EMERGENCE OF COMPLEXITY FROM SYNCHRONIZATION AND COOPERATION

Elvis L. Geneston, B.S., M.S.

Dissertation Prepared for the Degree of

DOCTOR OF PHILOSOPHY

UNIVERSITY OF NORTH TEXAS

May 2008

APPROVED:

Paolo Grigolini, Major Professor
Arkadii Krokhin, Committee Member
William Deering, Committee Member
Chris Littler, Chairman of the Department of Physics
Sandra L. Terrell, Dean of the Robert B. Toulouse School of Graduate Studies

Geneston, Elvis L. Emergence of Complexity from Synchronization and Cooperation. Doctor of Philosophy (Physics), May 2008, 111 pp., 27 illustrations, bibliography, 83 titles.

The dynamical origin of complexity is an object of intense debate and, up to moment of writing this manuscript, no unified approach exists as to how it should be properly addressed. This research work adopts the perspective of complexity as characterized by the emergence of non-Poisson renewal processes. In particular I introduce two new complex system models, namely the two-state stochastic clocks and the integrate-and-fire stochastic neurons, and investigate its coupled dynamics in different network topologies. Based on the foundations of renewal theory, I show how complexity, as manifested by the occurrence of non-exponential distribution of events, emerges from the interaction of the units of the system. Conclusion is made on the work's applicability to explaining the dynamics of blinking nanocrystals, neuron interaction in the human brain, and synchronization processes in complex networks.

ACKNOWLEDGEMENTS

All praise belongs to God for without Him I am nothing. I am thankful to many people who made the completion of this challenging work successful and a very enjoyable one. I thank my wife and my parents for the inspiration and untiring support. I am thankful and indebted to my research supervisor Professor Paolo Grigolini for the excellent ideas, encouragement, a very extended patience, and the everlasting friendship. I also extend a warm gratitude to Dr. Paolo Paradisi and Dr. Massimiliano Ignaccolo for all the very informative discussions. Special thanks go to Nagaraj, Vali, Nelson, Parts Lemy, Pahmz, Cesar, Rey and the Sapian and Stanley families for a very pleasurable stay in Denton.

I acknowledge the financial support from the Army Research Office and the Welch Foundation through grants W911NF-05-1-0205 and B-1577, respectively.

TABLE OF CONTENTS

Page

LIST OF FIGURES

Page

CHAPTER 1

INTRODUCTION

The Science of Complexity, in its infancy, is a known debated topic [1, 2, 3] and, as of the writing of this manuscript, no unified approach as to its dynamical origin has been established. Complexity, commonly viewed as a condition intermediate between total randomness and total order, is a physical state resulting from the cooperation of a large number of strongly interacting units of a complex system and that as a result of this cooperative behavior, the single components widely depart from the properties that they would have in isolation. The interaction among these units results to a non-predictable or anomalous time evolution of the properties of the system. The single components in solitude, that is, behaving independently, are normally characterized by Poisson statistics while its cooperative behavior in general exhibits anomalous relaxations in the form of non-exponential (non-Poisson) statistical distributions. The collective behavior of these coupled[1] units is a long standing problem [4, 5, 6, 7, 8] and the understanding of the dynamical properties of these complex systems have triggered the need of abandoning the traditional concepts of statistical physics, paving the way to the birth of several *Complexity Theories*.

Much of the complexity phenomena evolving from the interaction of units take place in a special structural form of complex system called *Complex Networks*. Complex networks form one of the most challenging areas of modern research encompassing a broad class of discipline, from physical and life sciences to sociology and economics. Recent studies [9, 10] went beyond the traditional concept of random networks [11] and established two new classes of networks, with high clustering [9] and power law distribution of edges [10]. More recently a new type of network has been proposed [12] with both high clustering and power-law distribution of edges. Herein, we adopt a regular network and the complex networks of Refs.

[1]May also refer to interacting units.

[9, 10, 11, 12] to study the dynamical properties of interacting units. The results of this manuscript show that complex networks indeed play a significant role in the synchronization and cooperation phenomena of oscillators. Herein, we do not discuss the properties and statistical mechanics of complex networks but rather we merely adopt complex networks topologies to model complexity and propose a theory as to what is the dynamical origin of the anomalous collective properties emerging from the coupling of the single components. The reader interested in complex networks is referred to the extensive review of Ref [13]. In particular, we adopt a two-state stochastic clock and an integrate-and-fire stochastic neuron as single components in the network to support the theory. As we shall see, the latter is a promising model for the physics of blinking quantum dots and the former aims at mimicking the dynamics of human brain.

The dynamical origin of complexity has attracted an increasing number of researchers in the past two decades. The discovery of the $1/f$ noise [14], a well-known manifestation of complexity, in many systems has given a clue as to what is the proper theoretical tool to investigate complexity. Bak et al [15] proposed that the problem with the $1/f$ noise should be settled with their theoretical perspective known as the Self Organized Criticality (SOC). Recently [16], another theoretical tool known as *superstatistics* has been advocated to be a proper approach to complexity. However, it has been shown with clarity in the book by Jensen [17] that SOC and superstatistics share the same view on complexity as both are based on the slow fluctuation of Poisson parameters, a class to which we refer herein as belonging to *modulation*, a non-renewal process. However, technological advancements, such as the single molecule spectroscopy and electroencephalography (EEG) among others, have revealed that many processes in complex real systems obey renewal properties, thereby signaling the need of a new approach to complexity assessing the renewal character of the system. Herein, to explain complex phenomena arising from the interaction of units in a system, we adopt a statistical technique called *Renewal Aging* to assess whether or not the time series of events

generated from a complex process is renewal and we attempt to explain the emergence of non-Poissonian statistical distributions from the perspective of *Subordination Theory*.

In this manuscript, we adopt complexity science as a field of investigation of multi-component systems characterized by non-canonical distributions. By this notion we mean the deviation from the canonical distribution as the breakdown of the conditions on which Boltzmann's view is based: short-range interaction, no memory, and no cooperation among the constituents of the system. The complexity approach herein rests on the purpose of addressing the problem on the departure from canonical distribution of complex systems, focusing on the waiting time distribution from the time series of events rather than the energy distribution. Thus, canonical and non-canonical distributions are represented here as exponential and non-exponential waiting time distributions respectively. The latter is generally manifested in the form of a stretched exponential and inverse power-laws in the time asymptotic limit.

1.1. Chapter Summaries

The next chapter offers an introduction to the basics of probability theory applied throughout the manuscript and gives a brief review of diffusion processes and theoretical tools such as the Fokker-Planck Equation, the Generalized Langevin Equation and the Continuous Time Random Walk. Chapter 3 is devoted to understanding how several complexity approaches are categorized based on addressing the renewal property of the system. Chapter 4 is the discussion of Subordination Theory which rests its foundations on the Continuous Time Random Walk and the Renewal Theory. The theory attempts at discussing the origin of non-Poisson statistical processes. In Chapter 5 we introduce the two-state stochastic clock model and investigate its dynamics in regular and complex topologies. Another model to explain complexity is discussed in Chapter 6. Here we use as single units the stochastic version of the well-adopted integrate-and-fire neurons. We conclude the dissertation in Chapter 7 by discussing issues that need further clarification and discuss plausible future research work.

CHAPTER 2

DIFFUSION PROCESSES

This chapter is devoted to the introduction of the basic mathematical concepts used throughout the entire manuscript. The chapter reviews the basic concepts in probability theory and derives the equations necessary to explain diffusion processes. It is not intended as a comprehensive material about diffusion, the continuous time random walk (CTRW), and the generalized langevin equation (GLE) that the reader is referred to Refs. [18, 19] for detailed discussions on the topics.

2.1. Probability Theory

Let us start by considering a stochastic variable $\xi(t)$ which can get a value x with a probability density function (PDF) $P(x,t)$. The joint probability density that the stochastic variable gets x_1 at time t_1, x_2 at time t_2, $\ldots x_n$ at time t_n is expressed as $P_n\left(x_1,t_1;x_2,t_2;\ldots;x_n,t_n\right)$ which has the property:

$$P_{n-1}\left(x_{n-1},t_{n-1};x_{n-2},t_{n-2};\ldots;x_1,t_1\right)=\int \mathrm{d}x_n P_n\left(x_n,t_n;x_{n-1},t_{n-1};\ldots;x_1,t_1\right) \qquad (2.1)$$

where the ordering of the pairs $\{x_i,t_i\}$ does not change the meaning of $P_n\left(\ldots\right)$. The probability that the stochastic variable $\xi(t)$ at time t_n gets the value (later we use the term *event* to refer to this process) x_n given that at time t_1 gets the value x_1, at time t_2 gets the value x_2, and so on is known as the conditional probability (CP) and is formally written as

$$P\left(x_n,t_n|x_{n-1},t_{n-1};x_{n-2},t_{n-2};\ldots;x_1,t_1\right)=\frac{P\left(x_n,t_n;x_{n-1},t_{n-1};\ldots;x_1,t_1\right)}{P\left(x_{n-1},t_{n-1};x_{n-2},t_{n-2};\ldots;x_1,t_1\right)}. \qquad (2.2)$$

The CP concept can be used to extract the information about the subensembles of a stochastic process. In general for events at $n+1$ to $n+l$ given the events 1 to l, Eq.(2.2) is written as

$$P_{l|n}\left(x_{n+l},t_{n+l};\ldots;x_{n+1},t_{n+1}|x_n,t_n;\ldots;x_1,t_1\right)=\frac{P_{n+l}\left(x_{n+l},t_{n+l};\ldots;x_1,t_1\right)}{P_n\left(x_n,t_n;\ldots;x_1,t_1\right)}. \tag{2.3}$$

We use the concept of conditional probability to define a *Markov process*. The variable $\xi(t)$ that we are considering is a Markov process if the following property holds true:

$$P_{1|n-1}\left(x_n,t_n|x_{n-1},t_{n-1};x_{n-2},t_{n-2};\ldots;x_1,t_1\right)=P_{1|1}\left(x_n,t_n|x_{n-1},t_{n-1}\right) \tag{2.4}$$

for all n where $t_1<t_2,\ldots,<t_n$. This means that given the actual state of the system (x_{n-1},t_{n-1}) we can calculate the probability for the occurrence of (x_n,t_n), and that the transition taking place when moving from t_{n-1} to t_n does not depend on earlier times. Using Eq. (2.2) the Markov process is described by the following equation:

$$P_n\left(x_n,t_n;x_{n-1},t_{n-1};\ldots;x_1,t_1\right)=\prod_{m=2}^{n}P_{1|1}\left(x_m,t_m|x_{m-1},t_{m-1}\right)P_1\left(x_1,t_1\right). \tag{2.5}$$

Applying Eq. (2.5) to Eq. (2.1) gives us

$$P_{1|1}\left(x_3,t_3|x_1,t_1\right)p_1\left(x_1,t_1\right)=\int \mathrm{d}x_2 P_{1|1}\left(x_3,t_3|x_2,t_2\right)P_{1|1}\left(x_2,t_2|x_1,t_1\right)p_1\left(x_1,t_1\right) \tag{2.6}$$

which yields:

$$P_{1|1}\left(x_3,t_3|x_1,t_1\right)=\int \mathrm{d}x_2 P_{1|1}\left(x_3,t_3|x_2,t_2\right)P_{1|1}\left(x_2,t_2|x_1,t_1\right). \tag{2.7}$$

This is the fundamental equation known as the $Chapman-Kolmogorov\ equation$.

2.1.1. *Stationary Markov Processes and the Master Equation*

Let us assume that the Markov process described above is stationary. This means that the process depends only on the time difference and does not depend on the absolute time. It is easy to show that integrating (2.6) with respect to x_1 and applying the recurrence relation (2.1) yields, after relabeling of indices,

$$P_1(x_2, t_2) = \int P_1(x_1, t_1) P_{1|1}(x_2, t_2|x_1, t_1) \mathrm{d}x_1. \tag{2.8}$$

Let us assume that the process takes place in a time interval $\tau = |t_2 - t_1| \to 0$. Thus, (2.8) becomes

$$P_1(x_2, t_1 + \tau) = \int P_1(x_1, t_1) P_{1|1}(x_2, t_1 + \tau|x_1, t_1) \mathrm{d}x_1. \tag{2.9}$$

Using Taylor series expansion and noting that $P_{1|1}(x_2, t_1|x_1, t_1) = \delta(y_1 - y_2)$, we obtain

$$P_{1|1}\left(x_2, t_1 + \tau|x_1, t_1\right) = \tau W(x_2|x_1) + (1 - W_0(x_1)\tau)\delta(x_1 - x_2) + o(\tau'). \tag{2.10}$$

Here $W(x_2|x_1)$ is the transition probability density per unit time that the system changes from x_1 to x_2 and $(1 - W_0(x_1)\tau)$ is the probability that no transition takes place during the time interval $t \to t_1 + \tau$ where

$$W_0(x_1) = \int W(x|x_1) \mathrm{d}x. \tag{2.11}$$

The last term has the property that $o(\tau')/\tau$ goes to zero as $\tau' \to 0$. Taking the time derivative (limiting case of $\tau \to 0$) of Eq. (2.9) and inserting Eqs. (2.10) and (2.11) to the Chapman-Kolmogorov equation (2.7), we get the *master equation*:

$$\frac{\partial}{\partial t} P(x, t) = \int \left[W(x|x') P_(x', t) - W(x'|x) P(x, t)\right] \mathrm{d}x \tag{2.12}$$

where proper relabeling of indices has been applied. In a discrete probability space (2.12) takes the form:

$$\frac{\partial}{\partial t}P(n,t) = \sum_{n'}\big[W(n|n')P(n',t) - W(n'|n)P(n,t)\big]. \tag{2.13}$$

2.1.2. *Kramers-Moyal Expansion and the Fokker-Planck Equation*

The Chapman-Kolmogorov equation (2.7) is a consistency equation for the conditional probabilities of a Markov process and a starting point for deriving the equations of motion describing a Markov process. Let us derive the famous $Fokker-Planck\ equation$ from this equation. To do that we assume x to be a continuous variable and that changes in $x(t)$ can only take place in small jumps. This makes $W(x'|x)$, the transition probability per unit time, decreases rapidly with increasing $|x-x'|$, the size of the jump. If we let the size to be $r = x - x'$, we can write $W(x'|x) \equiv W(x'; x-x') \equiv W(x'; r)$. Eq. (2.12) then becomes

$$\frac{\partial P(x,t)}{\partial t} = \int \mathrm{d}r W(x-r;r)P(x-r;t) - P(x,t)\int \mathrm{d}r W(x;-r). \tag{2.14}$$

Taylor expansion in $(x-r)$ around $r=0$ gives us

$$\begin{aligned}\frac{\partial P(x,t)}{\partial t} &= P(x,t)\int W(x;r)\mathrm{d}r - P(x,t)\int W(x;-r)\mathrm{d}r - \\ &\int r\frac{\partial}{\partial x}\big[W(x;r)P(x,t)\big]\mathrm{d}r + \frac{1}{2}\int r^2\frac{\partial^2}{\partial x^2}\big[W(x;r)P(x,t)\big]\mathrm{d}r\end{aligned} \tag{2.15}$$

yielding the so-called $Kramers-Moyal\ expansion$ of the master equation:

$$\frac{\partial P(x,t)}{\partial t} = \sum_{n=1}^{\infty}\frac{(-1)^n}{n!}\frac{\partial^n}{\partial x^n}\big[A_n(x)P(x,t)\big] \tag{2.16}$$

with

$$A_n(x) = \int_{-\infty}^{\infty} r^n W(x;r)\mathrm{d}r. \tag{2.17}$$

For slowly varying transition rates, $W(x-r;r) \approx W(x;r)$, we can truncate (2.16) up to an approximate order of derivatives. Considering only the second order gives us, with $A_1(x) = A(x)$ and $A_2(x) = B(x)$, the celebrated $Fokker - Planck\ equation$:

$$\frac{\partial}{\partial t}P(x,t) = -\frac{\partial}{\partial x}A(x)P(x,t) + \frac{1}{2}\frac{\partial^2}{\partial x^2}B(x)P(x,t) \tag{2.18}$$

2.2. Diffusion and the Central Limit Theorem

2.2.1. *Random Walks*

Let us review the random walk [20] problem in one dimension and denote with $P_n(j)$ the probability that the random walker is in the site j at a discrete natural time n. As shown in the figure, we assign p as the probability of the walker to make a jump from the left to the right (site $j-1$ to j) and q as the probability of jumping backward (site $j+1$ to j). This process can be modeled by the following master equation

$$P_{n+1}(j) = pP_n(j-1) + qP_n(j+1). \tag{2.19}$$

with the normalization condition $p + q = 1$. Moving to the continuous space-time representation, we assign

$$\begin{cases} t = n\Delta t \\ x = j\Delta x \end{cases} \tag{2.20}$$

and assume $n \gg 1$ and $j \gg 1$, thereby making x and t continuous allowing us to assume

$$P(x,t) = P_n(j) \tag{2.21}$$

and consequently,

$$P(x, t + \Delta t) = pP(x - \Delta x, t) + qP(x + \Delta x, t). \tag{2.22}$$

The continuum limit in space and time (2.20) allows us to make the following Taylor expansions in Δt and Δx up to the first few terms:

$$\begin{cases} P(x, t + \Delta t) = P(x, t) + \Delta t \frac{\partial}{\partial t} P(x, t) \\ P(x \pm \Delta x, t) = P(x, t) \pm \Delta x \frac{\partial}{\partial x} P(x, t) + \frac{1}{2}(\Delta x)^2 \frac{\partial^2}{\partial x^2} P(x, t) \end{cases} \tag{2.23}$$

Inserting (2.23) to (2.22) gives us a special form of Fokker-Planck equation (2.18) called *diffusion equation*:

$$\frac{\partial}{\partial t} P(x, t) = -V \frac{\partial}{\partial x} P(x, t) + D \frac{\partial^2}{\partial x^2} P(x, t) \tag{2.24}$$

with

$$D \equiv \frac{1}{2} \frac{(\Delta x)^2}{\Delta t} \tag{2.25}$$

and

$$V \equiv (p - q) \frac{\Delta x}{\Delta t}. \tag{2.26}$$

It is easy to show that the solution of (2.24), with the initial condition $x = 0$, is given by the Gaussian (normal) distribution

$$P(x, t) = \frac{1}{(4\pi D t)^{1/2}} exp\Big[-\frac{(x - Vt)^2}{4Dt}\Big] \tag{2.27}$$

which for the unbiased case $V = 0$, corresponding to the case $p = q = 1/2$, gives the familiar form

$$P(x, t) = \frac{1}{(4\pi D t)^{1/2}} exp\Big[-\frac{x^2}{4Dt}\Big]. \tag{2.28}$$

2.2.2. *The Central Limit Theorem*

The Gaussian distribution result (2.27) is an ubiquitous property of stochastic processes. This is a direct consequence of the *Central Limit Theorem* (CLT). The CLT states that for statistically independent and identically distributed (IID) random variables $x_1, \ldots, x_N$ with finite first and second moments, meaning $< x_i >< \infty$ and $< x_i^2 >< \infty$ respectively, then the sum variable

$$S_N = \frac{1}{N} \sum_{i=1}^{N} x_i \tag{2.29}$$

is distributed according to a normal distribution provided $N \to \infty$.

In the case of the random walk problem in Subsection 2.2.1, the jump distance's first and second moments, $(p-q)\Delta x$ and $(p+q)(\Delta x)^2 = (\Delta x)^2$ are obviously finite, thus giving us the normal distribution form (2.27). There are, however, cases commonly occurring in nature where the lowest moments of IID random variables diverge. The resulting distribution of the sum of these variables belongs to a class of distributions called the *Stable* or *Lévy Distributions* where the Gaussian (normal) distribution is a special case. This is the scope of the Generalized Central Limit Theorem (GCLT). For detailed wealthy discussion of CLT and GCLT, the reader is referred to the excellent book by Paul and Baschnagel [21].

2.3. Brownian Motion and Anomalous Diffusion

2.3.1. *Brownian Motion*

Let us consider a one-dimensional motion of a mesoscopic particle, called "Brownian particles", of mass M immersed in a fluid (bath) with relatively lighter particles under the influence of an external field. The erratic motion of this particle is described by the following set of equations:

$$\dot{x} = v \tag{2.30}$$

$$\dot{v} = -\gamma v + \frac{F(x)}{M} + f(t). \tag{2.31}$$

The term $-\gamma v$, where $\gamma = 6\pi\eta r$, is the irreversible dissipative force arising from the effects of Stokes' Law for a spherical object of radius r moving through a fluid (environment) with viscosity η. It has the effect of transferring the kinetic energy of the Brownian particle into the thermal energy of the environment. For simplicity, let us assume that this friction term does not contain memory effects. The term $f(t)$ is a random force that mimics the influence of the collisions between the Brownian particle with the much lighter particles of the fluid and $F(x)/M$ is added to take into account any external force affecting the motion of the particle.

Let us consider the velocity process and assume that there are no external forces acting on the particle. The resulting equation is the *Langevin equation*:

$$\frac{\mathrm{d}v}{\mathrm{d}t} = -\gamma v + f(t). \tag{2.32}$$

A more general form of (2.32) is the so-called *Generalized Langevin equation* [22]:

$$\frac{\mathrm{d}v}{\mathrm{d}t} = -\int_{-\infty}^{t} \mathrm{d}t' \gamma_{mem}(t-t')v(t') + f(t) \tag{2.33}$$

where the function $\gamma_{mem}(t-t')$ takes into account the memory of the dissipative force.

To solve the Langevin equation, let us make the following assumptions. First, we approximate the collisions between the Brownian particle and the environment particles as occurring instantaneously and imparting a random velocity change onto the Brownian particle. Furthermore, we assume that these collisions are totally uncorrelated. Let us also assume that the random force $f(t)$ has the following properties:

(i) $f(t)$ is independent of the position x,

(ii) $f(t)$ varies rapidly compared to the variation of $x(t)$,

(iii) $f(t)$ has zero-centered Gaussian property

$$< f(t) >= 0, \tag{2.34}$$

and

(iv) the correlation of the random force takes the following form:

$$< f(t')f(t) >= \mathcal{N}\delta(t'-t) \qquad t' > t, \tag{2.35}$$

where the notation $< ... >$ denotes the statistical average over an ensemble of realizations. The symbol δ is the Dirac delta function and $\mathcal{N}$ is the intensity of the random force whose exact expression is solved below.

Formally, the solution of Eq.(2.32) is:

$$v(t) = e^{\gamma t}\int_0^t e^{\gamma t'} f(t')\mathrm{d}t' + e^{-\gamma t}v(0). \tag{2.36}$$

Taking the first moment $< v(t) >$ and using Eq.(2.34) gives us

$$< v(t) >= e^{-\gamma t} < v(0) > \tag{2.37}$$

which coincides with the deterministic prescription of macroscopic bodies.

To get more significant results, let us evaluate the second moment $< v^2(t) >$. Using (2.36) and the random force property (2.35), we get

$$\begin{aligned} < v^2(t) > &= < v^2(0) > e^{-2\gamma t} + \mathcal{N}e^{-2\gamma t}\int_0^t \mathrm{d}t' \int_0^t \mathrm{d}t'' e^{-\gamma(t+t')}\delta(t'-t'') + \\ &\quad 2e^{-2\gamma t}\int_0^t \mathrm{d}t' e^{\gamma(t')} < v(0)f(t') > \\ &= < v^2(0) > e^{-2\gamma t} + \frac{\mathcal{N}}{2\gamma}\Big(1 - e^{-2\gamma t}\Big). \end{aligned} \tag{2.38}$$

where we considered the simplified case where v_0 and $f(t)$ are uncorrelated.

Allowing the system to reach equilibrium ($t \to \infty$), we obtain

$$< v^2(\infty) >= \frac{\mathcal{N}}{2\gamma}, \tag{2.39}$$

which when compared to the equipartition principle in one dimension:

$$\mathbf{E} = \frac{1}{2}M < v^2(\infty) >= \frac{1}{2}k_B T \tag{2.40}$$

gives an expression for the noise intensity:

$$\mathcal{N} = \frac{2\gamma k_B T}{M}. \tag{2.41}$$

Eqn (2.41) is one of the forms of the so-called *fluctuation-dissipation relation.*

Let us now proceed with the position process $x(t)$. Using Eqns. (2.30) and (2.36), we get

$$x(t) = \frac{v_0}{\gamma}(1 - e^{-\gamma t}) + \int_0^t e^{-\gamma t'} \mathrm{d}t' \int_0^{t'} e^{\gamma t''} f(t'') \mathrm{d}t'' \tag{2.42}$$

where we assumed the initial condition to be $x(0) = 0$. Thus, the assumption (2.34) leads to the expression of the mean position of the particle at time t.

$$< x(t) >= \frac{v_0}{\gamma}(1 - e^{-\gamma t}) \tag{2.43}$$

Let us proceed with the mean squared displacement of the particle. Squaring (2.42) and applying the random force correlation (2.35) gives

$$\begin{aligned} < x^2(t) > &= \frac{v_0^2}{\gamma^2}(1 - e^{-\gamma t})^2 + \mathcal{N} \int_0^t e^{-\gamma t'} \mathrm{d}t' \int_0^t e^{-\gamma t''} \mathrm{d}t'' \\ &\quad \times \int_0^{t'} e^{\gamma \tilde{t}'} \mathrm{d}\tilde{t}' f \int_0^{t''} e^{\gamma \tilde{t}''} \mathrm{d}\tilde{t}'' \delta(|\tilde{t}'' - \tilde{t}'|) \\ &= \frac{2k_B T}{M\gamma} t + \frac{v_0^2}{\gamma^2}(1 - e^{-\gamma t})^2 - \frac{k_B T}{M\gamma^2}(3 - 4e^{-\gamma t} + e^{-2\gamma t}). \end{aligned} \tag{2.44}$$

In the limiting case $t \to \infty$, we obtain

$$< x^2(t \to \infty) > \propto 2Dt \tag{2.45}$$

with

$$D = \frac{k_B T}{M\gamma} \tag{2.46}$$

Eqn. (2.46) is the famous *diffusion coefficient* derived by Einstein [23].

2.3.2. *Anomalous Diffusion*

The mean squared displacement of particles in many systems is, however, not limited to the form of (2.44). A number of diverse systems [24, 25, 26, 27, 28, 29, 30, 31, 32, 33, 34, 35, 36] departs from the direct linear time dependence of the mean squared displacement (2.44). This phenomenon is known as *Anomalous Diffusion* and takes the nonlinear form

$$< x^2(t) > \sim D_\alpha t^\alpha. \tag{2.47}$$

The factor D_α is the generalized diffusion coefficient. The processes with the property $0 < \alpha < 1$ belong to the class called *Subdiffusion* and for $\alpha > 1$ *Superdiffusion*. For an extensive discussion of these processes, the reader is referred to a review by Metzler and Klafter [37].

2.4. First Passage Times and the Kramers Problem

One of the most important problems concerning Brownian motion is to calculate the probability density function $\psi(t)$ for a Brownian particle described by stochastic process $x(t)$ to reach for the first time the position x_F (one-dimension) or to cross a boundary of a spatial dimension (multi-dimension). Problems of this type is ubiquitous in a variety of physical systems. This whole class of problems is the scope of the *first passage times* formalism [38]. Here, after formulating the general first passage times solution of a one-dimensional Fokker-Planck equation, we tackle the famous problem pertaining to reaction kinetics known as the *Kramers Problem* [39] where the reaction particles are taken to be Brownian particles in a potential.

2.4.1. *First Passage Times*

Let us consider a one-dimensional stationary Markovian stochastic process $x(t)$ where the probability of getting $x \leq x(t) < x + \mathrm{d}x$ for $x(0) = x_0$, is defined by $P(x,t|x_0)\mathrm{d}x$. The first passage times probability $F(x_F,t|x_0)\mathrm{d}t$ is defined as the probability that a continuous function $x(t)$ passes the boundary x_F for the first time in the time interval $(t, t+\mathrm{d}t)$ given an initial condition $x(0) = x_0$. $F(x_F,t|x_0)$ is obtained by observing that for $x_0 < x_F$

$$F(x_F,t|x_0) \equiv -\frac{\partial}{\partial t}\int_{-\infty}^{x_F} P_a(x,t|x_0)\mathrm{d}x, \tag{2.48}$$

where $P_a(x,t|x_0)\mathrm{d}x$ is the probability that the particle is in $(x, x+\mathrm{d}x)$ at time t and that at no time between 0 and t the particle has reached the point x_F. The probability $P_a(x,t|x_0)\mathrm{d}x$ can be visualized as the probability of finding the particle in $(x, x+\mathrm{d}x)$ at t if an absorbing barrier is present at x_f, and can thus be obtained as the fundamental solution of the diffusion equation with boundary conditions

$$P_a(-\infty,t|x_0) = P_a(a,t|x_0) = 0. \tag{2.49}$$

The fundamental integral equation is obtained by classifying the functions $x(t')$ for which $x(0) = x_0$ and $(x \leq x(t) < x + \mathrm{d}x)$ according to the time $\tau_F > 0$ at which they reach the point x_F for the first time $(x_0 < x_F \leq x)$. One thus obtains:

$$P(x,t|x_0) = \int_0^t F(x_F,\tau_F|x_0)P(x,t-\tau_F|x_F)\mathrm{d}\tau_F. \tag{2.50}$$

Laplace transforming[1] (2.50) and taking advantage of its time-convoluted structure gives us

$$\hat{P}(x,u|x_0) = \hat{F}(x_F,\tau_F|x_0)\hat{P}(x,u|x_F) \tag{2.51}$$

and consequently we obtain

$$\hat{F}(x_F,\tau_F|x_0) = \frac{\hat{P}(x,u|x_0)}{\hat{P}(x,u|x_F)}. \tag{2.52}$$

[1] $\hat{f}(x,u) \equiv \int_0^\infty e^{-ut} f(x,t)\mathrm{d}t$

For cases where the left-hand side of Eq. (2.51) satisfies the Fokker-Planck equaton (2.18) of ordinary diffusion process, the first passage times probability density function can be easily solved by taking the anti-Laplace transform [2] of Eq. (2.52) and using the diffusion solution (2.27) with a suitable initial condition.

2.4.2. *One-Dimensional Fokker-Planck Equation First Passage Times Moments*

Let us consider the one-dimensional Fokker-Planck equation (2.18) written in terms of the conditional probabilities:

$$\frac{\partial}{\partial t}P\left(x,t|x_0,t_0\right) = L_{FP}(x)P\left(x,t|x_0,t_0\right) \tag{2.53}$$

with

$$L_{FP} = -\frac{\partial}{\partial x}A(x) + \frac{1}{2}\frac{\partial^2}{\partial x^2}B(x). \tag{2.54}$$

Let us assume that at $t = 0$ the motion of the particle is governed by Eq. (2.53) in the domain $x\epsilon(-\infty, x_F)$. The region $x \to -\infty$ is a reflecting boundary and when the particle reaches x_F, the particle is absorbed. Thus, giving us the following boundary conditions:

$$\left.\begin{aligned} P\left(x_F,t|x_0,0\right) = &\quad 0 \\ \frac{\partial}{\partial x}P\left(x\to-\infty,t|x_0,0\right) \longrightarrow &\quad 0 \end{aligned}\right\}. \tag{2.55}$$

The probability for the particle to remain in the interval $(-\infty, x_F)$ at time t is

$$Q\left(x_0,t\right) = \int_{-\infty}^{x_F} P\left(x,t|x_0,0\right)\mathrm{d}x \tag{2.56}$$

which is also the probability that the first passage time τ from x_0 to x_F is larger than t:

$$Q\left(x_0,t\right) = Prob(\tau \geq t) = \int_t^{\infty} F\left(x_0,\tau\right)\mathrm{d}\tau \tag{2.57}$$

[2] $f(x,t) \equiv \frac{1}{2\pi i}\int_{\gamma-i\infty}^{\gamma+i\infty} e^{ut}\hat{f}(x,t)\mathrm{d}u$

and consequently,

$$F\left(x_0,t\right)=-\frac{\partial G(x_0,t)}{\partial t}. \tag{2.58}$$

Thus, $Q(x_0,t)$ takes the following boundary conditions:

$$Q(x_0,t)=\begin{cases}1 & \text{if } x_0\leq x_F,\\ 0 & \text{if } x_0>x_F,\end{cases} \tag{2.59}$$

$$Q(x_F,t)=0, \tag{2.60}$$

$$\frac{\partial}{\partial x_0}Q(x_F,t)\xrightarrow{x\to-\infty}0. \tag{2.61}$$

Using Eq. (2.58) and the fact that $\lim_{t\to\infty}t^nQ(x_0,t)=0$, the first passage times moments can be written as

$$<\tau^n>=-\int_0^\infty t^n\frac{\partial}{\partial t}Q(x_0,t)\mathrm{d}t=n\int_0^\infty t^{n-1}Q(x_0,t)\mathrm{d}t. \tag{2.62}$$

Let us go back to the Fokker-Planck equation (2.53). The homogeneity condition $P\left(x,t|x_0,0\right)=P\left(x,0|x_0,-t\right)$ gives $L_{FP}(x)=L_{FP}^{+}(x_0)$. This allows us to write Eq. (2.53) as

$$\frac{\partial}{\partial t}P\left(x,t|x_0,t_0\right)=L_{FP}^{+}(x_0)P\left(x,t|x_0,t_0\right) \tag{2.63}$$

with

$$L_{FP}^{+}(x_0)=A(x_0)\frac{\partial}{\partial x_0}+\frac{B(x_0)}{2}\frac{\partial^2}{\partial x_0^2}. \tag{2.64}$$

Taking the time derivative of (2.56) and using (2.63), we get

$$\frac{\partial}{\partial t}Q\left(x_0,t\right)=\Big[A(x_0)\frac{\partial}{\partial x_0}+\frac{B(x_0)}{2}\frac{\partial^2}{\partial x_0^2}\Big]Q\left(x_0,t\right). \tag{2.65}$$

Going back to Eq. (2.62) and applying (2.65) gives us

$$-n < \tau^{n-1}(x_0) >= \Big[A(x_0)\frac{\partial}{\partial x_0} + \frac{B(x_0)}{2}\frac{\partial^2}{\partial x_0^2}\Big] < \tau^n(x_0) > . \tag{2.66}$$

Let us solve the first moment $< \tau(x_0) >$. Equation (2.66) has to be solved with the boundary conditions

$$< \tau(x_F) > \quad = \quad 0, \tag{2.67}$$

$$\frac{\partial}{\partial x_0} < \tau(x_0) > \quad \xrightarrow{x_0 \to -\infty} \quad 0. \tag{2.68}$$

The homogeneous part of (2.66) for $n = 1$ when $B(x_0) \neq 0$ has the solution

$$\frac{\mathrm{d} < \tau(x_0) >}{\mathrm{d}x_0} =< \tau_0 > exp\Big[-2\int_0^x \frac{A(x')}{B(x')}\mathrm{d}x'\Big]. \tag{2.69}$$

To get a particular solution for the first moment case of (2.66), we apply the variation of the constant method. Choosing $< \tau_0 >=< \tau_0(x_0) >$ and inserting (2.69) into $n = 1$ case of (2.66), we get

$$\frac{\mathrm{d} < \tau_0 >}{\mathrm{d}x_0} exp\Big[-2\int_0^x \frac{A(x')}{B(x')}\mathrm{d}x'\Big] = \frac{-2}{B(x_0)}. \tag{2.70}$$

A particular solution of this equation is

$$< \tau_0(x_0) >= -2\int_0^x \frac{\mathrm{d}x'}{B(x')} exp\Big\{\int^{x'} \mathrm{d}x'' \frac{2A(x'')}{B(x'')}\Big\}. \tag{2.71}$$

Thus, we get the complete derivative of the mean first passage time:

$$\frac{\mathrm{d} < \tau(x_0) >}{\mathrm{d}x_0} = \left[< \tau_0 > -2\int_0^x \frac{\mathrm{d}x'}{B(x')} exp\Big\{\int^{x'} \mathrm{d}x'' \frac{2A(x'')}{B(x'')}\Big\}\right] exp\Big\{-2\int_0^x \frac{A(x')}{B(x')}\mathrm{d}x'\Big\}. \tag{2.72}$$

As $\frac{\mathrm{d} < \tau(x_0) >}{\mathrm{d}x_0}$ has to vanish for $x_0 \to -\infty$, only the particular solution remains. Using the conditions (2.67), the first moment is written as

$$< \tau(x_0) >= 2\int_{x_0}^{x_F} \mathrm{d}x' \phi^{-1}(x') \int_{-\infty}^{x'} \mathrm{d}x'' \frac{\phi(x'')}{B(x'')}. \tag{2.73}$$

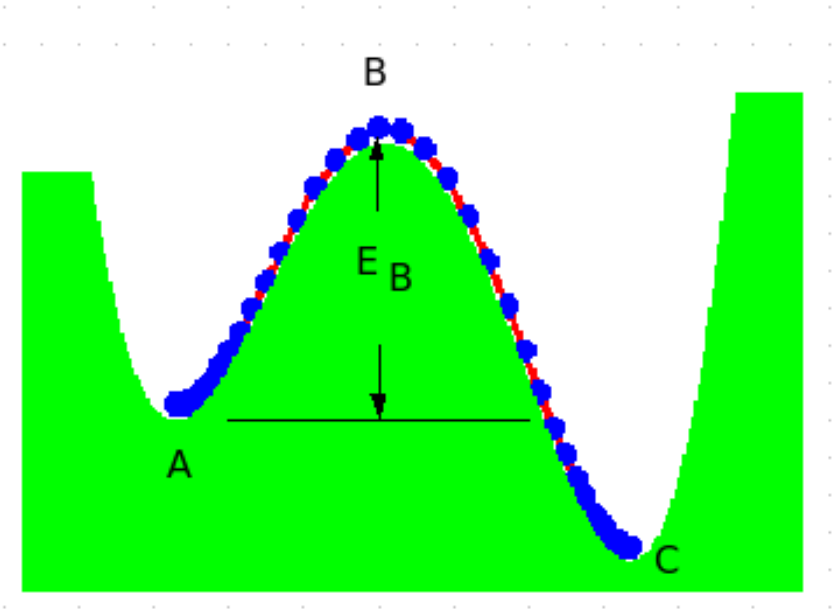

Figure 2.1: The Kramers problem. The Brownian particles must pass through the barrier E_B at B to reach the stable state C.

with

$$\phi(x) = exp\Big[\int_{-\infty}^{x_0} \mathrm{d}x' \frac{2A(x')}{B(x')}\Big].$$

In the following section we shall use Eqn. (2.73) to solve the chemical reaction rate considered by Kramers [39].

2.4.3. *The Kramers Problem*

The famous Kramers problem is illustrated in Figure 2.1. In the chemical reaction problem considered by Kramers, state A, which is a metastable state, corresponds to the reactants and state C, which is a stable equilibrium state of absolute minimum energy, to the products. The reaction can only take place when the system in state A crosses the barrier at x_B of energy difference E_B with respect to state A. Let us solve the rate at which the system changes state from A to C.

Kramers used the same set of equations (2.30) to model the problem:

$$\dot{x} = v \tag{2.74}$$

$$\dot{v} = -\gamma v + \frac{F(x)}{M} + f(t). \tag{2.75}$$

To solve (2.74) for the Kramer's problem in Figure 2.1, we first make the following assumptions on the time scales of the reaction process:

$$\tau_{env} \ll \tau_{eq} \ll \tau_{esc}, \tag{2.76}$$

where τ_{env} is the time scale of the bath particles, τ_{eq} is the equilibration time of the reacting particles, and τ_{esc} is the time scale of the particle to escape the reactants well and cross the barrier. The condition has to be satisfied for the reacting particles to reach thermal equilibrium first with the bath particles to allow on the thermal fluctuations of the particles to drive the system over the barrier. This is further fulfilled by the adoption of the following relation between the mean thermal energy of the particles and the barrier height E_B:

$$k_B T \ll E_B. \tag{2.77}$$

This relation prevents the particles to diffuse freely between the states A and C.

Kramers solved this problem in two-extreme cases:

(i) strong friction, $\gamma/\omega_B \gg 1$

(ii) weak friction, $\gamma/\omega_B \ll 1$

where $\omega_B = \sqrt{U''(x_B)/M}$ is the time scale for the exchange between kinetic and potential energy during the barrier crossing and U'' is the second derivative of the potential U at x_B with respect to the reaction coordinate x. Herein, we only consider the first case, which is also commonly known as the *Smoluchowski regime*. Considering that $1/\gamma$ (see deterministic part of (2.36)) is the time scale over which the Brownian particle loses information about the starting velocity, after this time inertia effects vanish. Thus, the strong friction condition

allows us to use the Smoluchowski approximation $\mathrm{d}v/\mathrm{d}t = 0$. Hence, from (2.74) we get

$$\frac{\mathrm{d}x}{\mathrm{d}t} = \frac{F(x)}{\gamma M} + \frac{f(t)}{\gamma}. \tag{2.78}$$

The corresponding Fokker-Planck equation (2.18) of (2.78) is

$$\frac{\partial}{\partial t}P\left(x,t\right) = \Big[-\frac{\partial}{\partial x}\frac{F(x)}{\gamma M} + D\frac{\partial^2}{\partial x^2}\Big]P\left(x,t\right) \tag{2.79}$$

with D the diffusion coefficient (2.46). Comparing (2.79) with (2.18) we find the relation

$$\begin{aligned} A(x) &= \frac{F(x)}{\gamma M} \\ \frac{B(x)}{2} &= D. \end{aligned} \tag{2.80}$$

Therefore, Eqn. (2.73) becomes

$$< \tau > \approx \frac{M\gamma}{k_B T}\int_x^{x_C} \mathrm{d}x' exp\Big[\frac{U(x')}{k_B T}\Big]\int_{-\infty}^{x_B} \mathrm{d}x'' exp\Big[-\frac{U(x'')}{k_B T}\Big] \tag{2.81}$$

where we made use of the fact that $F(x) = -\mathrm{d}U(x)/\mathrm{d}x$. To simplify the solution of (2.81), we make a Taylor expansion of the potential around $x = x_B$ in the first integral and around $x = x_A$ in the second:

$$U(x') = U(x_B) - \frac{1}{2}M\omega_B^2(x' - x_B)^2 \tag{2.82}$$

$$U(x'') = U(x_A) + \frac{1}{2}M\omega_A^2(x'' - x_A)^2 \tag{2.83}$$

where we substituted $U''(x_A) = M\omega_A^2$ and $U''(x_B) = M\omega_B^2$. The expansions (2.82) and (2.83) allow us to change the limits of integration in (2.81) to $(\infty, -\infty)$. Thus, Eqn. (2.81)

becomes

$$< \tau > \approx \frac{M\gamma}{k_B T}\int_{-\infty}^{\infty} \mathrm{d}x' exp\Big[\frac{U(x_B) - \frac{1}{2}M\omega_B^2(x' - x_B)^2}{k_B T}\Big] \times \int_{-\infty}^{\infty} \mathrm{d}x'' exp\Big[-\frac{U(x_A) + \frac{1}{2}M\omega_A^2(x'' - x_A)^2}{k_B T}\Big] \tag{2.84}$$

which, after solving the Gaussian integrals, gives

$$< \tau > \approx \frac{2\pi\gamma}{\omega_B\omega_A} exp\Big[\frac{E_B}{k_B T}\Big]. \tag{2.85}$$

Therefore, we obtain the Kramers reaction rate formula from state A to state C:

$$r = < \tau >^{-1} \approx \frac{\omega_B\omega_A}{2\pi\gamma} exp\Big[-\frac{E_B}{k_B T}\Big] \tag{2.86}$$

in accordance with the Arrhenius behavior [40].

2.5. Continuous Time Random Walk

In the random walk problem in section 2.3.1 we notice that this formalism has the walks done with certain prescribed jump-distance distributions but at discrete fixed times. This problem can be extended to a case where the time between successive steps (waiting times) is random rather than being fixed. This is the continuous time random walk (CTRW) formalism. If the length of the jumps l and the waiting times τ elapsing between two successive jumps are drawn from a probability distribution, say $\phi(l, \tau)$, which therefore represents the probability density to move a distance l in time τ in a single motion event, we can deduce the length distribution $\lambda(l)$ and the waiting times distribution $\psi(\tau)$ as follows:

$$\lambda(l) = \int_0^{\infty} \mathrm{d}\tau \phi(l, \tau), \tag{2.87}$$

$$\psi(\tau) = \int_{-\infty}^{\infty} \mathrm{d}l \phi(l, \tau). \tag{2.88}$$

Here the probability that a jump length is between $[l, l+\mathrm{d}l]$ is $\lambda(l)\mathrm{d}l$ and the probability for a jump to occur in the time interval $[\tau, \tau+\mathrm{d}\tau]$ when the last step occurred at time $\tau = 0$ is $\psi(\tau)\mathrm{d}\tau$. Denoting $\psi_n(\tau)$ as the probability density for the n-th step to occur after a time τ, we get the following recurrence relation:

$$\psi_n(\tau) = \int_0^\tau \psi(\tau - \tau')\psi_{n-1}(\tau')\mathrm{d}\tau'. \tag{2.89}$$

Applying the convolution theorem of the Laplace transforms, Eq.(2.89) results to

$$\hat{\psi}_n(u) \equiv \int_0^\infty \mathrm{d}\tau e^{-u\tau}\psi_n(\tau) = \hat{\psi}(u)\hat{\psi}_{n-1}(u) = [\hat{\psi}(u)]^n. \tag{2.90}$$

Let us now solve for the probability $p(x,t)$ of finding the position of the walker at x at time t. This is done by introducing two functions. First, let us define the survival probability (SP) $\Psi(\tau)$. This is the probability that no jumps occurred in the time interval $[0,\tau]$ and is written as:

$$\Psi(\tau) \equiv 1 - \int_0^\tau \psi(\tau')\mathrm{d}\tau' = \int_\tau^\infty \psi(\tau')\mathrm{d}\tau'. \tag{2.91}$$

The other one is the probability that the walker arrives exactly at x at time t:

$$Q(x,\tau) = \int_{-\infty}^\infty \mathrm{d}x' \int_0^\tau \mathrm{d}\tau' Q(x-x',\tau')\phi(x',\tau') + \delta(x)(\tau). \tag{2.92}$$

The probability $p(x,t)$ is related to Eq.(2.91) and Eq.(2.92) by the following equation:

$$p(x,t) = \int_0^t \Phi(t-\tau)Q(x-x',\tau)\mathrm{d}\tau. \tag{2.93}$$

Fourier-Laplace ($x \to k, \tau \to u$) transforming Eq.(2.93) gives:

$$\hat{P}(k,u) = \frac{1-\hat{\psi}(u)}{u}\frac{1}{1-\hat{\lambda}(k)\hat{\psi}(u)}. \tag{2.94}$$

This is the famous Montroll-Weiss equation [41] for the standard CTRW. In the next two chapters we use this equation as a building foundation of the renewal aging concept and subordination theory.

CHAPTER 3

COMPLEXITY AND AGING

In this chapter we review two dynamical approaches to complexity, namely the *renewal* and *modulation*. As we show herein, these two approaches generate the same non-exponential waiting time distribution function $\psi(\tau)$. Though both yield the same waiting time distribution, this does not indicate, as we show in the succeeding sections, that they are statistically equivalent and do not necessarily refer to the same physical properties. The next two sections cover the generation of time series t_i in the renewal and modulation perspective. In the renewal case, the time series is generated having the condition that every time the process produces a waiting time τ_i, the system's memory is reset to zero thereby making the waiting times τ_i statistically independent. The time series from a modulation approach, on the other hand, is realized in a way that from time to time a transition from a given exponential scale to another occurs, in such a way that the resulting waiting time distribution, which is therefore, the superposition of infinitely many exponential distributions, is the same non-exponential form generated from a renewal perspective. This outcome may lead to a confusion as to which is the correct approach for a given complex process under consideration. The remaining sections of the chapter attempts to distinguish one from the other base on two statistical techniques known as renewal aging and diffusion scaling.

3.1. Renewal Theory

Let us start with the renewal approach. Let us consider the following dynamical model:

$$\frac{\mathrm{d}y\left(t\right)}{\mathrm{d}t} = ay^{z}\left(t\right) \tag{3.1}$$

with $a > 0$ and $z \geq 1$. Simple as it may appear, it nevertheless serves the complete purpose of realizing the non-Poisson renewal condition, to which in this manuscript is considered as a tool for a proper model of complexity . Equation (3.1) is an equation of motion describing a particle moving in the positive y-axis direction and confined in the interval $\mathbf{I} = [0, 1]$. Statistics come into play in this deterministic equation when we determine the waiting times generated in the process by the following prescription: every time the particle reaches the border at $y = 1$, we inject the particle back in a random position with uniform probability distribution in the interval $[0, 1]$. We consider the times it takes the particle to reach the border $y = 1$ as the *waiting times* of the process and we shall refer to the back injection as *events*. With this condition, Eq.(3.1) can be rewritten in the integral form:

$$\int_{y_0}^{1} \frac{\mathrm{d}y}{y^z} = a\tau. \tag{3.2}$$

Solving this integral gives us the random initial position y_0 of the particle in relation to the waiting times τ through the following expression:

$$y_0 = \frac{1}{\left[1 - (1 - z)\, a\tau\right]^{\frac{1}{1-z}}}. \tag{3.3}$$

Let us now find the distribution density $\psi(\tau)$ of the waiting times. The probability that the particle reaches the border in the time interval $[\tau, \tau + \mathrm{d}\tau]$ is determined by

$$\psi(\tau)\mathrm{d}\tau = p_0(y_0)\mathrm{d}y_0. \tag{3.4}$$

Due to the re-injection process of the particle when it reaches the border, we get $p_0(y_0) = 1$. Thus giving us, using Eq. (3.3), the non-exponential distribution of waiting times:

$$\psi(\tau) = \left|\frac{\mathrm{d}y_0}{\mathrm{d}\tau}\right| = (\mu - 1)\frac{T^{\mu-1}}{(\tau + T)^{\mu}} \tag{3.5}$$

where

$$\mu = \frac{z}{z-1} \tag{3.6}$$

and

$$T = \frac{\mu - 1}{a}. \tag{3.7}$$

Eq. (3.5) is a properly normalized distribution function. The parameter T has the purpose of bearing the information on the lapse of time necessary to reach the time asymptotic condition when $\psi(\tau)$ becomes identical to an inverse power-law.

3.1.1. *Evolution of Probability*

Let us find the probability distribution function $p(y,t)$ of the dynamical variable $y(t)$ in the form:

$$\frac{\partial}{\partial t}p(y,t) = \mathcal{L}p(y,t). \tag{3.8}$$

The equation of motion for $y(t)$ consists of two contributions in the interval **I**: (a) the deterministic motion within the interval; (b) the random re-injection. The Heisenberg-like picture for (a) is :

$$\mathcal{L}_H^{(a)} \equiv -\alpha y^z \frac{\partial}{\partial y} \tag{3.9}$$

which therefore gives us the Schrödinger-like picture

$$\mathcal{L}^{(a)} = \mathcal{L}_H^{(a)+} = \alpha \frac{\partial}{\partial y} y^z. \tag{3.10}$$

The Schrödinger-like picture for the random part (b) is written as

$$\mathcal{L}^{(b)}p(y,t) = \alpha p(1,t). \tag{3.11}$$

In fact,

$$\frac{\partial}{\partial t}p(y,t) = \mathcal{L}^{(b)}p(y,t) = \alpha p(1,t) \tag{3.12}$$

yields

$$p(y,t) = \alpha \int_0^t p(1,t')\mathrm{d}t'. \tag{3.13}$$

This means that $p(y,t)$ increases due to the uniform back injection. If the population intensity with **I** increases, $p(1,t)$ must decrease so as to keep constant the total population. We are going to assess this in a little while. In conclusion, we get the following time evolution of the probability function:

$$\frac{\partial}{\partial t}p(y,t) = \alpha\Big[-\frac{\partial}{\partial y}y^z p(y,t) + p(1,t)\Big]. \tag{3.14}$$

It is easy to show that this equation satisfies the normalization condition $\int_0^1 p(y,t)\mathrm{d}y = 1$, which is fulfilled at all times in the interval **I**.

From (3.8), we can find the equilibrium distribution[1]

$$p_{eq}(y) = \frac{2-z}{y^{z-1}}, \tag{3.15}$$

which is also properly normalized. The equilibrium condition (3.15) implies $z < 2$ ($\mu > 2$). We see that $1/y^{z-1}$ is incompatible with the normalization request for $z > 2$. In fact, in this case the integrand is faster than $1/y$, thereby making the integral become equal to ∞.

Let us prepare the system in the flat distribution

$$p(y,0) = 1. \tag{3.16}$$

This distribution becomes the equilibrium distribution (3.15) as $t \to \infty$. The physical reason is evident. The closer to $y = 0$, the slower the particle's motion. Thus, there is a natural tendency for the distribution to become denser as $y \to 0$.

[1] In fact, $\mathcal{L}p_{eq}(y) = 0$.

Let us find the waiting time distribution for the re-injection event to occur and denote t_a as the beginning of the observation time. Starting the observation at $t_a = 0$ is equivalent to the concept yielding Eq. (3.4). Thus, we get

$$\psi_{t_a=0} = (\mu - 1)\frac{T^{\mu-1}}{(\tau + T)^{\mu}}. \tag{3.17}$$

The case where the observation and preparation times are not the same yields a different result. To illustrate this point, let us find the waiting time distribution for the infinitely aged condition case $t_a = \infty$. In this case we have for the infinitely aged condition waiting time distribution density:

$$\psi_{t_a=\infty}(\tau) = p_{eq}(y)\left|\frac{\mathrm{d}y}{\mathrm{d}\tau}\right|. \tag{3.18}$$

Using (3.1), (3.6), and (3.7), we get

$$\psi_{t_a=\infty}(\tau) = (\mu - 2)\frac{T^{\mu-2}}{(\tau + T)^{\mu-1}}. \tag{3.19}$$

The corresponding survival probabilities of (3.17) and (3.19) are:

$$\Psi_0(\tau) = \left(\frac{T}{\tau + T}\right)^{\mu-1}, \tag{3.20}$$

$$\Psi_\infty(\tau) = \left(\frac{T}{\tau + T}\right)^{\mu-2}, \tag{3.21}$$

thereby telling us that the relaxation of the system becomes slower and slower as time goes by. This phenomenon is called the *Aging Effect*. The older you get, the slower you become. A thorough discussion of this interesting effect will be presented in the later sections.

3.2. Modulation

It is known that a superposition of infinitely many exponentially decaying functions yields an inverse power-law distribution [42]. In this section we show how a power-law distribution

of the form (3.5) emerges from the superposition of exponentials through the process called *modulation*.

To illustrate modulation, let us consider the following multiplicative stochastic process of the relaxation times $T_r = 1/\lambda$:

$$\frac{\mathrm{d}T_r}{dt} = -\nu\left(T_r - T_0\right) + T_r\xi\left(t\right) \tag{3.22}$$

where $\xi(t)$ is taken to be a delta correlated Gaussian random process

$$\left\langle \xi\left(t\right)\xi\left(t'\right)\right\rangle = 2D\delta\left(t - t'\right) \tag{3.23}$$

and the rate ν keeps under control the modulation rate. The deterministic part of (3.22) gives a relaxation to the rate $1/T_0$ in a time $1/\nu$. The time dependent Poisson rates λ are uniquely derived from an exponential distribution

$$\psi_\lambda(\tau) = \lambda e^{-\lambda\tau}. \tag{3.24}$$

Modulation implies that given a suitable form of distribution $\Pi(\lambda)$ of the Poisson rates λ, the waiting time distribution $\psi(\tau)$

$$\psi\left(\tau\right) = \int_0^\infty d\lambda\Pi(\lambda)\psi_\lambda(\tau) \tag{3.25}$$

gets an inverse power law form (3.5).

The corresponding Fokker-Planck equation of (3.22) is written as

$$\frac{\partial}{\partial t}P(T_r,t) = \nu\frac{\partial}{\partial T_r}\Big[\left(T_r - T_0\right)P(T_r,t)\Big] + D\frac{\partial}{\partial T_r}\left[T_r\frac{\partial}{\partial T_r}\Big\{T_rP(T_r,t)\Big\}.\right] \tag{3.26}$$

The steady-state solution to (3.26) is given by the solution to

$$\frac{\partial P(T_r,t)}{\partial t} = 0, \tag{3.27}$$

which for the zero flux case yields

$$\frac{1}{T_r P(T_r)} \frac{\partial}{\partial T_r} \Big\{ T_r P(T_r) \Big\} = -\frac{(T_r - T_0)}{D T_r^2} \tag{3.28}$$

The solution to (3.28) is given by

$$P(T_r) = \frac{C_{norm}}{T_r^{\alpha+1}} e^{-\gamma/T_r} \tag{3.29}$$

where C_{norm} is the normalization constant and the parameter values are given by

$$\alpha = \frac{\nu}{D} \tag{3.30}$$

$$\gamma = \frac{\nu}{D} T_0 = \alpha T_0. \tag{3.31}$$

Normalizing the distribution (3.29) yields

$$P(T_r) = \frac{\gamma^\alpha}{\Gamma(\alpha)\, T_r^{\alpha+1}} e^{-\gamma/T_r}. \tag{3.32}$$

Since

$$\Pi(\lambda) \mathrm{d}\lambda \equiv P(T_r) \mathrm{d}T_r, \tag{3.33}$$

we get, using (3.24) and (3.25),

$$\begin{aligned} \psi(t) &= \frac{\gamma^\alpha}{\Gamma(\alpha)} \int_0^\infty dT_r \frac{e^{-\gamma/T_r} e^{-t/T_r}}{T_r^{\alpha+2}} = \frac{\Gamma(\alpha+1)}{\Gamma(\alpha)} \frac{\gamma^\alpha}{(\gamma+t)^{\alpha+1}} \\ &= \frac{\alpha \gamma^\alpha}{(\gamma+t)^{\alpha+1}}. \end{aligned} \tag{3.34}$$

Thus, with $\alpha = \mu - 1$ and $\gamma = T$, we obtain the inverse power-law distribution density (3.5) from the superposition of an infinite number of exponential functions with different rates.

Taking into account that

$$\Pi(\lambda) = \frac{P(1/\lambda)}{\lambda^2}, \tag{3.35}$$

we obtain the $\Pi-$distribution of order $\mu - 1$ proposed by Beck [43] and used in later work [44]:

$$\Pi(\lambda) = \frac{T^{\mu-1}}{\Gamma(\mu-1)}\lambda^{\mu-2}\exp(-\lambda T). \tag{3.36}$$

This is the statistical weight to adopt in Eq. (3.25) to get an inverse power law distribution of waiting times.

It is convenient to stress that the slow modulation condition is realized by setting ν very small. In this case, as we shall see, the theory here illustrated does not produce aging effects. In the opposite limit of very large ν the dynamical approach of this Section yields a renewal condition, but at that stage the process is Poissonian again. To realize a non-Poisson renewal condition, we must ensure that after drawing a given waiting time τ for the next drawing we shall use a different λ. This is an ideal condition, difficult if not impossible to realize dynamically. In the following section we introduce a statistical analysis that tells us if a process is renewal or not.

3.3. Aging Effects in Renewal and Modulation Theories

3.3.1. *The Aging Experiment Analysis*

A way to establish if a process is renewal or not is the so-called *Aging Experiment*. To understand the nature of this experiment we have to be aware that, in general, the distribution of waiting times depend on the time at which the observation begins. Let us consider a Gibbs ensemble of time sequences produced by the same complex process shown in Figure 3.1. For the case where we start the observation process at $t = 0$, corresponding to an event on each of the time sequences, the waiting time probability density of the occurrence

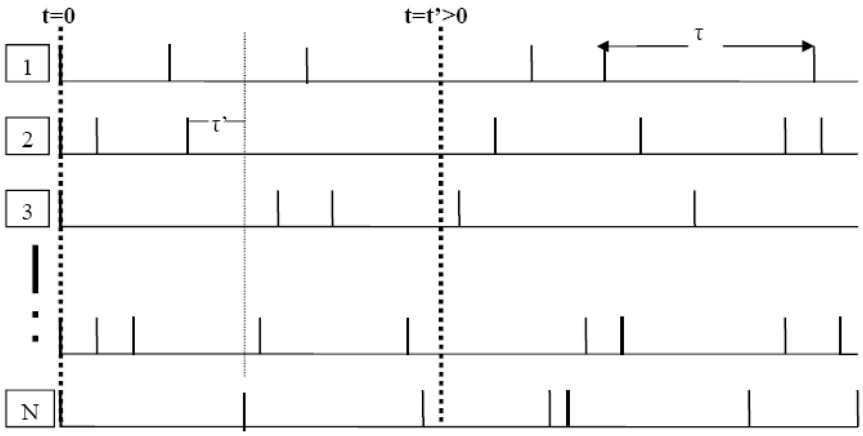

Figure 3.1: Gibbs ensemble of time sequences.

of an event on any of the time series is the same form as that of Eqn. (3.17):

$$\psi(\tau') = (\mu - 1)\frac{T^{\mu-1}}{(\tau' + T)^{\mu}}. \tag{3.37}$$

The observation process starting at $t' \neq t$ for a non-exponential process gives a form different than that of (3.37). Let us denote $\psi(t, t')$ as the waiting distribution density obtained by an observer at time t with the observation process beginning at $t' > 0$. If the process is renewal, that is, the occurrrence of an event has the effect of erasing the system's memory, we obtain

$$\psi(t, t') = \psi(t) + \sum_{n=1}^{\infty} \int_0^{t'} \mathrm{d}t'' \psi_n(t'')\psi(t - t''). \tag{3.38}$$

Let us discuss the meaning of this equation. The first term on the right hand side is the probability distribution if no event occurred before the observation time $t' > 0$. Thus, it is equivalent to (3.37) provided an event took place at time $t = 0$. The second term is added to take into account all the events that took place at an arbitrary time $t'' < t'$. Let us imagine that $n \geq 1$ events occurred and the last of which exactly at time $t'' < t$. The probability density of these events is given by $\psi_n(t'')$. The factor $\psi(t - t'')$ is the probability of event

occurrence after t'. This is so because the probability of having an event after t' depends on the last event occurring prior to t' which in this case took place at time t''.

If the process fits the prescription of ordinary statistical physics we expect that

$$\psi(t,t') = \psi(t-t') = \psi(\tau) \tag{3.39}$$

which indicates that the system does not age. In the next section we show that a process yielding Poisson distribution does not age.

Let us now proceed with the aging experiment analysis [45]. We generate a sequence of times $\{t_i\}$, which are recorded as vertical lines on the t-axis. Then we use a mobile window of size t_a, corresponding to the age that we want simulate. The beginning of the window is located on each of the times of the sequence $\{t_i\}$ and we measure the time distance between the end of the window and the first event time after it. These truncated time distances are used to build up a t_a-aged histogram, which is then used to defined the *aged* probability density distribution $\psi_{t_a}(\tau)$ and the corresponding survival probability

$$\Psi_{t_a}(\tau) = \int_{\tau}^{\infty} \psi_{t_a}(\tau')d\tau' = 1 - \int_{0}^{\tau} \psi_{t_a}(\tau')d\tau'. \tag{3.40}$$

Note that with this notation the exact prescription of Eq. (3.38) becomes

$$\psi_{t_a}(\tau) = \psi(\tau + t_a) + \sum_{n=1}^{\infty} \int_{0}^{t_a} dy \psi(y+\tau)\psi_n(t_a - y). \tag{3.41}$$

3.3.2. *Aging of an Exponential Renewal Process*

Let us consider Eqn. (3.1) for the case $z = 1$. Following the entire procedure in Section 3.1, we obtain the renewal exponential distribution of waiting times

$$\psi(\tau) = ae^{-a\tau}. \tag{3.42}$$

Let us now find the probability distribution $\psi_n(t)$. Following the prescription in Section 2.5 leading to Eqn. (2.90), we have the following properties in the Laplace domain:

$$\hat{\psi}_n(u) = \left[\hat{\psi}(u)\right]^n. \tag{3.43}$$

Therefore, inserting the Laplace transform of (3.42) to (3.43) yields, after anti-Laplace transformation, the Poisson distribution

$$\psi_n(t) = \frac{a(at)^{n-1}}{(n-1)!}e^{-at}. \tag{3.44}$$

To evaluate the aging property of a renewal exponential distribution, we use (3.38). Thus, we get

$$\begin{aligned}
\psi(t,t') &= \psi(t) + \sum_{n=1}^{\infty}\int_0^{t'} \mathrm{d}t''\psi_n(t'')\psi(t-t'') \\
&= ae^{-at} + a^2\sum_{n=1}^{\infty}\int_0^{t'} \mathrm{d}t''\frac{(at'')^{n-1}}{(n-1)!}e^{-at''} \\
&= ae^{-a(t-t')}.
\end{aligned} \tag{3.45}$$

This means that the exponential renewal process does not produce aging. The probability distribution of observing an event with the observation starts at $t = 0$ is the same probability distribution as if the observation was began at $t' > 0$. The next subsection shows that this is not the case for a process yielding a non-exponential distribution.

3.3.3. *Aging of a Non-exponential Renewal Process*

Let us consider the waiting time distribution (3.37)

$$\psi(\tau) = (\mu-1)\frac{T^{\mu-1}}{(\tau+T)^{\mu}}. \tag{3.46}$$

The Laplace transform of (3.46) is given by [48]:

$$\hat{\psi}(u) = \frac{(\mu-1)\Gamma(1-\mu)}{(uT)^{1-\mu}}\Big[e^{uT} - E^{uT}_{\mu-1}\Big] \tag{3.47}$$

where

$$E^{uT}_{\mu-1} \equiv \sum_{n=0}^{\infty} \frac{(uT)^{n+1-\mu}}{\Gamma(n+2-\mu)} \tag{3.48}$$

is the generalized exponential relaxation [46]. Taylor series expansion of (3.47) gives us the following asymptotic expressions in the limiting case $u \to 0$:

$$\hat{\psi}(u) = 1 - \Gamma(2-\mu)(uT)^{\mu-1} \qquad 1 < \mu < 2, \tag{3.49}$$

$$\hat{\psi}(u) = 1 - < \tau > u - \Gamma(2-\mu)(uT)^{\mu-1} \qquad 2 < \mu < 3, \tag{3.50}$$

where $< \tau >= T/(\mu-2)$ is the mean waiting time.

The corresponding probability that no event occurs up to time t, the survival probability, of (3.38) is

$$\Psi(t,t') = \int_t^{\infty} dt'' \psi(t'',t'). \tag{3.51}$$

Note that by taking the t'-derivative of (3.51) and using (3.38) we obtain

$$\frac{d}{dt'}\Psi(t,t') = P(t')\Psi(t-t'), \tag{3.52}$$

where

$$\mathcal{P}(t) = \sum_{n=0}^{\infty} \psi_n(t). \tag{3.53}$$

is the rate of events occurring at time t, under the condition that an event occurred at $t = 0$. Laplace-transforming Eqn. (3.53) gives

$$\hat{\mathcal{P}}(u) = \sum_{n=0}^{\infty} \hat{\psi}_n(u) = \sum_{n=0}^{\infty} (\hat{\psi}(u))^n = \frac{1}{1 - \hat{\psi}(u)}. \tag{3.54}$$

From Appendices B and C, we get the following results:

$$\mathcal{P}(t) = \frac{1}{<\tau>} + \frac{T^{\mu-2}}{(3-\mu)<\tau>} \frac{1}{t^{\mu-2}} \qquad 2 < \mu < 3, \tag{3.55}$$

$$\mathcal{P}(t) = \frac{1}{\Gamma(\mu-1)\Gamma(2-\mu)T^{\mu-1}} \frac{1}{t^{2-\mu}} \qquad 1 < \mu < 2. \tag{3.56}$$

In conclusion, the renewal aging, in the case $\mu < 2$ is characterized by the property that the rate of event occurrence, tends to decrease as a function of time.

3.3.4. *Modulation and Renewal Aging*

Let us assume that the system is prepared at time $t = -t_a < 0$. The first measured waiting time is denoted by τ_1. The first waiting time, distinct from the observation of the successive waiting times, does not necessarily correspond to the total time duration of a laminar region. The resulting histogram records time lengths that are generally smaller than those corresponding to preparing the system at time $t = 0$. Nevertheless, in the case when the waiting time distribution is exponential, both long and short time lengths are reduced by the same percent. Thus, turning the histogram into a normalized waiting-time distribution density has the effect of recovering the same exponential form. As shown in Section 3.3.2 renewal exponential process does not age. In the non-exponential case delaying the observation process has the effect of producing a percent cut of the short-time laminar regions larger than that of the long-time laminar regions. As a consequence, with the normalization of the distribution, the weight of the short-time laminar regions is reduced

and the weight of the long-time laminar regions is enhanced, thereby generating a slower decay of the survival probability $\Psi(t)$ as we previously see in Section 3.1.1.

The work of Allegrini *et al.* [47] compared the results of aging analysis on artificial waiting time sequences, leading to the same power-law distribution with the same power index μ, generated by the renewal and modulation prescriptions with different numbers of drawings N_d from the distribution (3.24) . The waiting times for the modulation process are extracted based on the numerically-generated $\Pi(\lambda)$ distribution (3.36). After N_d drawings, they selected from $\Pi(\lambda)$ a new rate λ. It is evident that if $N_d = 1$, and only one waiting time is drawn from the Poisson distribution with a given λ and immediately afterward a different λ is selected from the distribution density $\Pi(\lambda)$, the resulting sequence is renewal. Increasing N_d has the effect of realizing the prescriptions of superstatistics [16], which requires a long-time sojourn in a given Poisson condition, for the system to adapt to the local thermodynamic condition.

The results of this aging experiment are illustrated in Fig. 3.2. We see that when we draw only a waiting time τ and then we use a different $\psi_\lambda(\tau) \equiv \lambda exp(-\lambda\tau)$ for the drawing of the next waiting time, the process is totally renewal. If we increase the number of waiting times drawn from the same $\psi_\lambda(\tau)$, the intensity of aging is reduced till the condition of a total lack of aging is reached when the number of waiting times drawn from the same waiting time distribution becomes very large.

The aging experiment can be used to establish if a real sequence is renewal or not. The earlier described aging experiment is applied to a real sequence so as to determine the aged histogram and through it the corresponding survival probability, called $\Psi_{t_a}^{(exp)}(\tau)$. We have to establish also a criterion to determine the form of the survival probability produced by the renewal condition. This is not quite straightforward to do, due to the fact that the exact form of Eq. (3.38) is not a simple functional of $\psi(\tau)$. A simple functional is given by Eq. (3.59) that makes it possible to get $\psi_{t_a}(\tau)$ from $\psi(\tau)$ by means of a simple expression, and thus to derive from the form that the renewal theory assigns to the aged survival probability, denoted

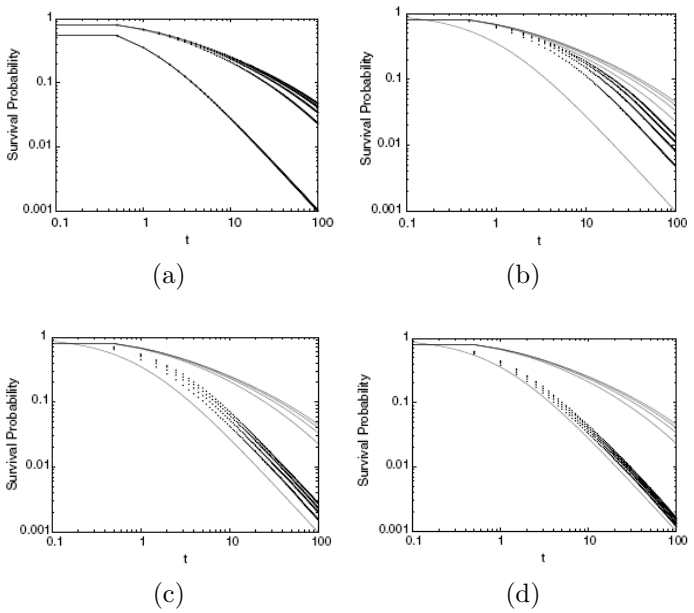

Figure 3.2: Comparison between the function $\Psi_{t_a}(t)$ of a renewal process (continuous lines) and the function $\Psi_{t_a}(t)$ produced by a modulation approach with a changing value of N_d (dotted lines). The curves from bottom to top refer to the ages $t_a = 0, 50, 100, 150, 200$. $(a) N_d = 0; (b) N_d = 10; (c) N_d = 100; (d) N_d = 500$. Taken from Ref. [47].

by $\Psi_{t_a}(t)$. If these two procedures applied to the same sequence generate the condition

$$\Psi_{t_a}^{(exp)}(t) = \Psi_{t_a}^{(ren)}(t), \tag{3.57}$$

we consider the process to be renewal. Note that a virtually exact criterion is obtained by shuffling the time distances between two consecutive events to produce a more reliable $\Psi_{t_a}^{(ren)}(t)$.

3.3.5. *Aging and Rejuvenation*

To discuss the interesting effect of a time dependent μ and of rejuvenation, let us adopt a simplified formula rather than the exact formula Eq. (3.41).

As in the earlier subsection we set the condition that the system is prepared at $t_a < 0$ and that observation begins at $t = 0$. The exact expression for $\psi_{t_a}(t)$ (3.41) can be written

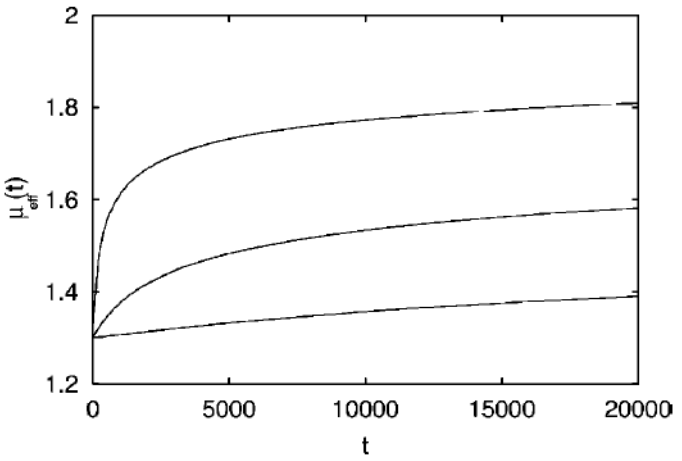

Figure 3.3: The effective power index μ_{eff} of Eq. (3.63) as a function of time. The curves refer, from top to bottom, to $t_a = 100, 1000, 10000$. Taken from Ref. [49]

in the form

$$\psi_{t_a}(t) = \int_0^{t_a} dy P(y)\psi(y+t), \tag{3.58}$$

where $P(y)$ is defined by Eq. (3.53). We have seen that for $\mu < 2$, this quantity is not constant and it decreases as $1/t^{2-\mu}$ (see Eq. (B-7)). Under the simplifying assumption that $P(y)$ is constant, we get [49]:

$$\psi_{t_a}(t) = \frac{\int_0^{t_a} \psi(t+y)dy}{K(t_a)}, \tag{3.59}$$

where $K(t_a)$ is the normalization factor defined by

$$K(t_a) \equiv \int_0^{t_a} \Psi(t')dt', \tag{3.60}$$

and $\Psi(t)$ is the probability that no event occurs throughout the time interval of length t. We then introduce the aged survival probability by means of Eq. (3.40). This expression can be used for the comparison of Eq. (3.38), even if it is not exact, insofar as it is expected to be reliable in both the short and the long-time limit.

Using for $\psi(t)$ the explicit form (3.46), it is straight forward to show that (3.59) reduces to

$$\psi_{t_a}(t) = (\mu - 2)\frac{(t+T)^{(1-\mu)} - (t+T+t_a)^{(1-\mu)}}{T^{(2-\mu)} - (t_a+T)^{(2-\mu)}}. \tag{3.61}$$

This formula establishes that for $t << t_a$ the index of the distribution is $\mu - 1$, whereas for $t >> t_a$ the index becomes μ. This result for the age-dependent waiting time distribution function agrees with the predictions by Barkai [50] and by the authors of [51]. Notice that the formula (3.61) is equivalent to drawing the initial condition for y from an aged distribution of this variable.

Here, we are in a position to evaluate the waiting time index at a generic time, where, we write $\psi_{ta}(t)$, as

$$\psi_{ta}(t) = \frac{A(T, t_a)}{(t+T)^{\mu_{eff}(t)}}. \tag{3.62}$$

Using (3.61) we arrive at the following formula for the time dependence of the effective power-law index

$$\mu_{eff}(t) = -\frac{ln[(t+T)^{(1-\mu)} - (t+T+t_a)^{(1-\mu)}]}{ln[t+T]}. \tag{3.63}$$

Fig. 3.3 illustrates the regression of the effective power-law index to μ with two different ages, and shows clearly that the regression is slower for older systems.

CHAPTER 4

SUBORDINATION THEORY

4.1. Single Subordination

Let us imagine a fair coin tossing process occurring at every discrete time $t(n)$ where getting a head corresponds to assigning the value 1 and tail the value -1 to the variable ξ so as to generate the fluctuation shown in Figure 4.1. We refer to the head and tail as states $|1>$ and $|2>$ respectively. Let us adopt a Gibbs representation of the fluctuation of $\xi(t)$ and consider that at every time step n we count the number of systems located in each of the two states. We assign N_1 and N_2 as the number of states in state $|1>$ and $|2>$ respectively. For $N = N_1 + N_2$ very large, we can assume the ratio $p_1 = N_1/N$ as the probability of finding the system in the state $|1>$ and $p_2 = N_2/N$ as the probability of finding the system in state $|2>$. Thus, in a discrete time representation we get time evolution of the probabilities:

$$\mathbf{p}(n+1) - \mathbf{p}(n) = \mathbf{M}\mathbf{p}(n), \tag{4.1}$$

where

$$\mathbf{p} \equiv (p_1, p_2) \tag{4.2}$$

and

$$\mathbf{M} \equiv \frac{1}{2}\begin{bmatrix} -1 & 1 \\ 1 & -1 \end{bmatrix}. \tag{4.3}$$

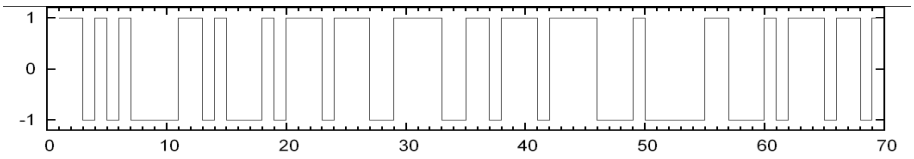

Figure 4.1: Fluctuation generated by the coin-tossing procedure where getting a head corresponds to assigning the value 1 and tail the value -1.

Let us consider the case where the coin tossing event, instead of occurring at every time step, only takes place in a specific time interval

$$\tau_n = t(n+1) - t(n) \tag{4.4}$$

derived from a given distribution density $\psi^{(S)}(\tau)$ to which we refer as the *subordination function*. In this case, following the CTRW prescription, Eq. (4.1) becomes

$$\mathbf{p}(t) = \sum_{n=0}^{\infty} \int_0^t dt' \psi_n^{(S)}(t') \Psi^{(S)}(t-t') \mathbf{K}^n \mathbf{p}(0), \tag{4.5}$$

where we denote

$$\mathbf{K} \equiv 1 + \mathbf{M}. \tag{4.6}$$

Here, $\psi_n^{(S)}(t')$ is the probability of drawing from the waiting time distribution $\psi^{(S)}(\tau)$ n times where the last coin tossing event occurs exactly at time t'. This generates the vector $\mathbf{K}^n\mathbf{p}(0)$ whose form remains unchanged up to time t provided that in between the times t' and t no further drawing occurs . This last condition is ensured by the survival probability $\Psi^{(S)}(t-t')$. In fact

$$\Psi^{(S)}(t) \equiv \int_t^{\infty} dt' \psi^{(S)}(t') \tag{4.7}$$

is the probability that no event occurs up to time t. By Laplace transforming Eq. (4.5) we obtain

$$\hat{\mathbf{p}}(u) = \frac{1}{u - \frac{u\hat{\psi}^{(S)}(u)}{1-\hat{\psi}^{(S)}(u)}(\mathbf{K}-1)}\mathbf{p}(0). \tag{4.8}$$

It is easy to show that the Generalized Master Equation (GME) pertaining to (4.5) is

$$\frac{d}{dt}\mathbf{p} = \int_0^t dt' \Phi(t-t')\mathbf{M}\mathbf{p}(t'), \tag{4.9}$$

where the memory kernel, $\Phi(t)$, is related to the subordination function $\psi^{(S)}(t)$ in the Laplace domain by

$$\hat{\Phi}(u) = \frac{u\hat{\psi}^{(S)}(u)}{1-\hat{\psi}^{(S)}(u)}. \tag{4.10}$$

The Laplace transform of this GME coincides with Eq. (4.8), thereby establishing that Eq. (4.9) coincides with Eq. (4.5).

4.1.1. *Relaxation to Equilibrium*

The coin tossing process can be regarded as a two-state system that at every time step, with equal probability, either stays in the current state or jumps to the other state. Let us define the non-equilibrium indicator:

$$\Pi(n) = p_1(n) - p_2(n). \tag{4.11}$$

The adoption of the Gibbs ensemble perspective of the coin tossing process makes the relaxation of $\Pi(n)$ move from an out-of-equilibrium condition $\Pi(n) \neq 0$ to the equilibrium value $\Pi(n+1) = 0$ in one time step. Following Eq. (4.9), let us define the relaxation to equilibrium of the variable $\Pi(t)$. In fact, after straightforward algebra, Eq. (4.9) is shown to yield

$$\frac{d}{dt}\Pi(t) = \int_0^t dt' \Phi(t-t')\Pi(t'), \tag{4.12}$$

whose Laplace transform is

$$\hat{\Pi}(u) = \frac{1 - \hat{\psi}^{(S)}(u)}{u}\Pi(0), \tag{4.13}$$

thereby implying

$$\frac{\Pi(t)}{\Pi(0)} = \Psi^{(S)}(t). \tag{4.14}$$

This is an expected result, insofar as the probability that the quantity $\Pi(t)$ does not vanish is evidently equal to the probability that no event occurs up to time t.

We can also reverse this result. Any relaxation process described by the survival probability $\Psi^{(S)}(t)$ can be thought of as being subordinated to the coin tossing process described by the matrix $\mathbf{M}$ of Eq. (4.3) by means of the subordination function

$$\psi^{(S)}(t) = -\frac{d}{dt}\Psi^{(S)}(t). \tag{4.15}$$

Note that a significant restriction to the possibility of relating a generic relaxation to a subordination function is given by the fact that the subordination function is the distribution of waiting times between two consecutive events. Thus, it is always positive and the corresponding survival probability must correspond to a monotonic relaxation. A relaxation process given by damped oscillations cannot have a renewal origin.

4.2. Exponential and Non-exponential Subordination

Let us consider the action of the demon sketched in Figure 4.2. The demon has a box of very large number of black and white particles where the ratio of the black particles to the total number of particles is given by

$$g = \frac{N_B}{(N_B + N_W)} \ll 1, \tag{4.16}$$

where N_B and N_W denote the number of black and white particles contained in the box, respectively. Let us imagine that the coin-tossing event only happens when the demon draws

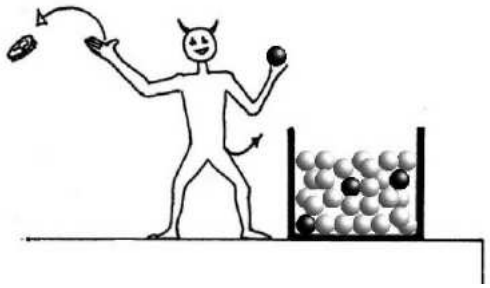

Figure 4.2: The demon randomly draws a ball from the box. The drawing of a black ball corresponds to an event occurrence.

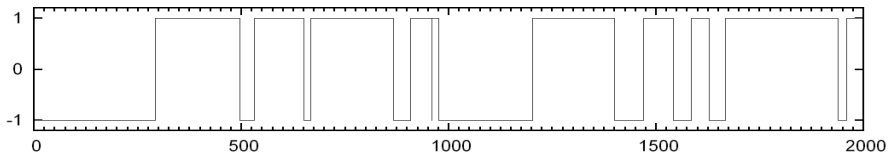

Figure 4.3: Fluctuation produced by the Demon where coin-tossing is realized only when a black ball is drawn.

a black ball. The probability that no events occur up to time $t \to \infty$ is given by

$$\Psi(t) = (1-g)^t = exp(-gt). \tag{4.17}$$

The renewal nature of the ball drawing process allows us to use Eq. (4.15), thus we get the exponential subordination function

$$\psi^{(S)}(t) = gexp(-gt). \tag{4.18}$$

Using (4.18), Eq. (4.9) yields

$$\hat{\Phi}(u) = g, \tag{4.19}$$

which corresponds to

$$\Phi(t) = g\delta(t). \tag{4.20}$$

Thus the GME Eq. (4.9) becomes identical to the ordinary master equation

$$\frac{d}{dt}\mathbf{p} = g\mathbf{M}\mathbf{p}(t). \tag{4.21}$$

The stochastic trajectory, of which this master equation is the Gibbs representation is illustrated in Fig. 4.1.

In conclusion, subordination to the coin tossing process, which can be interpreted as a lazy demon that tosses coin only according to the time prescribed by the subordination function $\psi^{(S)}(\tau)$, is equivalent to the hardworking demon who draws ball at every time but has a very small success rate ($g \ll 1$) of getting a black ball.

Let us assume that the Demon's box is affected by a leak that makes the number of black balls decrease as a function of time making the rate time dependent with the following form:

$$g(t) = \frac{g_0}{1 + g_1 t}. \tag{4.22}$$

In this case, (4.17) becomes

$$\Psi^{(S)}(t) = \prod_{t'=1}^{t} (1 - g(t')) \tag{4.23}$$

which in the time continuum limit becomes

$$\Psi^{(S)}(t) = exp(-\int_0^t dt' g(t')). \tag{4.24}$$

Inserting Eq. (4.22) into (4.24) gives

$$\Psi^{(S)}(t) = \left[\frac{T_S}{T_S + t}\right]^{\mu_S - 1}, \tag{4.25}$$

with

$$T_S = \frac{1}{g_1} \tag{4.26}$$

and

$$\mu_S - 1 = \frac{g_0}{g_1}. \tag{4.27}$$

Using (4.15), we obtain the corresponding properly normalized subordination function:

$$\psi^{(S)}(t) = (\mu_S - 1)\frac{T_S^{\mu_S - 1}}{(t + T_S)^{\mu_S}}, \tag{4.28}$$

The inverse power-law form Eq. (4.28) is a simple way of connecting the short time properties, where the inverse power law form does not yet appear, to the long-time limit $t >> T_S$, where the inverse power law form becomes evident. The parameter T_S keeps under control the time extent through which the transition from microscopic dynamics, with no power law, to macroscopic dynamics with inverse power-law, occurs. As we shall see, the non-renewal aging is related to this parameter becoming larger and larger as an effect of aging. It is important to remark, however, that this regime of transition to the long-time regime bearing signs of complexity under the form of the power law index μ_S, does not afford by itself any information on the system's complexity. For simplicity's sake, it is convenient to assume this transition regime to be as short as possible. Thus, it is convenient to assign to T the shortest possible value, $T = 1$, if we set for the elementary time step the condition $\Delta t = 1$. We shall see, however, that when the non-exponential waiting time $\psi^{(S)}(t)$ is used as the subordination function, a new intermediate time regime appears, and this time regime contains information on the system's complexity.

The adoption of Eq. (4.15) is made possible only when the renewal condition applies [52]. This is an important property that requires some comments. Let us examine two distinct conditions:

(a) The leaking of the black balls makes the Demon upset that every time he draws a black ball, he replaces the box with a new one having the same property as the original box (see Fig. 4.4). This is a Homogeneous Non-Poisson Process and the replacement of the box makes it renewal.

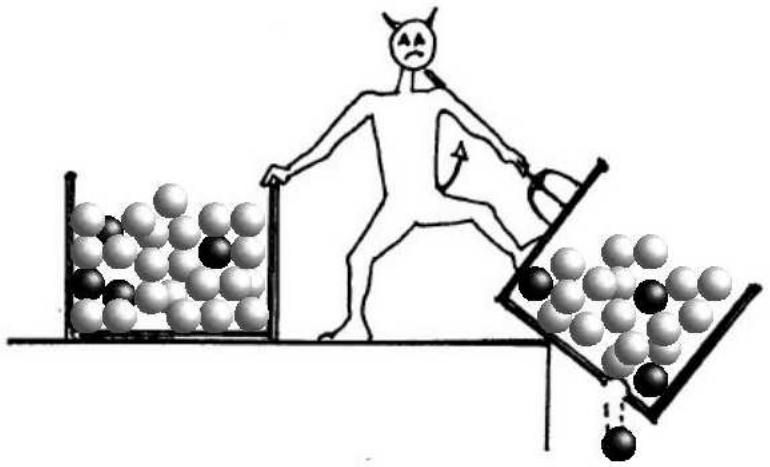

Figure 4.4: The demon randomly draws a ball from the box. The drawing of a black ball corresponds to an event occurrence.

(b) The demon keeps using the same box. In the case where the time dependence of $g(t)$ (4.22) is slow enough, this process is virtually equivalent to the slow modulation method discussed in Chapter 3 which therefore tells us that the process is not renewal, preventing us to use the prescription (4.15). This is a Non-Homogeneous Poisson (NHP) process.

It is important to notice that, according to the perspective emerging from the work of Barabasi [53] and Vazques *et al.* [54], on e-mail users, as well as on the Einstein and Darwin correspondence, the inverse power law of the waiting time distribution is an ineluctable consequence of the social nature of human activities. Thus, it is perhaps more convenient to interpret the inverse power law distribution density $\psi(\tau)$ Eq. (4.28) as a consequence of the Demon's social life.

Let us focus now on the renewal case. It is possible to demonstrate that the subordination function $g^{(S)}(t)$, of whatever analytical form, can be realized with the Demon model (a). In fact, for a given $\psi^{(S)}(t)$ we use Eq. (4.15) to derive the survival probability $\Psi^{(S)}(t)$. Then,

using Eq. (4.24) we obtain

$$g^s(t) = \frac{\psi^{(S)}(t)}{\Psi^{(S)}(t)}, \tag{4.29}$$

which is an important relation of Renewal Theory [52], which allows us to establish the time dependence of the number of black balls to realize a subordination function of any form.

Note that to take into account the renewal character of case (a), it is convenient to write the time dependent rate of event production $g(t)$ in the time region between the event occurring at time t_i and the next event, occurring at time $t_{i+1} > t_i$, in the form

$$g(t) = \frac{g_0}{1 + g_1 \Delta t}, \tag{4.30}$$

where

$$\Delta t = t_{i+1} - t_i. \tag{4.31}$$

The introduction of the *stochastic* time Δt is made necessary to generate a calculational algorithm that is a faithful representation of the case where the upset Demon throws away a box and replacing it with a new one when he eventually, after many drawings, finally gets a black ball. Note that the upset Demon throwing away a box is an intuitive representation of critical events. Unfortunately, the critical events are not so plainly evident, and special methods must be adopted to reveal their occurrence.

4.3. Renewal versus Non-renewal Aging

The cases (a) and (b) of the earlier subsection makes it convenient for us to go back to the aging issue of Chapter 3 to shed further light on the difference between *renewal* and *non-renewal* aging. The non-renewal aging is easier to understand. Therefore, let us begin discussing this case. Note that the subordination process is operated with the subordination function $\psi^S(t)$, which corresponds to a renewal process. We do not produce subordination by means of a non-renewal process. Therefore, let us discuss this case omitting the superscript S. Let us imagine that at a given time t', regardless of whether an event occurs or not, the

Demon focuses his attention only on the systems in the state $|1>$, and he evaluates the corresponding survival probability:

$$\Psi(t,t') = exp(-\int_{t'}^{t} dt'' g(t'')). \tag{4.32}$$

In fact, this is the same condition as that examined by means of Eq. (4.24). The survival probability $\Psi(t) = 1$ at $t = t'$ as a consequence of the fact that at the moment when observation begins, the Demon focuses his attention only on the systems in the state $|1>$. This is a way generating out of equilibrium conditions, without perturbing system's dynamics [51]. In the special case when at $t = t'$ an event occurs, equilibrium would be realized. However, if this is also the beginning of the observation process, the Demon creates an out of equilibrium condition that is not associated however to the replacement of the old box with a new one. This Demon keeps drawing balls from the same box. After some straightforward algebra in this case we get

$$\Psi(t,t') = \left[\frac{T_S}{T_S+t}\right]^{\mu_S-1}\left[\frac{T_S+t'}{T_S}\right]^{\mu_S-1} = \left[\frac{T_S+t'}{T_S+(t-t')+t'}\right]^{\mu_S-1}. \tag{4.33}$$

We see that this kind of aging, non renewal, corresponds to the parameter T_S becoming larger and larger as a consequence of the increasing time. If the out of equilibrium condition corresponding to observation beginning is realized at time $t' > 0$, while the ball box is brand new at time $t = 0$, T_S is replaced by $T_S + t'$. In conclusion, the non-renewal aging yields a survival probability characterized by the property that the emergence of the inverse power law behavior occurs at larger and larger times with increasing t', the age of the system.

Case (a) is characterized by different properties. First of all the survival probability, this time, depends on whether or not the beginning of observation process coincides with an event occurrence. Let us denote by $\Psi(t|t_i)$ the survival probability referred to the initial time t_i, under the condition that the beginning of observation process corresponds to an event occurrence. We have

$$\Psi^{(S)}(t|t_i) = \Psi^{(S)}(t-t_i). \tag{4.34}$$

This result is easily obtained by plugging Eq. (4.30) into Eq. (4.32). Thus, we see that a first big difference between renewal and non-renewal case is that the non-renewal aging is independent of whether the observation beginning coincides or not with the event occurrence. In the renewal case we have

$$\Psi^{(S)}(t|t') \neq \Psi^{(S)}(t,t'). \tag{4.35}$$

Let us now address the problem of evaluating $\Psi^{(S)}(t,t')$ in the case of renewal aging. This problem has been discussed in depth in the recent literature [51]. From a formal point of view, the waiting time distribution density of age t' is given by (see also Eq. (3.38))

$$\psi^{(S)}(t,t') = \psi^{(S)}(t) + \sum_{n=1}^{\infty} \int_0^{t'} \psi_n^{(S)}(t'')\psi^{(S)}(t-t'')dt''. \tag{4.36}$$

We refer the reader to Section 3.3.1 for the physical meaning of this exact expression.

4.4. Double Subordination

Let us now address the problem of creating a process subordinated to the fluctuations $\xi_S(t)$ illustrated in Fig. 4.3. In the long-time limit, the survival probability $\Psi(t) = exp(-gt)$ is indistinguishable from the coin-tossing survival probability itself. Thus, to create a process departing from the conditions of ordinary statistical mechanics, we adopt for the second subordination process the subordination function given by Eq. (4.28).

To shed light on the nature of this resulting process, we can evaluate analytically the resulting survival probability $\Psi_{SP}(t)$ by means of the following formula

$$\Psi_{SP}(t) = \sum_{n=0}^{\infty} \int_0^t dt' \psi_n^{(S)}(t')\Psi^{(S)}(t-t')exp(-gn). \tag{4.37}$$

This formula rests on the same arguments as those leading to Eq. (4.5), with a different physical meaning, though. We are using the very small rate condition Eq. (4.16). Thus, we imagine that the original Poisson process rests on the unit time step $\Delta t = 1$, and we assume

that it refers to a natural time scale, where time is the discrete number $n = 1, 2, ...$ The exponential survival probability of Eq. (4.17) now reads

$$\Psi(n) = exp(-gn). \tag{4.38}$$

Let us consider now the generic time t. How many times did the Demon of Fig. 4.2 draw balls from his box filled mainly with white balls? He may have done no drawing, one drawing, two drawings, and so on. When he draws a black ball, he tosses a fair coin, and consequently, he realizes equilibrium. The survival probability becomes smaller and smaller with increased number of drawings. This explains the exponential weight $exp(-gn)$ on the right-hand side of Eq. (4.37). As in the case of Eq.(4.5), the probability that the last of a sequence of n drawings occurs at time t' is given by $\psi_n^{(S)}(t')$, and the probability that no drawing occurs after this last drawing up to time t is given by $\Psi^{(S)}(t - t')$.

Using the same Laplace transform method as that adopted to derive Eq. (4.8) we now obtain

$$\hat{\Psi}_{SP}(u) = \frac{1}{u + \frac{u\hat{\psi}^{(S)}(u)}{1-\hat{\psi}^{(S)}(u)}\,(1 - exp(-g))}. \tag{4.39}$$

Note that in accordance with the condition of Eq.(4.16) we may expand the exponential and write Eq. (4.39) as

$$\hat{\Psi}_{SP}(u) = \frac{1}{u + \frac{u\hat{\psi}^{(S)}(u)}{1-\hat{\psi}^{(S)}(u)}g}. \tag{4.40}$$

At this point we have to stress the difference between the power indices $\mu_S > 2$ and $\mu_S < 2$. As mentioned earlier we are using the subordination function Eq. (4.28). The mean waiting time is therefore given by

$$< \tau >= \frac{T_S}{\mu_S - 2}. \tag{4.41}$$

which diverges at $\mu_S = 2$ and remains divergent in the whole range from $\mu_S = 2$ to $\mu_S = 1$. When $\mu_S > 2$, the mean waiting time is finite and we have for $u \to 0$

$$\hat{\psi}^{(S)}(u) = (1 - < \tau > u). \tag{4.42}$$

Thus Eq. (4.40) becomes

$$\hat{\Psi}_{SP}(u) = \frac{1}{u + \frac{g}{<\tau>}}. \tag{4.43}$$

whose inverse Laplace transform yields an exponential survival probability again. In the latter the exponential lifetime $1/g$ is turned into $< \tau > /g$, which becomes much larger than the original lifetime in the vicinity of the border with the non-ergodic region, $\mu_S = 2$. In other words, a second subordination process, resting on an exponential subordination function is equivalent to a trivial time dilatation.

The non-ergodic condition $\mu_S < 2$ is much more interesting than the $\mu_S > 2$ situation. In this case, the Laplace transform of $\psi^{(S)}(t)$ is given by Eq. (3.49). Thus, using Eq. (4.39), we obtain, for $u \to 0$

$$\hat{\Psi}_{SP}(u) \to e^g \hat{E}_\alpha(u), \tag{4.44}$$

where

$$\hat{E}_\alpha(u) = \frac{1}{u + \lambda^\alpha u^{1-\alpha}}, \tag{4.45}$$

with

$$\alpha \equiv \mu_S - 1 \tag{4.46}$$

and

$$\lambda = \left(\frac{e^g - 1}{\Gamma(2 - \mu_S)(T_S)^\alpha} \right)^{1/\alpha}. \tag{4.47}$$

Thanks to the relation of Eq. (4.46), when $\mu_S = 2$, and thus $\alpha = 1$, Eq. (4.45) becomes the Laplace transform of an exponential. This is expected, since $\mu_S = 2$ is the border with the region where, as earlier shown, the mean waiting time $< \tau >$ is finite, and consequently the non-exponential subordination is not efficient enough as to establish a significant departure from the mere time dilatation produced by a second subordination resting on an exponential subordination function.

We note that Eq. (4.45) is the celebrated Mittag-Leffler proposal for the generalization of exponential relaxation [46]. According to the Mittag-Leffler theory, the stretched exponential

$$E_\alpha(t) = exp(-(\lambda t)^\alpha) \tag{4.48}$$

occurs for $t < 1/\lambda$, and the inverse power-law

$$E_\alpha(t) \propto \frac{1}{t^\alpha} \tag{4.49}$$

occurs for $t > 1/\lambda$. We see that decreasing g has the effect of making more and more extended the region where the stretched exponential relaxation of Eq. (6.17) applies. If we increase the parameter g we can significantly reduce the time over which stretched exponential dominates even making it completely disappear. Although the double subordination method that we have used rests on the condition $g \ll 1$ making it impossible to get rid of the stretched exponential regime, we notice that by increasing g we come close to the condition corresponding the direct application of subordination procedure to the coin-tossing process, yielding

$$\Psi_{SP}(t) = \Psi^{(S)}(t), \tag{4.50}$$

thereby making the resulting survival probability identical to the subordination survival probability (4.25). In conclusion, the direct subordination to the coin-tossing process does not create any significant intermediate complexity. The transition regime does not afford

any information on the network complexity. The subordination to a sufficiently slow Poisson process, or sufficiently slow fluctuation-dissipation process, as we shall see in Section 4.6, has, on the contrary, the significant effect of creating an extended intermediate regime with important information on the network's complexity. If there exists an extended regime of transition to the inverse power law behavior of the survival probability, which significantly departs from the stretched exponential behavior, this may be an indication that the subordination function $\psi^{(S)}(\tau)$ of Eq.(4.28) has a very large T_S, or, more in general, it is characterized by its own slow regime of transition to the inverse power law regime. In this case we do not get a reliable information on the complexity parameter μ_S, characterizing the Demon's social life. If, on the contrary, this extended regime of transition to the inverse power law behavior is distinctly a stretched exponential with the stretching coefficient $\alpha < 1$, then $\mu_S = 1 + \alpha$ may afford reliable information on Demon's social life. Note that the time series emerging from complex processes are usually of finite time duration. Consequently, if the stretched exponential regime is very extended in time, it may be the only form of complexity experimentally accessible. In the opposite condition when the stretched exponential regime is significantly reduced by the adoption of large values of g, the inverse power law part of the survival probability may become the only one experimentally observable if the finite-seize induced truncation of the waiting time distribution density is not drastic .

As a final remark, we want to support our claim that $\mu_S > 2$ does not make the subordination process to produce visible effects of departure from ordinary statistical physics, with an example afforded by Metzler and Klafter [55]. Let us imagine that there are no truncation effects and that we can explore time asymptotic regime, where the inverse power law behavior distinctly appears. The quantity

$$v_t = \xi_S(t) - \xi_S(t-1) \tag{4.51}$$

is almost everywhere vanishing, and becomes finite only in the correspondence of an event occurrence. It is equivalent to the fluctuations responsible for the sub-diffusion process

studied by Metzler and Klafter [55]. The model of sub-diffusion proposed by these authors yields for $t \to \infty$

$$\left\langle x^2(t) \right\rangle \propto t^{\beta}, \tag{4.52}$$

where

$$\beta \equiv \frac{\alpha}{2} = \frac{\mu_S - 1}{2}. \tag{4.53}$$

We shall come back to discussing the scaling β as a complexity indicator in Section 4.6. Here we limit ourselves to noticing that for $\mu_S > 2$, the diffusion regime is characterized by the ordinary scaling $\beta = \frac{1}{2}$, which is a clear manifestation of the fact that for $\mu_S > 2$ the Demon's social life does not produce ostensible deviations from ordinary statistical physics.

4.5. Alternative Physical Interpretation of the Double Subordination

Probably a more attractive interpretation of the results of the earlier subsection is obtained by going back to the Demon of Figure 4.2. This Demon takes action at every time step of the natural time scale. However not all his actions produce events insofar as not all his actions correspond to the drawing of a black ball. We do not make the assumption that $g \ll 1$ instead we make the weaker assumption

$$g \leq 1. \tag{4.54}$$

Repeating the same calculations as those of the earlier subsection we obtain

$$\hat{\Psi}_{SP}(u) = \frac{1}{u + g\hat{\Phi}(u)}, \tag{4.55}$$

where $\Phi(u)$ is given by Eq. (4.10). Setting $g = 1$, we immediately recover Eq. (4.50), thereby establishing that when each of the Demon's actions generate an event, then the survival probability $\Psi_{SP}(t)$ coincides with $\Psi^{(S)}(t)$, and consequently with the inverse power law of Eq. (4.25).

When $g < 1$, we obtain

$$\hat{\Psi}_{SP}(u) = A_g \hat{E}_\alpha(u), \tag{4.56}$$

with

$$\hat{E}_\alpha(u) = \frac{1}{u + \lambda_\alpha(g) u^{1-\alpha}}, \tag{4.57}$$

$$\lambda_\alpha \equiv \left[\frac{g}{(1-g)} \frac{1}{T^\alpha \Gamma(1-\alpha)} \right]^{1/\alpha} \tag{4.58}$$

and

$$A_g \equiv \frac{1}{(1-g)}. \tag{4.59}$$

Note that the overall factor A_g is an artifact of the approximation done when we moved from the discrete to the continuous time picture. In fact the survival probability up to the occurrence of the first event is $1 - g$, which would cancel with the denominator of A_g. A more satisfactory way of expressing the result of this section is given by

$$\Psi_{SP}(t) = E_\alpha \left(-(\lambda_\alpha(g) t)^\alpha \right), \tag{4.60}$$

where the survival probability is given by a Mittag-Leffler function. This is equivalent to neglecting the regime of transition from the microscopic, discrete-time regime, to the Mittag-Leffler regime. We have to keep in mind that the stretched exponential, $exp(-(\lambda t)^\alpha)$, although fitting the condition $\Psi_{SP}(0) = 1$ corresponds to a time asymptotic rather than microscopic time regime.

We have virtually recovered the same result as that of the earlier section. This shows that the emergence of a stretched exponential can be interpreted in two different but equivalent ways. The former is based on the concept of double subordination. The first subordination process is based on the adoption of an exponential subordination function, which, as shown

in Section 4.2, is equivalent to the Demon acting with no rest but with a very limited success rate. The second subordination process is determined by the Demon's social life and is characterized by $\mu_S < 2$. Thus, it is evident that this process of double subordination can be interpreted as a single subordination applied to a Demon with a very limited success rate. In fact, as shown here, this second procedure yields essentially the same result as the application of the earlier.

We have to stress the big difference with the Demon of Fig. 4.2. As we have earlier seen, in that case decreasing g has the effect of producing a trivial time dilatation. Here decreasing g does more than producing time dilatation, insofar as it changes the balance between the time extension of the stretched exponential regime and that of the inverse power law regime. As a consequence, a mere time re-scaling is not enough to connect processes with lower values of g to processes with higher values of this parameter.

4.6. Subordination to an Ordinary Fluctuation-dissipation Process

Let us now address the problem of generalizing the double subordination of the earlier subsection. We have seen that the double subordination is equivalent to creating a process subordinated to a dichotomous Poisson process with rate g. Here we consider the case where the leading process, in the natural time scale n, is given by the ordinary Langevin equation

$$\frac{d}{dn}y = -\gamma y(n) + f(n), \tag{4.61}$$

where $f(n)$ is a noise of intensity

$$< f^2 >_{eq} = \frac{D}{\tau_c}, \tag{4.62}$$

wtih the equation subscript referring to the equilibrium thermal bath. According to the Einstein fluctuation-dissipation relation, the mean square value of y is given by

$$< y^2 >_{eq} = \frac{D}{\gamma}. \tag{4.63}$$

We again assume for the elementary time step the condition $\Delta t = 1$, and we assume the noise $f(n)$ to have the correlation time $\tau_c = 1$. This is a noise with no correlation, and the diffusion coefficient D becomes identical to the noise intensity.

We note that in this case, the time scale is given by $1/\gamma$, thereby playing the role $1/g$. As in the case of the process subordinated to dichotomous Poisson fluctuations, the condition

$$\gamma << 1 \tag{4.64}$$

makes the time n of the order of $1/\gamma$ virtually continuous.

Applying the same approach as that used to derive Eq. (4.9) from Eq. (4.5), we obtain [80]

$$\frac{\partial}{\partial t}p(y,t) = \int_0^t \Phi(t-t') \left[\gamma \frac{\partial}{\partial y} y + < y^2 >_{eq} \frac{\partial^2}{\partial y^2}\right] p(y,t')dt', \tag{4.65}$$

where the memory kernel in the Laplace domain is defined, through the Laplace transform of the subordination function $\psi^{(S)}(t)$, by Eq. (4.10).

It is important to point out that the regression to equilibrium of the moments of the dynamic variable $< y^q(t) >$ from an initial out-of-equilibrium state $< y(0) >$ can be derived using the same arguments as those adopted to derive Eq. (4.37). Thus we obtain

$$Y_q(t) \equiv < y^q(t) > = \sum_{n=0}^{\infty} \int_0^t dt' \psi_n^{(S)}(t') \Psi^{(S)}(t-t') exp(-\gamma q n). \tag{4.66}$$

and, instead of Eq. (4.44) we now have

$$\hat{Y}_q(u) \to e^{\gamma q} \hat{E}_\alpha(u), \tag{4.67}$$

with $\hat{E}_\alpha(u)$ given, as in the earlier case, by Eq. (4.45), and λ_α defined by

$$\lambda_\alpha = \left(\frac{e^{q\gamma} - 1}{\Gamma(2-\mu_S)(T_S)^\alpha}\right)^{1/\alpha}. \tag{4.68}$$

It is evident that increasing q has the effect of reducing the size of the time interval of the stretched exponential relaxation. Note that these results are obtained by assuming $\langle y^2(0)\rangle \gg \langle y^2\rangle_{eq}$ so as to neglect the influence of the stochastic force. The same results are obtained using Eq. (4.65) with only the friction term on its right hand side.

The stochastic trajectory $y(t)$ fluctuates within a strip of size $\langle y^2\rangle_{eq}$, thereby making it possible to make predictions based on disregarding the first rather than the second term on the right hand side of Eq. (4.65). This allows us to evaluate the distribution of the time intervals between two consecutive re-crossings of the origin, $y = 0$.

Note that when we disregard the friction term on the right-hand side of Eq. (4.65), this equation becomes equivalent to the Continuous Time Random Walk of Montroll and Weiss [41] whose scaling index β is known to be

$$\beta = \frac{\mu_S - 1}{2}. \tag{4.69}$$

This scaling can be proved using Eq. (4.65). In the case where dissipation can be neglected Eq. (4.65) becomes

$$\frac{\partial}{\partial t}p(y,t) = \gamma \int_0^t \Phi(t-t') < y^2 > \frac{\partial^2}{\partial y^2}p(y,t')dt'. \tag{4.70}$$

Moving to the Laplace-Fourier domain, we obtain for $\hat{p}(k,u)$

$$\hat{p}(k,u) = \frac{1}{u + k^2\hat{\Phi}(u)}. \tag{4.71}$$

Using Eq. (4.10) and (3.49) and considering the limit $u \to 0$ we arrive at

$$\hat{p}(k,u) = \frac{1}{u + \gamma\frac{k^2u^{2-\mu_S}}{\Gamma(2-mu_S)T^{\mu_s-1}}}. \tag{4.72}$$

Diffusion scaling implies that

$$y \propto t^{\beta}, \tag{4.73}$$

and consequently that the Fourier and Laplace variables are related by

$$k \propto u^{\beta}. \tag{4.74}$$

Invariance by scaling implies that plugging Eq. (4.74) into Eq. (4.72) so as to make $\hat{p}(k,u)$ depend only on u, has the effect of producing a quantity proportional to $1/u$, which is, in fact, the aged memory of an invariant, namely, time-independent quantity. This is realized by setting the scaling condition of Eq. (4.69), which is consequently proved. This is equivalent to the diffusion scaling of the fractional diffusion process of Metzler and Klafter [55] (see Eq. (4.53)). As we have pointed out earlier, the stochastic velocity creating, in the absence of friction, the diffusion process $y(t)$ is obtained through the subordination to the stochastic velocity responsible for ordinary diffusion.

A further way of expressing diffusion scaling is given by

$$p(y,t) = \frac{1}{t^{\beta}} F(\frac{y}{t^{\beta}}), \tag{4.75}$$

which is an obvious way to set the condition of Eq. (4.73), if we take into account that the prefactor $1/t^{\beta}$ serves only the purpose to guarantee normalization of $F(y)$ when the integration variable y is replaced by the new integration variable $z = y/t^{\beta}$.

The adoption of Eq. (4.75) allows us to determine the asymptotic properties of the waiting time distribution density $\psi^{D}(t)$ which is derived from the origin re-crossing histogram. We record the times t_i defined by

$$y(t_i) = 0 \tag{4.76}$$

and we define the time interval between successive re-crossings

$$\tau_i = t_{i+1} - t_i. \tag{4.77}$$

We note that these are renewal events, insofar as they have been proven [56] to fit the renewal criterion illustrated in Section 3.1. However, we must emphasize that these renewal events

are not as important as the renewal events associated with the subordination function $\psi^{(S)}(t)$. In fact, as we have seen, in the case of the subordination to a coin-tossing process, these events correspond to the choice of either $+1$ or -1. In the case of the double subordination, they correspond to the drawing of a ball, whose color may leave unchanged the sign of ξ_S, if the ball is white, or may also change it, with equal probability, if the ball is black. In the case of the subordination to an ordinary fluctuation-dissipation process, here under discussion, the leading Demon is creating a fluctuation $y(t(n))$. In other words, the times $t(n)$ are the times at which the fluctuation $y(t)$ may undergo an abrupt change, due to the fact that the stochastic force $f(n)$ is assumed to be white. The effect of subordination can also be interpreted as a way to turn this white noise into correlated noise, insofar as it is kept unchanged for the whole time interval between $t(n)$ and $t(n+1)$.

Consequently, the distribution densities $\psi^{(S)}(t)$ and $\psi^{(D)}(t)$ have a different physical meaning, although both become inverse power laws in the time asymptotic limit. The inverse power law of $\psi^{(S)}(t)$, with $\mu_S < 2$ is a choice dictated by the fact that, as we have established with Eq. (4.43), the adoption of a subordination function compatible with ergodicity would not establish a departure, in the macroscopic time regime, from the ordinary forms of exponential relaxation. The inverse power-law nature of $\psi^{(D)}(t)$, with $\mu_D < 2$ is a consequence of Eq. (4.75). In fact,

$$\sum_{n=1}^{\infty} \psi_n^{(D)}(t) = Q(t), \tag{4.78}$$

where

$$Q(t) \equiv p(0,t) = \frac{1}{t^{\beta}} F(0). \tag{4.79}$$

The rationale for Eqs. (4.78) and (4.79) is as follows. We locate our diffusing trajectory at $y = 0$ at time $t = 0$ and we wait for this trajectory to come back. In the time asymptotic regime where the scaling condition of Eq. (4.75) applies, the trajectory $y(t)$ can be found in the original position only as a result of the re-crossing process. This property is obvious in

the natural time condition. In the t time scale is justified by observing that the probability of not leaving the origin is proportional to $1/t^{\mu_S-1}$ and consequently faster than $1/t^{\frac{\mu_S-1}{2}}$, which is the probability of finding the particle at $y=0$ in the scaling regime.

From Eq. (4.78) we derive

$$\frac{\hat{\psi}^{(D)}(u)}{1-\hat{\psi}^{(D)}(u)} = \hat{Q}(u), \tag{4.80}$$

which yields

$$\hat{\psi}^{(D)}(u) = \frac{\hat{Q}(u)}{1-\hat{Q}(u)}. \tag{4.81}$$

Let us use Eq. (4.79) and the Tauberian theorem, according to which, for $\alpha < 1$

$$t^{\alpha-1} \rightarrow \frac{1}{u^{\alpha}} \tag{4.82}$$

. We set $1-\alpha = \beta$, which is a legitimate choice insofar as $\beta < \alpha$ and we get

$$\hat{Q}(u) = \frac{const}{u^{1-\beta}} \tag{4.83}$$

and consequently

$$\frac{\hat{Q}(u)}{1-\hat{Q}(u)} \approx (1 - \frac{u^{1-\beta}}{const}). \tag{4.84}$$

By plugging Eq. (4.84) into the right side of Eq. (4.81) and using Eq. (3.49) again we find

$$\mu_D = 2 - \beta. \tag{4.85}$$

This is an interesting result. It means that also the re-crossing events are not ergodic. However, we have to warn the reader about the fact that these events do not correspond to objective facts. They are the consequence of assigning to the re-crossing of the origin a special physical significance that may not correspond to reality. Here we are making the assumption that, due to the Demon's action, the index μ_S corresponds to a sequence of real

physical events. It is interesting to notice that the condition

$$\mu_S = \mu_D \tag{4.86}$$

is realized when

$$\beta = \frac{1}{3}, \tag{4.87}$$

which is the well known scaling of the Kardar-Parisi-Zhang renormalization theory (KPZ) [57]. Thus, we conclude that the identification of re-crossings with significant renewal events, in the case of the KPZ condition does not generate a quite unsatisfactory scenario. In fact, in this case re-crossings and subordination events are characterized by the same non-ergodic index

$$\mu = \frac{5}{3} \tag{4.88}$$

However, the adoption of the re-crossing technique can be used to establish a distinction between μ_S and μ_D, when a renormalization approach different from the KPZ theory applies. To make this aspect clearer, let us go back to the natural time scale, and let us establish the time distribution of time distances between two consecutive re-crossing of the level $R > \langle y^2 \rangle_{eq}^{1/2}$. In this case, the dissipation process cannot be neglected, and it has the effect of establishing a re-crossing distribution that involves directly μ_S. To get analytical results we proceed as follows. We go back to the natural time scale, and we let the network evolve until it reaches the equilibrium distribution described by

$$p_{eq}(y) = \frac{1}{\left(2\pi \left\langle y^2 \right\rangle_{eq}\right)^{1/2}} exp\left(-\frac{y^2}{2\left\langle y^2 \right\rangle_{eq}}\right). \tag{4.89}$$

We now study the recrossing of the level $R > \langle y^2 \rangle_{eq})^{1/2}$. This is again using Eq. (4.78). In this case $Q(t)$ is time independent. We set the condition

$$Q(t) = g_R \equiv \gamma R p_{eq}(R), \tag{4.90}$$

where g_R coincides with the Kramers rate [39]. Thus, we obtain

$$\psi_R(n) = g_R exp\left(-g_R n\right). \tag{4.91}$$

The transition from n- to t-time scale is achieved in the usual way, as described by Eq. (4.37) with $exp(-gn)$ replaced by $exp(-g_R n)$, thereby yielding

$$\Psi_R(t) = e^{g_R} E_\alpha(t), \tag{4.92}$$

where $E_\alpha(t)$ is derived from its Laplace transform that is identical to Eq. (4.45) with λ_α given by

$$\lambda_\alpha = \left(\frac{e^{g_R} - 1}{\Gamma(2-\mu_S)(T_S)^\alpha}\right)^{1/\alpha} \tag{4.93}$$

We note that with increasing R, the rate g_R becomes smaller and smaller thereby extending the time interval of the stretched exponential.

This has the effect of establishing a direct connection with the subordination process. In fact, thanks to Eq. (4.46) we can relate the stretched exponential relaxation directly to the subordination process. In practice, the determination of μ_S through this procedure can be hard, due to the fact that the statistics become poorer with increasing R. For a valuable determination of μ_S we can express this parameter as a function of μ_D. Using Eq. (4.53) and Eq. (4.85) we obtain

$$\mu_S = 5 - 2\mu_D, \tag{4.94}$$

which, of course, in the KPZ case, yields $\mu_S = \mu_D = 5/3$.

It is convenient to mention that this subordination perspective, in the case of the random growth of surfaces leads to a remarkably good agreement between theory and numerical simulation [80]. This fact requires a proper comment. The time series generated by complex systems are finite, and their own generators are networks of finite size. The authors of Ref.[80, 59] have remarked that the adoption of the subordination function with a non

truncated inverse power law distribution density is not realistic, because it rests on the idealized condition that the time series under study are infinite. As pointed out in Ref. [80], a convenient way to take truncation effects into account rests on replacing Eq. (4.45) with

$$\hat{Y}(u) = \frac{1}{u + (\lambda_\alpha)^\alpha (u + \Gamma_{trunc})^{1-\alpha}}, \tag{4.95}$$

where the parameter Γ_{trunc} defines the time parameter

$$T_{trunc} \equiv \frac{1}{\Gamma_{trunc}}. \tag{4.96}$$

This choice implies that also the the subordination function $\psi^{(S)}(t)$ is truncated. This is so because, according to Eq. (4.95) the real $\Phi(t)$ is related to to the ideal by means of the relation

$$\Phi(t) = \Phi_0(t) exp(-\Gamma_{trunc} t), \tag{4.97}$$

which, in turn, thanks to Eq. (4.10) yields

$$\hat{\psi}^{(S)}(u) = \frac{\hat{\Phi}_0(\Gamma_{trunc} + u)}{u + \hat{\Phi}_0(\Gamma_{trunc} + u)}. \tag{4.98}$$

Thus, when $u \ll \Gamma_{trunc}$, $\hat{\psi}^{(S)}(u)$ becomes the Laplace transform of an exponential subordination function. In the case where Γ_{trunc} is, due to the finite network size is of the order of λ_α, the inverse power law of the Mittag-Leffler function does not emerge, and the whole process is virtually described by a stretched exponential relaxation. This does not mean that the inverse power-law does not contribute to the process. It does, although within the limits established by the finite size of the networks under study. The authors of Ref.[80] found an excellent agreement between theory and numerical experiment by adopting this perspective. As we shall see in Chapter 6, this truncation effect can be due to the deterministic periodicity of the interacting units in a system.

We have also to point out that when $g_R << 1$, Eq. (4.93), yields

$$T_S \gg \frac{1}{\lambda_\alpha}. \tag{4.99}$$

As a consequence, the renewal events of the subordination process keeps their inverse power law nature in the time scale where the survival probability maintains its form of stretched exponential function.

Finally, it is important to explain why the survival probability $Y(t)$ (q = 1) of Eq. (4.67) can be obtained from the survival probability of Eq. (4.44) by replacing g with γ. This can be explained again using the concept of success rate. In fact, as we have seen in this section, in the natural time scale the time distance between two big fluctuations of y is under the control of the Kramers prescription that assigns to the corresponding waiting time distribution density the exponential form of Eq. (4.91). This interpretation is not quite satisfactory, due to the dependence on the threshold R, which seems to be to some extent arbitrary. A more compelling argument is given by the remark that the regression to equilibrium of a fluctuation y significantly larger than $\left(\langle y^2 \rangle_{eq}\right)^{1/2}$ is $exp(-\gamma t)$, thereby leading to $Y(t)$ (q = 1) of Eq. (4.67). In other words, here the success rate has to do with the attainment of a level much higher than that of the many more numerous fluctuations of small intensity.

CHAPTER 5

COMPLEXITY FROM SYNCHRONIZATION AND COOPERATION I: PHASE SYNCHRONIZATION OF STOCHASTIC CLOCKS

Phase synchronization is a growing field of research, which is fast developing from the seminal work of Winfree [60] and Kuramoto [61] on coupled oscillators. A number of physiologists use a clock, a form of oscillator, to represent single neurons. Stam [62] adopted the chaotic oscillator Rössler attractor [63], to describe the dynamics of a single neuron. The authors of Ref. [64] and of Ref. [66] have shown that coupled stochastic clocks can show cooperative (synchronized) behavior, but overlooked the emergence of non-ergodic fluctuations. Herein we consider the two-state version of stochastic clock used in Ref. [66] and show important properties making it a plausible model for the dynamics of human brain, the blinking quantum dots and numerous other complex systems exhibiting two-state properties.

The first section of the chapter will introduce the model of the stochastic clock. The succeeding sections will investigate its dynamics on several types of network topologies; all-to-all coupled, regular and several complex networks. We show that the cooperation of the individual clocks yields collective properties different as the clocks would have in isolation, behaving independently. We also show that synchronization is enhanced by the adoption of complex network topologies.

5.1. The Two-State Stochastic Clock Model

The two-state stochastic clock is illustrated in Figure 5.1. The hand of the clock can only move in two phases, $\Phi = 0$ and $\Phi = \pi$. We denote the former state $|1>$ and the latter as state $|2>$ and let g_{12} be the constant transition rate from $|1>$ to $|2>$ and g_{21} for the reverse.

Let us find the probability density function (PDF) $\psi(\tau)$ of the time of sojourn of the clocks in each of the two phases corresponding to the rates g_{12} and g_{21}. For simplicity, let us assume that the clocks has the same probability of staying in each state, allowing us to write $g = g_{12} = g_{21}$. The probability that the clock leaves its state is therefore

$$p(\tau) = \psi(\tau)\Delta\tau. \tag{5.1}$$

To find the form of $\psi(\tau)$, it is convenient to introduce the concept of Survival Probability (SP) $\Psi(\tau)$. This is the probability that clock remains in the same state after a time τ has elapsed. Thus, we have

$$\Psi(\tau) = \int_{\tau}^{\infty} \psi(\tau)\mathrm{d}\tau. \tag{5.2}$$

Using a discrete time representation, the SP of the clock after a time τ is given by

$$\Psi(\tau) = (1-g)^{\tau} \approx e^{-g\tau}. \tag{5.3}$$

where we assume in the second equality that $\tau \gg 1$. Thus, using (5.2) we get the waiting time distribution density

$$\psi(\tau) = \tau e^{-g\tau}. \tag{5.4}$$

Following the arguments that lead to Eqn. (3.44), we conclude that an individual clock is Poissonian. In the following sections we show that the collective behavior of a set of interacting stochastic clocks yields a dynamic complexity, that is, it departs from the Poisson statistics as obeyed by a single clock.

5.2. All-to-All Coupling

Let us consider a set of N two-state stochastic clocks and adopt an all-to-all coupling configuration. The master equation (2.13) for a single clock in the Gibbs ensemble system is

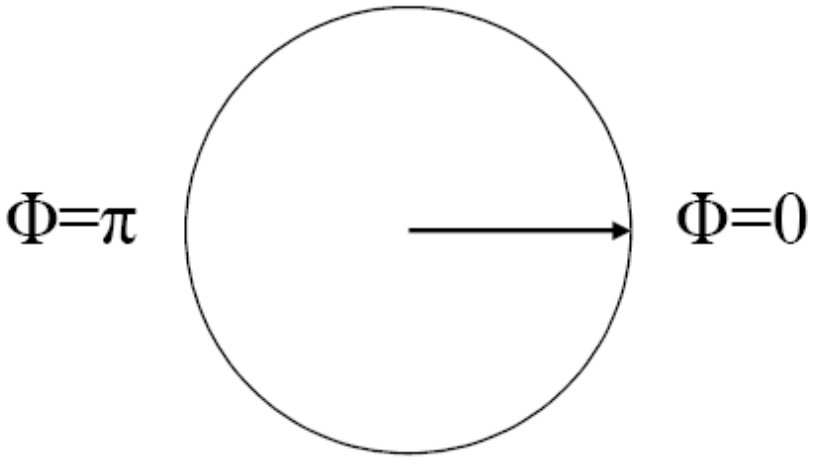

Figure 5.1: The two-state stochastic clock.

$$\begin{cases} \frac{\mathrm{d}}{\mathrm{d}t}P_1(t) = -g_{12}P_1 + g_{21}P_2 \\ \frac{\mathrm{d}}{\mathrm{d}t}P_2(t) = -g_{21}P_2 + g_{12}P_1 \end{cases} \tag{5.5}$$

where P_1 (P_2) is the probability of finding the clock in the state $|1>$ ($|2>$), and g_{12} (g_{21}) is the rate of transition from state $|1>$ ($|2>$) to the $|2>$ ($|1>$). The transition rates g_{12} and g_{21} are defined by means of the following prescription:

$$\begin{cases} g_{12}(t) = g_0 \exp\{-K(\pi_1(t) - \pi_2(t))\} \\ g_{21}(t) = g_0 \exp\{+K(\pi_1(t) - \pi_2(t))\} \end{cases} . \tag{5.6}$$

where g_0 is the unperturbed transition rate, $K > 0$ is a constant coupling parameter and $\pi_1(t)$ ($\pi_2(t)$) is the fraction $N_1(t)/N_c$ ($N_2(t)/N_c$) of the nearest neighbor[1] clocks N_c in the state $|1>$ ($|2>$) at time t. With the choice of the all-to-all coupling topology, $N_c = N - 1$.

[1]refers to the number of clocks to where the currently evaluated clock is coupled

Thus, in the limiting case $N \to 0$, the mean field approximation [65]

$$\pi_{1(2)} = P_{1(2)} \tag{5.7}$$

is an exact property.

Using the property (5.7) and the normalization condition $P_1 + P_2 = 1$, the master equation (5.5) reduces to

$$\frac{\mathrm{d}}{\mathrm{d}t}\Pi(t) = -2g\Pi\cosh(K\Pi) + 2g\sinh(K\Pi) = -\frac{\partial V(\Pi)}{\partial \Pi}, \tag{5.8}$$

where $\Pi = P_1 - P_2$ and $\Pi\epsilon[-1, 1]$. Eq. (5.8) describes the overdamped motion of a particle with position Π within the potential $V(\Pi)$ [39]. From (5.8), we find that the potential $V(\Pi)$ is symmetric and the values of its minima Π_{min} depend only on the coupling constant K. Moreover, we find that there is a critical value $K_c = 1$ of the coupling parameter K such that: 1) if $K \leq K_c$ the potential $V(\Pi)$ has only one minimum, $\Pi = 0$, 2) if $K \geq K_c$ the potential $V(\Pi)$ has two symmetric minima, $\Pi = \pm\Pi_{min}$ separated by a barrier (the maximum o f Π) centered in $\Pi = 0$. As shown in Figure 5.2, the value Π_{min} and the height of the barrier (V(0)) are increasing function of the coupling constant[2] is chosen to satisfy the condition $V(\pm\Pi_{min}) = 0$ for all values $K > K_c$. In particular $\Pi_{min} \to 1$ and $V(0) \to +\infty$ when $K \to +\infty$.

The time evolution of the variable $\Pi(t)$ is determined by the minima and maxima of the potential $V(\Pi)$. Thus, two types of dynamical evolution are possible: 1) If $K \leq K_c$, $\Pi(t)$ will reach, after a transient period, an asymptotic value $\Pi(\infty) = 0$ not depending on the initial conditions $\Pi(0)$. 2) If $K \geq K_c$, $\Pi(t)$ will reach, after a transient period, either of the two asymptotic values $\Pi(\infty) = \pm\Pi_{min} \neq 0$ depending on the initial condition. $\Pi(0) > 0$ results to the positive minimum and $\Pi(0) > 0$ to the negative minimum. The initial condition $\Pi(0) = 0$ will result in $\Pi_{min} = 0$ for all values of t. In Figure 5.3 we compare the

[2]The arbitrary constant in the definition of the potential $V(\Pi)$

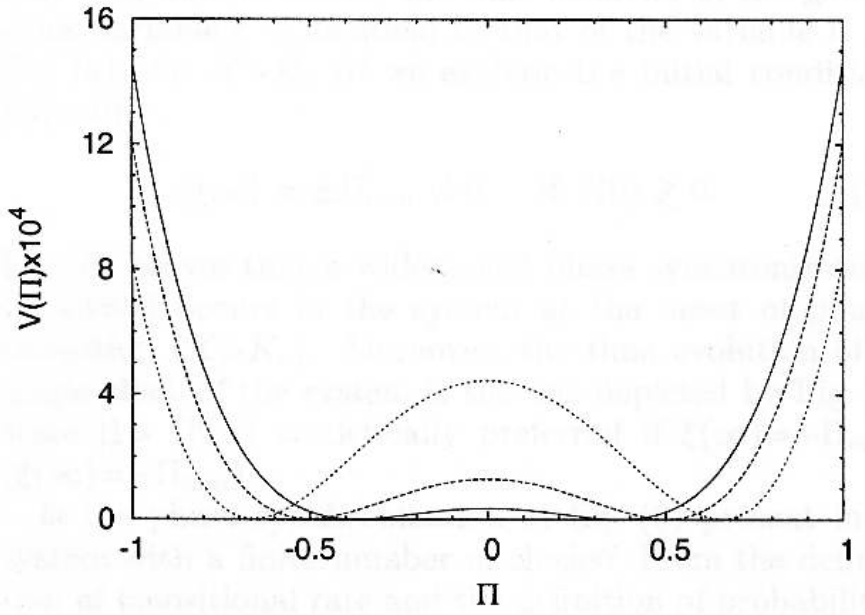

Figure 5.2: The potential $V(\Pi)$, rescaled by a factor 10^4, as a function of Π for g=0.01 for $K = 1.05$ (continuous line), $K = 1.1$ (dashed line), and $K = 1.2$ (dotted line).

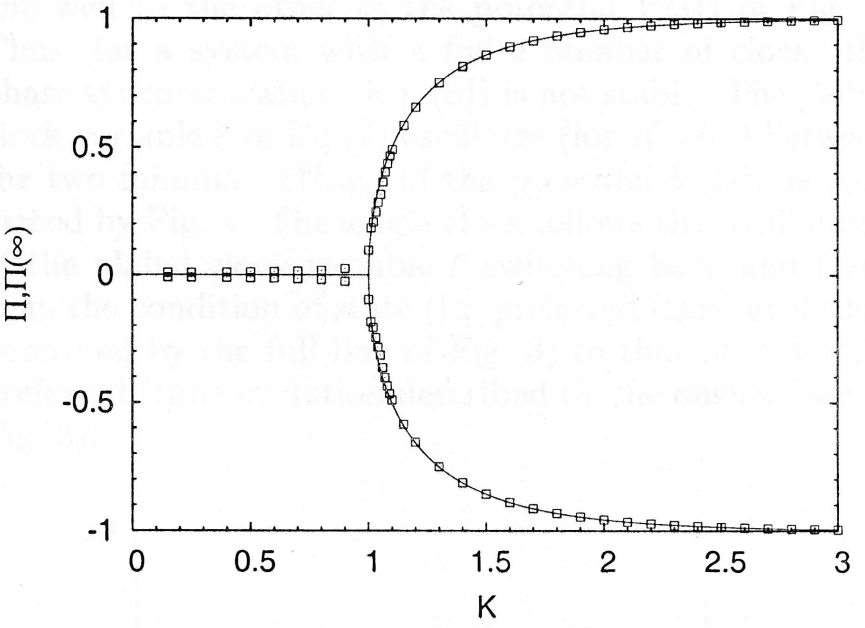

Figure 5.3: The minima Π of the potential $V(\Pi)$ and the asymptotic value $\Pi(\infty)$ as a function of the coupling constant K. The full line is the theoretical prediction for the minima $\tilde{\Pi}$ obtained from (5.8). The squares denote the result of the numerical evaluation of $\Pi(\infty)$ with a Gibbs ensemble consisting of $N = 10000$ clocks.

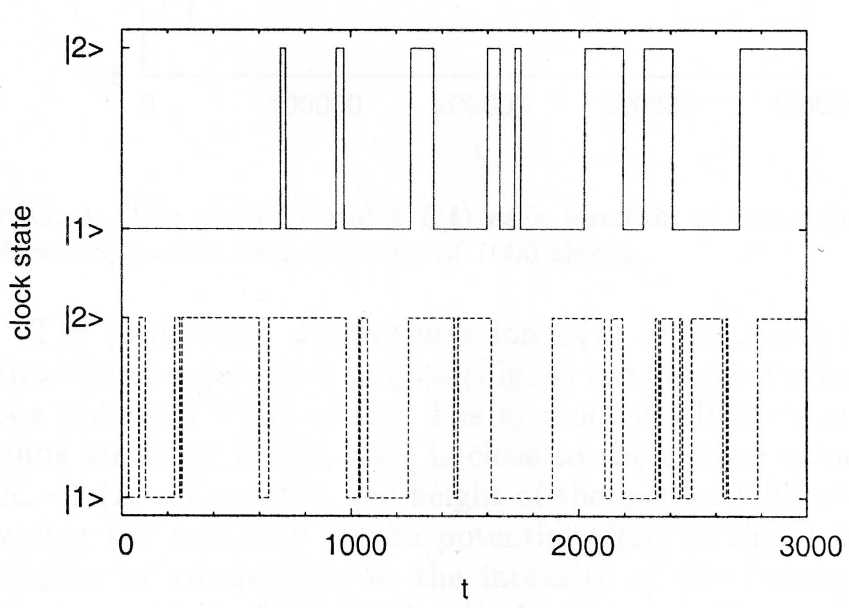

Figure 5.4: The typical time evolution of a single clock in a system of Gibbs ensemble. The solid (dashed line) refers to the case $\Pi(\infty) = +\Pi_{min}$ ($\Pi(\infty) = -\Pi_{min}$). The system is composed of 10000 clocks with unperturbed transition rate $g_0 = 0.01$ and the coupling constant $K = 1.05$.

minima $\tilde{\Pi}$ of the potential $V(\Pi)$ and the numerical evaluation of $\Pi(\infty)$ as a function of the coupling parameter K. The figure also shows that a second-order phase transition occurs at $K = K_c = 1$. This phase transition also signals the birth of a "statistical preference" ($\Pi = P_1 - P_2 \neq 0$) for a single clock in the system of Gibbs ensemble to be in state $|1>$ and $|2>$. This is a consequence of the fact that the transition rate g_{12} and g_{21} of Eq. (5.6) are different for $K > K_c$. Using the mean field approximation (5.7) and allowing $\Pi(t)$ to reach its asymptotic value, we get

$$g_{12}(t) = g_0 \exp\{-K\Pi(\infty)\} \neq g_{21}(t) = g_0 \exp\{K\Pi(\infty)\}. \tag{5.9}$$

Figure 5.4 confirms the prediction of Eq. (5.9). It shows that if $\Pi(\infty) = +\Pi_{min}$ ($\Pi(\infty) = +\Pi_{min}$) the single clock, on the average, spends more time in the state $|1>$ ($|2>$). The probability density function for the sojourn times in both of the preferred and not-preferred states are exponentials with different mean sojourn time.

5.2.1. *Collective Behavior*

Let us explore the collective behavior of a single system of N clocks under the all-to-all coupling condition. Adopting the method from [68], we define the global clock variable ξ as

$$\xi = \frac{\sum_{j=1}^{N} exp(i\Phi_j(t))}{N} = \frac{N_1(t) - N_1(t)}{N}. \tag{5.10}$$

The symbol i is the imaginary unit, Φ_j is the phase of the j^{th} clock, and $N_1 t$ and $N_2(t)$ are the number of clocks in the state $|1>$ and $|2>$ at time t respectively. When $N \to 0$, the single system becomes a Gibbs ensemble on its own as all the clocks are identical and, at the same time, the mean field approximation (5.7) becomes valid. In this case the master equation for the single system of infinite clocks is the master equation Eq. (5.5), where P_1 (P_2) is now the probability of finding a clock in the system with the state $|1>$ ($|2>$). From Eq. (5.10), in the limiting case $N \to 0$, we get $\xi(t) = P_1(t) - P_2(t) = \Pi(t)$. Thus, for a system with infinite clocks, the time behavior of the global clock variable ξ is identical to that of the variable Π of Eq. (5.8). Thus, for $K > K_c$,

$$\xi(\infty) = \pm\Pi_{min} \neq 0 \tag{5.11}$$

depending on the initial condition $\xi(0) < 0$ or $\xi(0) > 0$. Eq. (5.11) proves that a widespread phase synchronization ($\xi(\infty) \neq 0$) occurs in the system at the onset of phase synchronization ($K > K_c$). Moreover, the time evolution of a single clock of the system is the one depicted in Figure 5.4 where state $|1>$ is statistically preferred if $\xi(\infty) = +\Pi_{min}$ and state $|1>$ if $\xi(\infty) = -\Pi_{min}$.

5.2.2. *Finite Size Effects*

Is the phase synchronization of Eq. (5.11) present in a system with a finite number of clocks? From the definition of transitional rate and the definition of probability, it follows

that

$$\begin{cases} g_{12}P_1 = \lim_{N\to\infty} \frac{N_{1\to 2}}{N} \\ g_{21}P_2 = \lim_{N\to\infty} \frac{N_{2\to 1}}{N} \end{cases}, \tag{5.12}$$

where $N_{1\to 2}$ ($N_{2\to 1}$) is the number of clocks that undergo a transition from the state $|1>$ ($|2>$) to the state $|2>$ ($|1>$) per unit time, and N is the total number of clocks in the system. Using the law of large numbers [18], we get, for $1 << N < \infty$,

$$\begin{cases} \frac{N_{1\to 2}}{N} = g_{12}P_1 + \varepsilon_{12}P_2 \\ \frac{N_{2\to 1}}{N} = g_{21}P_2 + \varepsilon_{21}P_1 \end{cases}, \tag{5.13}$$

where ε_{12} and ε_{21} are fluctuating variables (white noise) whose intensities are $\propto 1\sqrt{N}$. Thus, from (5.12) and (5.13), we conclude that the master equation of a system with a finite number of clocks is equivalent to that of a system with an infinite number of clocks but with fluctuating transitional rates:

$$\begin{cases} \frac{\mathrm{d}}{\mathrm{d}t}P_1(t) = -(g_{12} + \varepsilon_{12})P_1 + (g_{21} + \varepsilon_{21})P_2 \\ \frac{\mathrm{d}}{\mathrm{d}t}P_2(t) = -(g_{21} + \varepsilon_{21})P_2 + (g_{12} + \varepsilon_{12})P_1 \end{cases}. \tag{5.14}$$

Thus, the mean field master equation (5.8) is now written as, taking into account the finite size effects,

$$\frac{\mathrm{d}}{\mathrm{d}t}\Pi(t) = -\frac{\partial V(\Pi)}{\partial \Pi} - \eta(t)\Pi(t) + \theta(t) \tag{5.15}$$

with $\eta = \varepsilon_{12} + \varepsilon_{21}$ and $\theta = \varepsilon_{12} - \varepsilon_{21}$. The presence of the fluctuations η and θ in (5.15) has the effect of triggering transitions from one well to the other of the potential $V(\Pi)$ of Figure 5.2. Therefore, for a system with a finite number of clocks the phase synchronization (5.11) is not stable. The global clock variable ξ Eq. (5.10) oscillates, for $K > K_c$ between the two minima, $\pm\Pi_{min}$, of the potential $V(\Pi)$, as confirmed by Figure 5.5. The single clock follows the oscillations of the global clock variable ξ switching back and forth from the condition of state $|1>$ to state $|2>$ and vice versa.

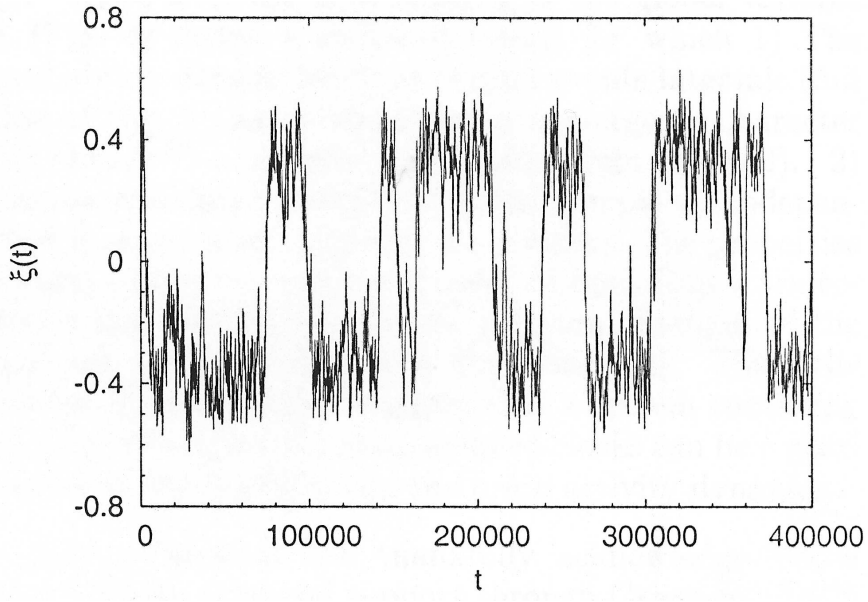

Figure 5.5: The global variable $\xi(t)$ as a function of time for $K = 1.05$ and $g = 0.01$ of a system with 1000 clocks.

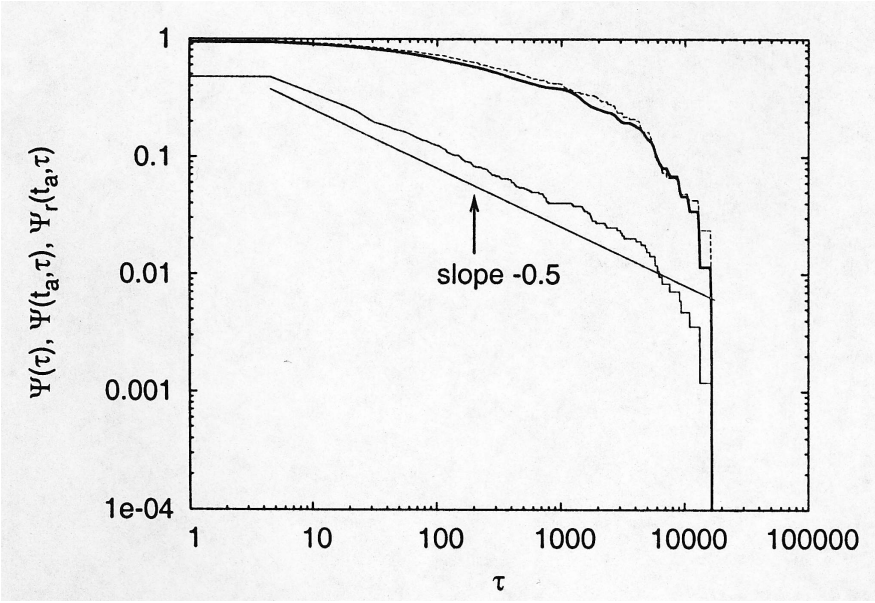

Figure 5.6: The survival probabilities $\Psi(\tau)$ (full line), $\Psi(t_a = 500, \tau)$(dashed line), and $\Psi_r(t_a = 500, \tau)$ (full thick line) as a function of the sojourn times τ.

5.2.3. *Renewal Property and the Origin of the System Power-Law Distribution*

The probability density function $\psi(\tau)$ of the sojourn times τ in the states $\xi > 0$ and $\xi < 0$ of Figure 5.5 are identical since the potential $V(\Pi)$ of Figure 5.2 is symmetric. If

the coupling constant K is close to the critical value $K_c = 1$, the height of the barrier $V(0)$ dividing the two wells of the potential in Figure 5.2 is smaller or comparable to the intensity of the fluctuations η and θ of Eq. (5.15). Under this condition, we expect [67] the power-law behavior $\psi(\tau) \propto 1/\tau^{1.5}$ for an extended interval of sojourn times. This is exactly what we observed in Figure 5.6 where the full line denotes the survival probability, the probability of observing a sojourn time larger than τ, $\Psi(\tau) \propto 1/\tau^{0.5}$. As the coupling parameter increases (above the critical value $K_c = 1$), the height of the barrier dividing the two wells of the potential $V(\Pi)$ of Figure 5.2 quickly overcomes the intensity of the fluctuations η and θ in Eq. (5.15). This time the power-law behavior disappears, the theoretical arguments of [67] loses validity, and an exponential behavior emerges, the Kramers theory [39] becomes valid. Finally, we show that the transition between the states $\xi > 0$ to $\xi < 0$ in Figure 5.5 is a renewal process. For this purpose we use the aging experiment of Ref. [45]. We evaluate the survival probability $\Psi(t_a, \tau)$ of age t_a : the probability of observing a sojourn time larger than τ if the observation starts at a time t_a after a crossing from $\xi > 0$ to $\xi < 0$ or vice versa ($\Psi(0, \tau) = \Psi(\tau)$). We then compare $\Psi(t_a, \tau)$ with the expected survival probability $\Psi_r(t_a, \tau)$ of age t_a in the renewal case. If $\Psi(t_a, \tau) = \Psi_r(t_a, \tau)$ for all values of t_a, the process described by $\Psi(\tau)$ is renewal. Figure 5.6 shows that the transition between the states $\xi > 0$ and $\xi < 0$ is a renewal process: the dashed line ($\Psi(t_a, \tau)$) and the full thick line ($\Psi_r(t_a, \tau)$) coincide (we choose $t_a = 500$ in Figure 5.6 for clarity).

5.3. Effects of Complex Networks Topology

The inverse power-law distribution (see Eqn. (3.5)) of the time of sojourn of the global clock (collective phase) in a specific state is not limited to the power index $\mu = 1.5$ as shown when the clocks interact in an all-to-all coupled network. A way to change the dynamic complexity of the system is by adopting complex networks topology. Herein we show the effects of different complex networks topologies on the dynamics of interacting clocks. In particular we adopt four familiar complex networks: the random or Erdös-Renyi (ER) network [11] (see Figure 5.7a) , the small-world network of Watts and Strogatz (WS)

[9] (see Figure 5.7b), the Barabasi-Albert model (BA) [10] (see Figure 5.7c), and the more recent model by Holme and Kim (HK) [12] (see Figure 5.7d). In addition, we also study the effect of a regular network (R) (see Figure 5.7e) to make a comparison with the complex networks.

To make a good comparison we created the networks in a way that all of them share the same average number of links m_l, which in the case of Figure 5.7 takes $m_l = 10$. Another interesting result is the effect of complex topology on the phase synchronization of the clocks. This is shown in Figure 5.9. Figure 5.9 shows that the regular network almost does not make, if it does with larger values of K, the global system into phase synchrony whereas the complex network topologies lead to the phase transition similar to the all-to-all coupled network but with the expense of larger coupling parameter K. It also shows that the HK network which is characterized with high clustering and power-law distribution of links is the most efficient network for synchronization at least for the model used herein. A deep understanding of these effects from complex networks is the subject of my future research work. Theoretical concepts applied to the all-to-all coupled networks, that is the mean field approximation, will no longer apply and new theory must be developed to explain the dynamical origin of the effects of complex network.

5.4. Chapter Conclusion

In conclusion, we have shown that the system of two-state coupled clocks undergoes a phase transition for a coupling parameter critical value $K = K_c = 1$. The onset of phase transition signals the birth to a phase synchronization in the system. If the number of constituents of the system is finite the phase synchronization is not stable and an oscillatory behavior appears for the variable ξ describing the collective motion of the system. At the onset of phase transition, the zero crossing of the global variable ξ defines a series of events for which the probability density function $\psi(\tau)$ of the inter-events interval has a non-Poisson non-ergodic behavior and exhibits a renewal property: independent inter-events interval. These properties are observed in blinking quantum dots trajectories [45, 70, 67] and of the

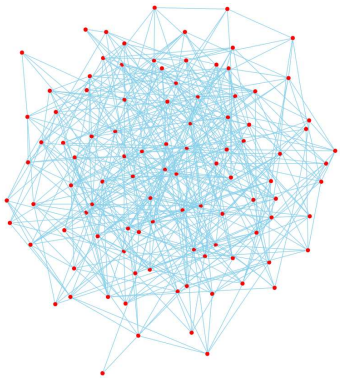

(a) Erdös-Renyi (ER) network [11]

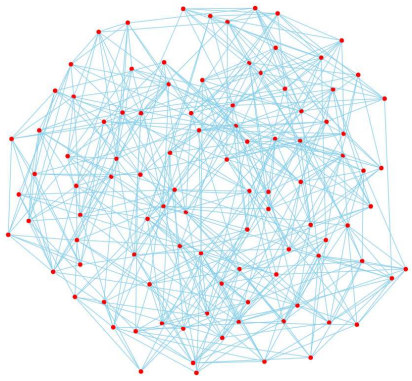

(b) Small World Network of Watts and Strogatz [9]

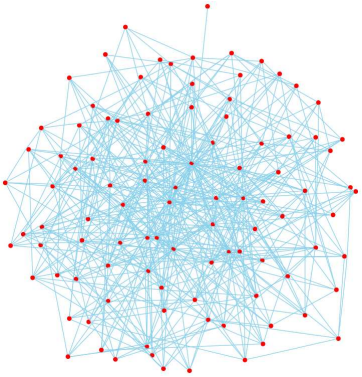

(c) The Barabasi-Albert model (BA) [10]

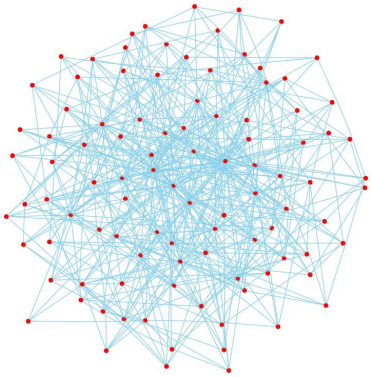

(d) Holme and Kim (HK) [12]

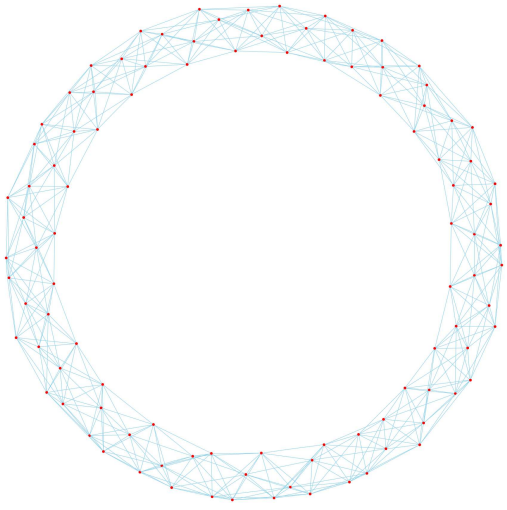

(e) A Regular Network

Figure 5.7: The four different complex networks and a regular network.

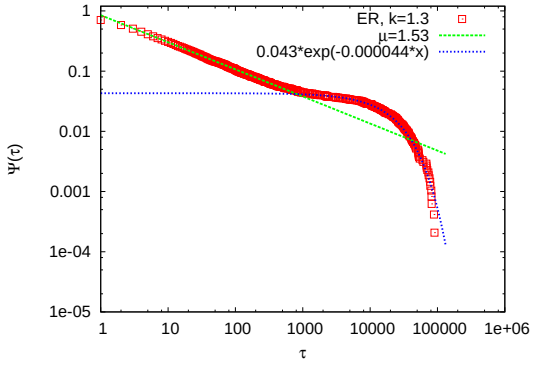

(a) SP from Erdös-Renyi (ER) network [11]

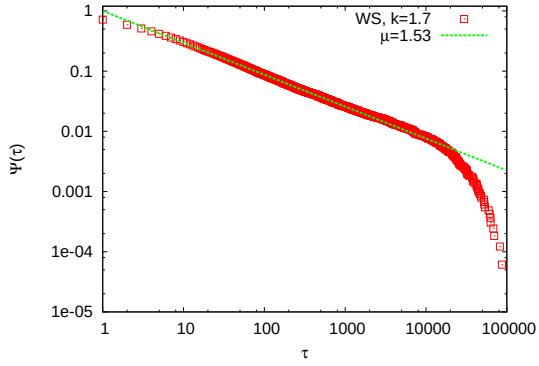

(b) SP from Small World Network of Watts and Strogatz [9]

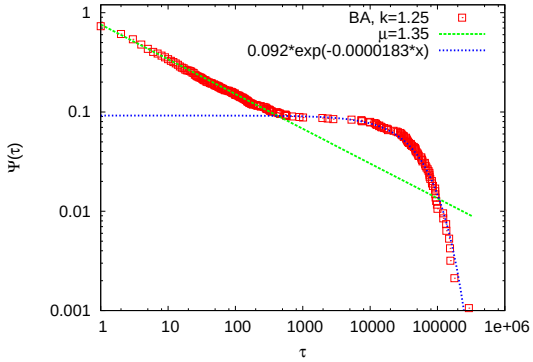

(c) SP from The Barabasi-Albert model (BA) [10]

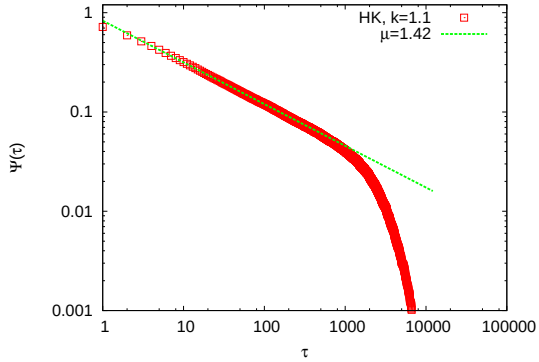

(d) SP from Holme and Kim (HK) [12]

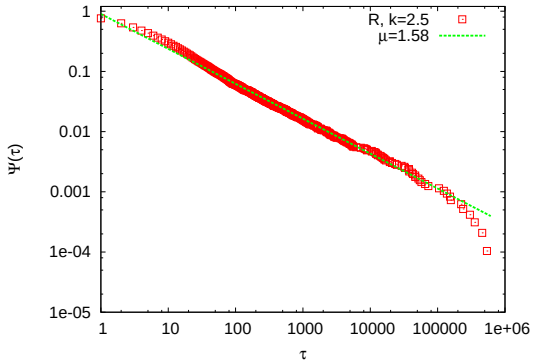

(e) SP from A Regular Network

Figure 5.8: Effect of complex network topology on the state sojourn time distribution.

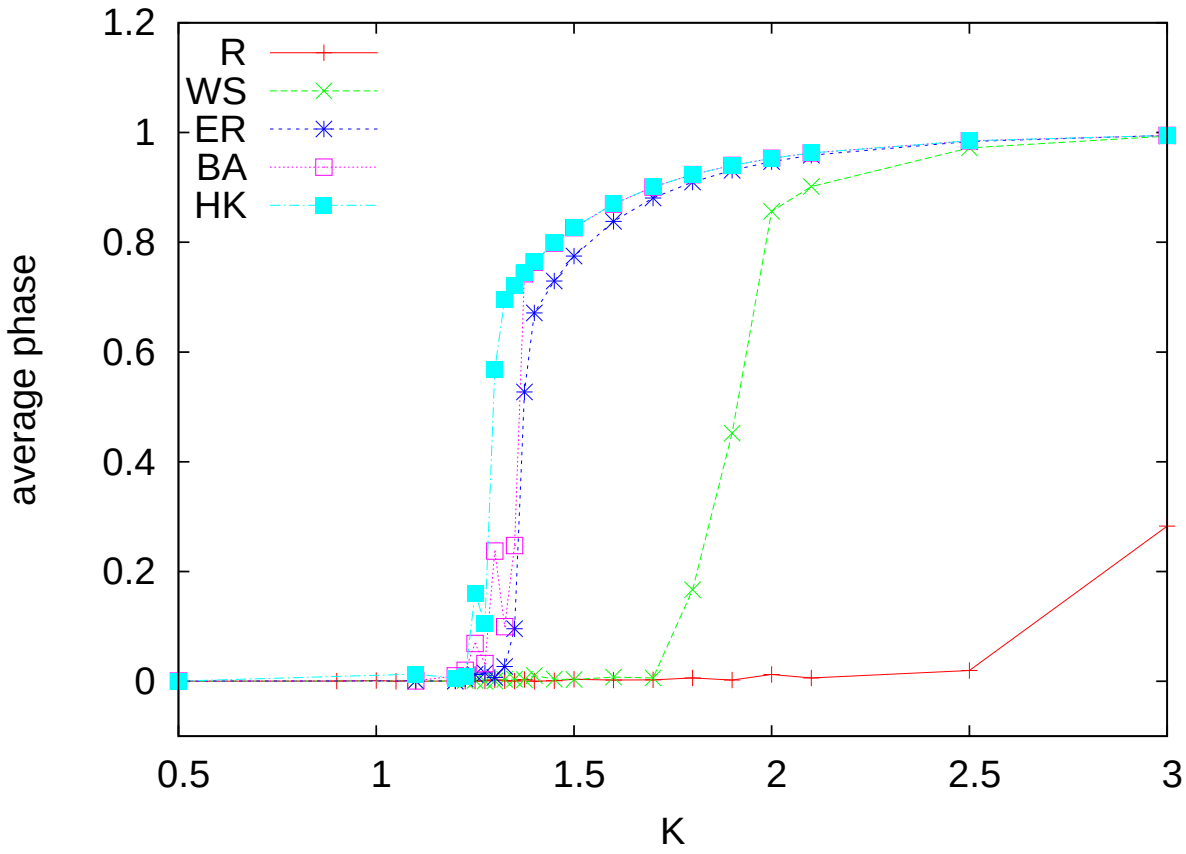

Figure 5.9: The effect of complex network on the global synchrony of the clocks.

temporal changes of the network topology of the brain [59]. Thus, these results suggest that a system consisting of a finite number of 2-state coupled clocks can be a good model for the dynamics of blinking quantum dots and human brain brain as well.

CHAPTER 6

COMPLEXITY FROM SYNCHRONIZATION AND COOPERATION II: STOCHASTIC SYNCHRONIZATION OF NEURONS

The occurrence of events described by inverse power laws is a clear manifestation of complexity. This phenomenon seems to be typical of processes characterized by the interaction among the elementary constituents, which can be neuronal [72] as well as human [53]. The authors of Ref. [72] have stressed the role of neuron synchronization as a source of neuronal avalanches and have concluded that the theoretical foundation of these processes is still open. It is worth mentioning that these real neurons are shown to interact in a scale free complex network [73]. A well model of neuron synchronization is that proposed years ago by Mirollo and Strogatz [74]. However, this model cannot be adopted as the prototype of complexity origin insofar as at synchronization all the neurons fire at the same time thereby realizing a perfectly periodic process. Herein, we modify the deterministic model by Mirollo and Strogatz by making it stochastic and we study its dynamics in complex networks.

In this chapter we argue that the complex structure of the brain and the emergence of non-exponential waiting time distribution as a result of neuron cooperation has a dynamic origin, which allows us to interpret the events experimentally detected as determined by the inverse power-law advocated by Barabási [53], even when the actions obeying this prescription are invisible. This explains why cooperation generates stretched exponential relaxation as well as inverse power-law decay [78].

6.1. The Mirollo-Strogatz Model

The Mirollo-Strogatz model [74] for synchronization of population of pulse-coupled oscillators is based on Peskin's model for self-synchronization of the cardiac pacemaker [75]. The model is a network of N integrate-and-fire oscillators (neurons) (see Tuckwell [76] and

references therein), each subject to the following equation of motion:

$$\frac{\mathrm{d}}{\mathrm{d}t}x_i = -\gamma x_i + S, \qquad i = 1, \ldots, N. \tag{6.1}$$

The variable x_i, in the case where the oscillators refer to neurons, denotes the potential and S is a positive constant making the potential essentially increase with time. When x_i reaches a threshold value Θ, the i_{th} neuron "fires" and instantly resets to $x_i = 0$, hence the name "integrate-and-fire" neuron. For the case of a single neuron with $\Theta = 1$, Eqn. (6.1) gives us the firing period

$$T_{MS} = -\frac{1}{\gamma}\ln\Big(1 - \frac{\gamma}{S}\Big). \tag{6.2}$$

Thus firing is only realize when $\gamma/S < 1$.

Let us consider the case when all the neurons interact through pulse-coupling: when one neuron fires, all the others are pulled up by an amount k or to firing, whichever comes first. That is,

$$x_i = 1 \Rightarrow x_j = min(1, x_j + k) \qquad \forall \quad j \neq i. \tag{6.3}$$

In addition to the coupling prescription above, Mirollo and Strogatz [74] assumed that x evolves according to $x = f(\Phi)$ where $f(\Phi)$ is a smooth, concave down and monotonically increasing function:

$$\frac{\mathrm{d}f}{\mathrm{d}\Phi} > 0 \tag{6.4}$$

$$\frac{\mathrm{d}^2 f}{\mathrm{d}\Phi^2} < 0, \tag{6.5}$$

with the phase variable $\Phi\epsilon[0, 1]$; 0 being the the phase at $x = 0$ and 1 when $x = 1$. With these conditions, they proved that at some later time all the neurons would synchronize, that

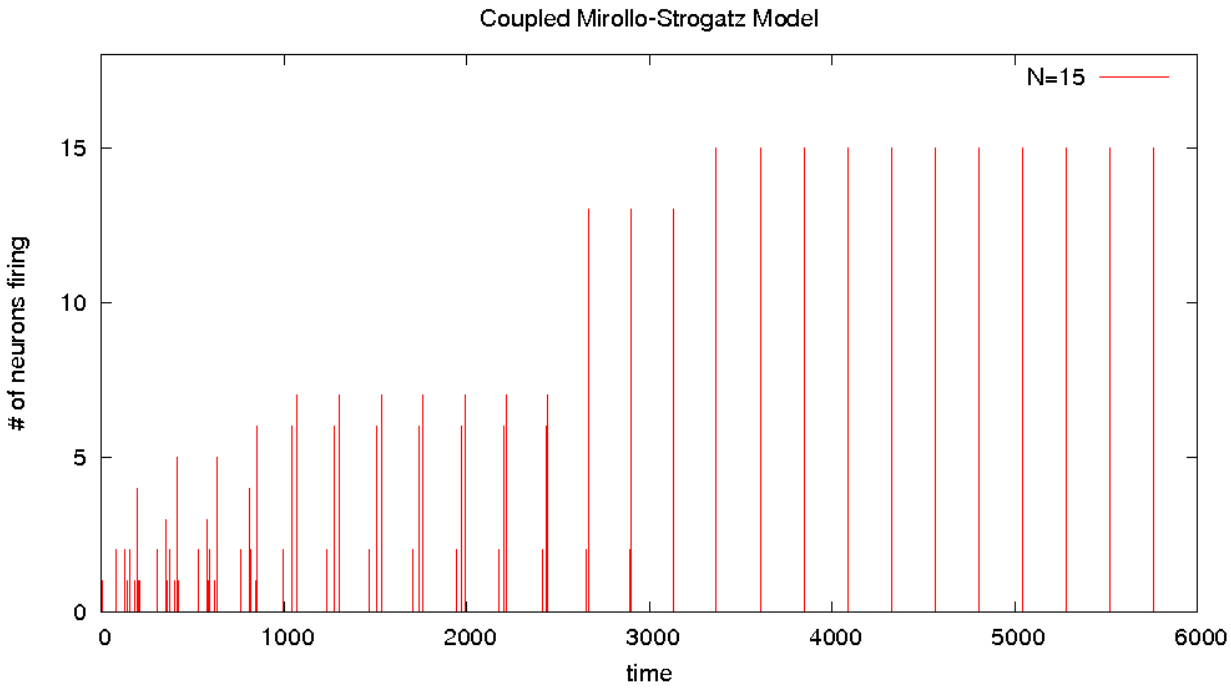

Figure 6.1: Synchronization of the Mirollo-Strogatz Model.

is, they fire at the same time with period T_{MS} (6.2) as shown in Figure 6.1. Thus, giving us the probability distribution density of times between two neuron firings (with τ being the usual waiting times):

$$\psi(\tau) = \delta(\tau - T_{MS}). \tag{6.6}$$

6.2. Stochastic version of the Mirollo-Strogatz Model

The Mirollo-Strogatz neuron model leading to the waiting times distribution (6.6) is clearly unrealistic due to its deterministic nature. To make the model realistic, it is appropriate to replace (6.1) with the stochastic equation

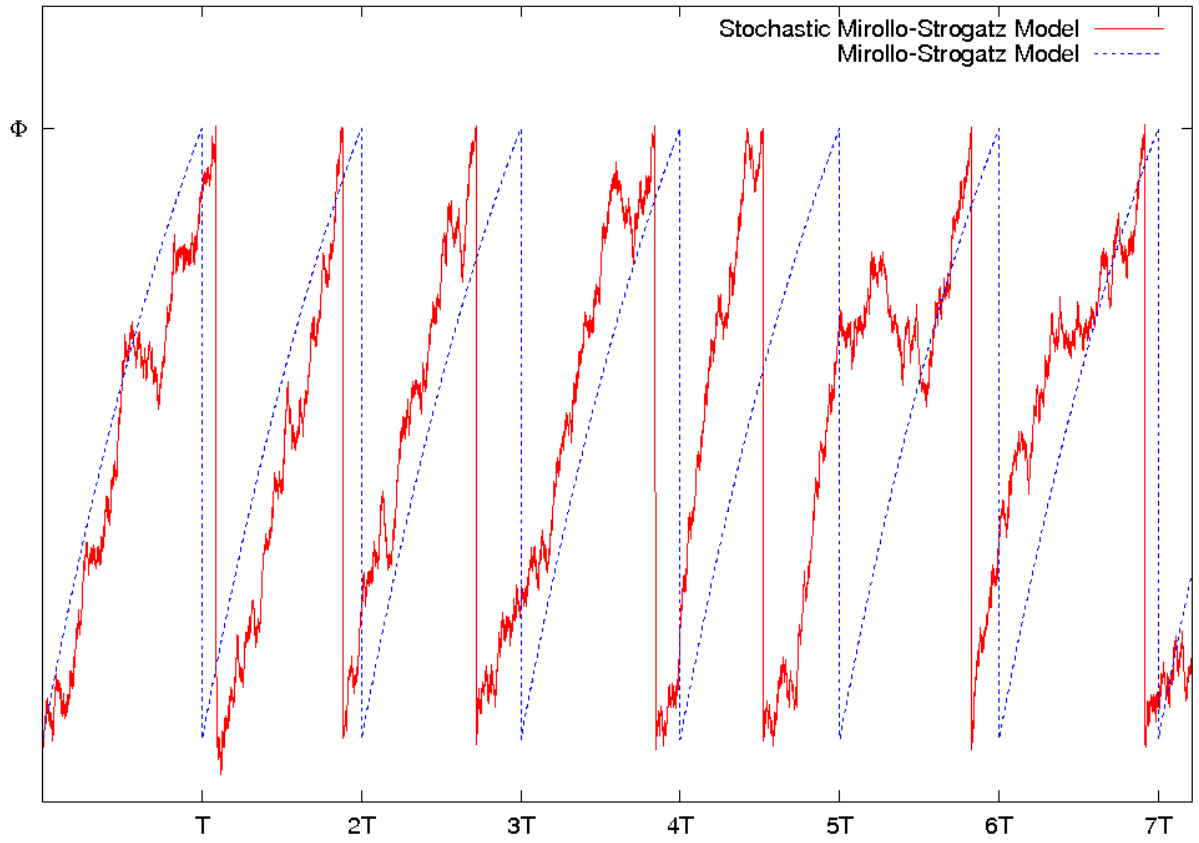

Figure 6.2: The trajectory of the single stochastic Mirollo-Strogatz neuron model as compared to its deterministic counterpart.

$$\frac{\mathrm{d}}{\mathrm{d}t}x_i(t) = -\gamma x_i(t) + S + \xi(t), \qquad i = 1, \ldots, N. \tag{6.7}$$

where $\xi(t)$ is a delta-correlated random function:

$$< \xi(t)\xi(t') >= \sigma^2\delta(|t - t'|). \tag{6.8}$$

The addition of the noise in (6.7) making the model stochastic has the effect of realizing the firing process of a single neuron earlier or later than than the period T_{MS} as shown in Figure 6.2. The waiting time distribution density $\psi(\tau)$ in the case where $\gamma = 0$ can be easily solved using the first passage time formalism introduced in Section 2.4.1. It can be shown

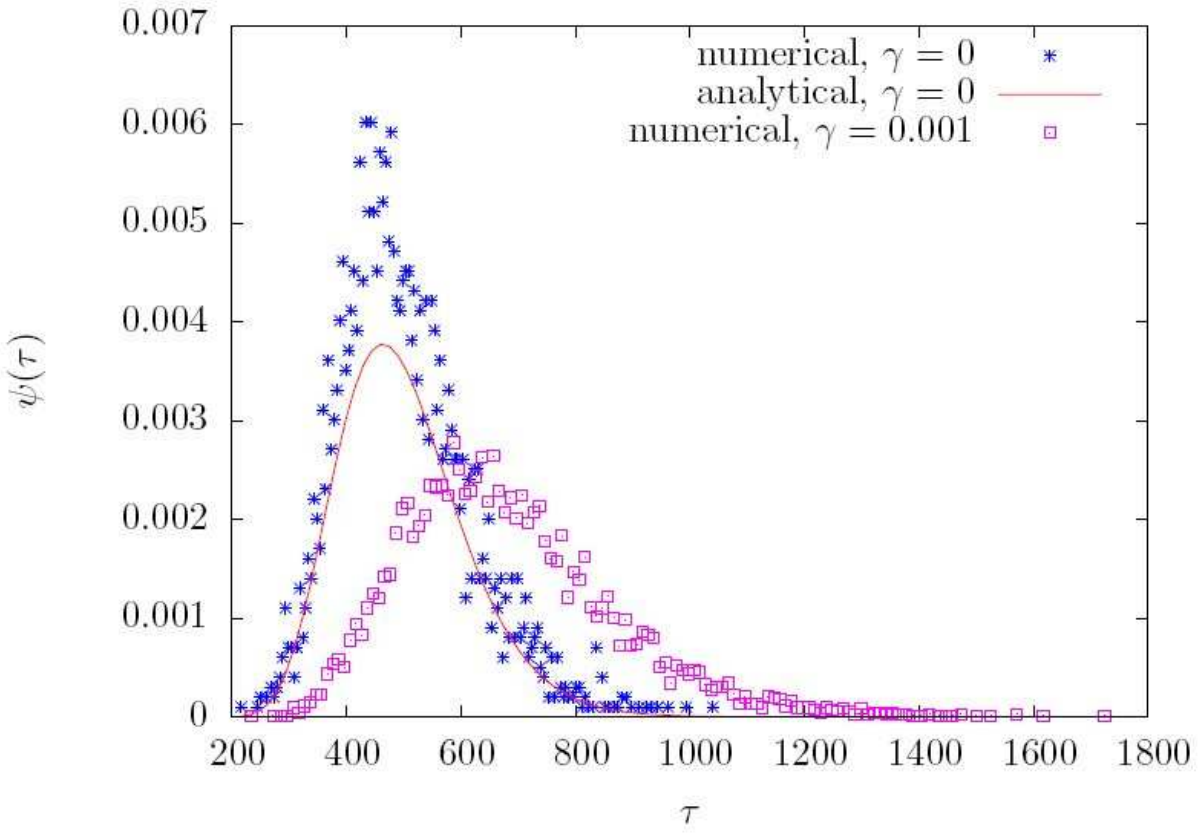

Figure 6.3: The trajectory of the single stochastic Mirollo-Strogatz neuron model as compared to its deterministic counterpart.

that this takes the inverse Gaussian form

$$\psi(\tau) = \frac{1}{(2\pi\sigma^2\tau^3)^{1/2}} exp\Big[-\frac{(1-S\tau)^2}{2\sigma^2\tau}\Big]. \tag{6.9}$$

We are not aware of any solution for the case $\gamma > 0$. However, as shown in Figure 6.3, it has the effect of making the mean waiting time larger.

6.3. Stochastic Firing Collective Behavior

Let us now study the collective behavior when the stochastic neurons obeying (6.7) are coupled according to the pulse-couling scheme of Section 6.1. To do this, let us first review some results in Section 4.4. Let us make the assumption that the rate $g < 1$. Thus we can

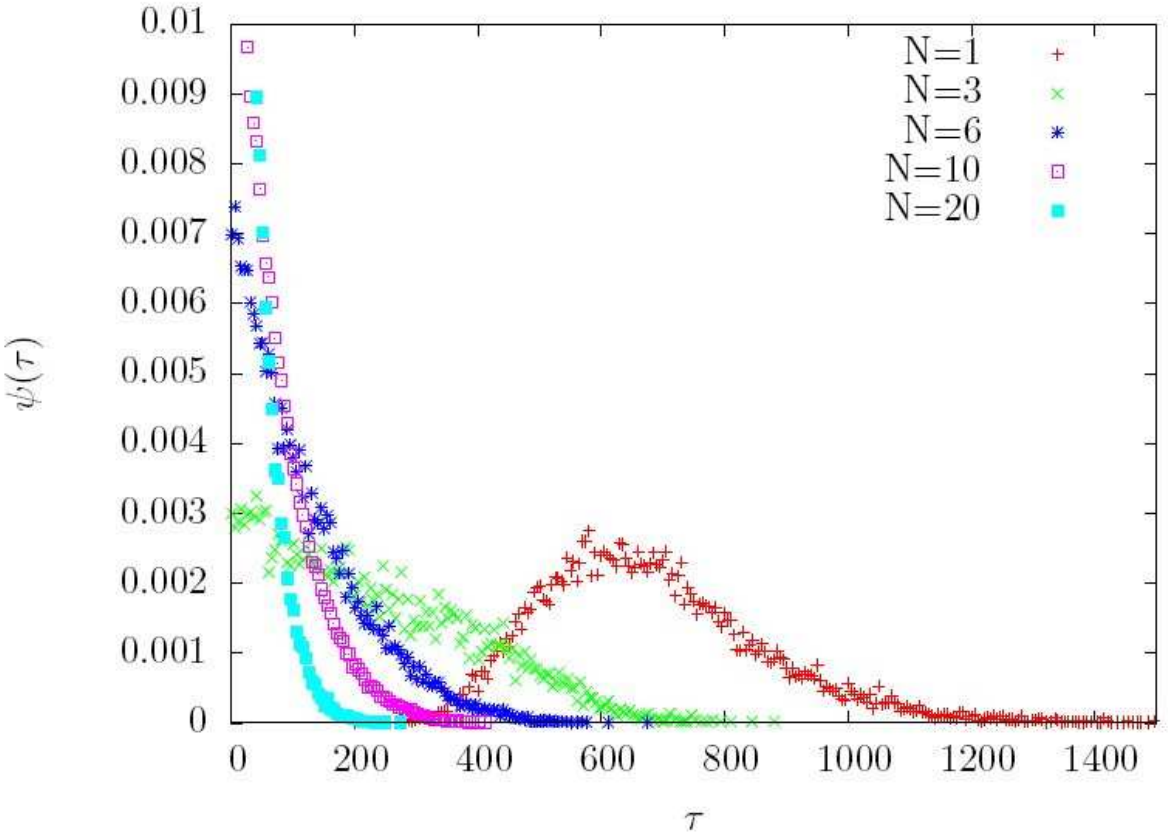

Figure 6.4: Decay of the waiting time distribution for different values of N.

write the Laplace-transform of the survival probability (4.44) as

$$\hat{\Psi}(u) = \frac{1}{u + \lambda^{\alpha}(u + \Gamma_t)^{1-\alpha}}, \tag{6.10}$$

with the introduction of the parameter Γ_t, to which, for the purposes herein, we refer to as the inverse of the truncation time. The recent work of Ref. [59] has revealed the existence of quakes on the human brain, and has proved that the time distance between two consecutive quakes is well described by a survival probability $\Psi(t)$, whose Laplace transform fits very well the prescription of Eq. 6.10. In the case $\Gamma_t = 0$ this is the Laplace transform of the Mittag-Leffler function [77], which interpolates between the stretched exponential relaxation $exp(-(\lambda t)^{\alpha})$, for $t < 1/\lambda$ and the inverse power law behavior $1/t^{\alpha}$, for $t > 1/\lambda$. The

parameter $\Gamma_t > 0$ has been introduced in the recent work of Refs. [80, 59] to take into account the truncation thought to be a natural consequence of the finite size of the time series under study. As a matter of fact, when λ is of the order of the time step and $1/\Gamma_t$ is much larger than the unit time step, the survival probability turns out to be virtually an inverse power law, whereas when $1/\lambda$ is of the order of $1/\Gamma_t$ and both are much larger than the unit time step, the survival probability turns out to be a stretched exponential function.

The noise $\xi(t)$ in (6.7) has the effect of making the neurons fire at times $t \ll T_{SM}$. Consequently, as an effect of setting $\sigma > 0$, a new, and much shorter time scale is generated. When we refer to this time scale as time scale of interest, the Mirollo and Strogatz period T_{MS} plays the role of truncation time:

$$\Gamma_t \approx \frac{1}{T_{MS}}. \tag{6.11}$$

To examine this condition let us set $k = 0$. In this case even if we assign to all the neurons the same initial condition, $x = 0$, due to the presence of stochastic fluctuation the neuron will fire at different times thereby creating a spreading on the initial condition that tends to increase in time, even if initially the firing will occur mainly at times $t = nT_{MS}$. The system will eventually reach a stationary condition with a constant firing rate G given by

$$G = \frac{N}{< \tau >}, \tag{6.12}$$

where $< \tau >$ denotes the mean time between two consecutive firings of the same neuron. For noise intensity $\sigma \ll 1$, $< \tau >= T_{MS}$. From the condition of constant rate G, we immediately derive the Poisson waiting time distribution

$$\psi(\tau) = Gexp(-G\tau). \tag{6.13}$$

We shall see hereby that this heuristic argument agrees very well with numerical results. For the numerical simulation we select the condition

$$G \ll 1 \ll N \ll T_{MS}, \tag{6.14}$$

with $N \gg 1$ and $N \ll T_{MS}$. As a consequence of this choice we get

$$\frac{1}{G} \approx \frac{T_{MS}}{N} \ll T_{MS}, \tag{6.15}$$

thereby realizing the earlier mentioned time scale separation. It is evident that this condition of non-interacting neuron fits Eq. (6.10) with $\alpha = 1$ and

$$\lambda(k = 0) = G. \tag{6.16}$$

In this case, the time truncation is not perceived, due to the condition $1/G \ll T_{MS}$.

To study the effect of coupling among neurons we adopt as benchmark the All-To-All coupling (ATA). Then, we consider four different networks. The first one is a regular (R) network (see Figure 5.7e), with the sites distributed on a circle with each site coupled to its $2m_{nn}$ nearest neighbors. The other three networks are complex: the Watts and Strogatz (WS) network (see Figure 5.7b) characterized by high clustering [9]; the Barabási and Albert (BA) network (see Figure 5.7c) [10], which is known to be scale free and finally the Holme and Kim (HK) network (see Figure 5.7d) [12], which shares with WS the high clustering and with BA the scale free condition. We assign to all three complex networks the same mean number of links, m_l, and we set $m_l = 2m_{nn}$.

We begin our analysis by discussing the ATA case. Fig. 6.5 refers to this condition. We adopt the values $N = 100$, $\gamma = 0.0001, S = 0.00019$. We have assessed numerically that $\langle\tau\rangle = 7431$ thereby yielding, thanks to Eq. (6.12), $G = 0.0135$, and $T_{MS} = 7472.14$. Curve 1 of Fig. 1 corresponds to $k = 0$. As earlier mentioned, this condition yields Eq. (6.13) and thus $\Psi(\tau) = exp(-G\tau)$. The log-linear representation of Fig. 6.6 fully confirms this expectation. Let us discuss now the effect of switching on the interaction among neurons.

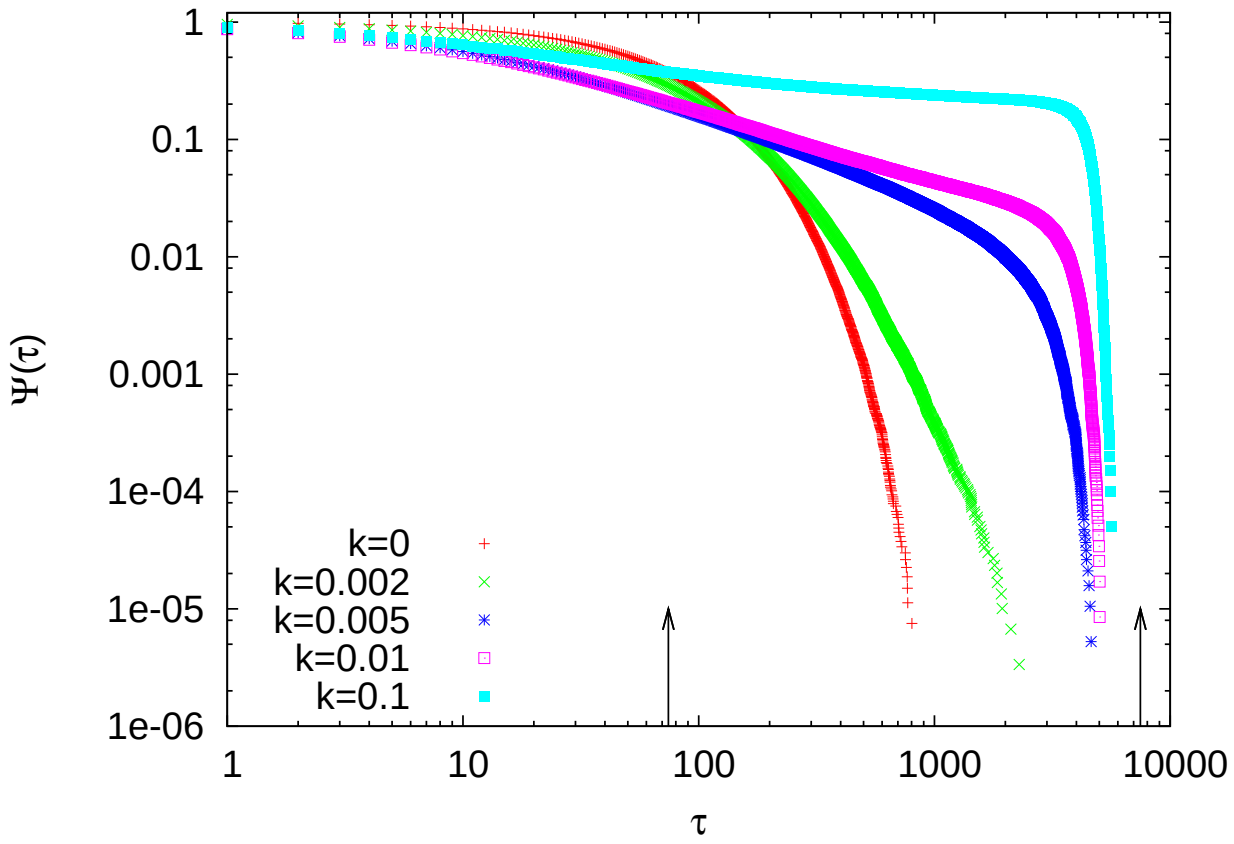

Figure 6.5: The survival probability $\Psi(\tau)$ as a function of τ.The vertical arrows denote $1/G = 74.31$ (left) and $T_{MS} = 7472.14$ (right). Curves 1, 2, 3, 4 and 5 refer to $k = 0, 0.002, 0.005, 0.01, 0.1$, respectively.

Fig. 6.5 shows that all the curves with $k > 0$ drop to zero at $\tau \approx T_{MS}$. This is an indication that the truncation parameter Γ_t of Eq. (6.10) is not a finite size effect, but rather a consequence of the fact that cooperation tends to fill the gap between $1/G$ and T_{MS} without significant effects in the time region exceeding the Mirollo and Strogatz time. The intuitive explanation is that no matter how small the coupling strength k is, the condition that at each time step only one neuron fires is lost. In the case of no interaction the probability that two neurons fire at the same time is G^2. Thanks to $G \ll 1$ (see Eq. (6.14)), the simultaneous firing of two neurons virtually does not happen. When we switch on the coupling, no matter how weak the interaction strength is, the simultaneous firing of more

than one neuron becomes frequent, and this explains why curve 2, corresponding to $k = 0.002$ has a much slower decay, so that it is still significantly large at $t = T_{MS}$.

Now, let us explore in detail the coupling interval $(0, k_{bd}]$, with $k_{bd} \approx 0.002$. This is the coupling region where the theoretical expectation of Eq. (6.10) is satisfactorily fulfilled. As earlier mentioned, in the time region $t < 1/\lambda$, we expect that

$$\Psi(t) = exp\,(-(\lambda t)^{\alpha})\,. \tag{6.17}$$

To prove this important fact, we focus our attention on the upper limit of this region, $k_{bd} = 0.002$, and in Fig. 6.7 we show $-log[\Psi(\tau)]$ in a log-log representation, where the stretched exponential should become a straight line with slope α. We see that this theoretical expectation is satisfactorily fulfilled with $\alpha = 0.77$. We note that at $\tau \approx 1000$ a significant departure from the straight line appears. This is a consequence of the earlier mentioned emergence of the power law regime $\Psi(\tau) \propto 1/\tau^{\alpha}$. To make this fact evident, we illustrate $\Psi(\tau)$ in a log-log representation in Fig. 6.8. We see that the numerical calculation confirms the Mittag-Leffler transition from the stretched exponential to the inverse power law behavior, supplemented by the truncation at $t \approx T_{MS}$, taken into account by the parameter $\Gamma_t \approx 1/T_{MS}$ of Eq. (6.10).

We note that Barabasi [53] stressed the emergence of the inverse power law behavior, properly truncated, as a consequence of the cooperative nature of human actions. Apparently, the numerical results of this Letter set a limit to the generality of this view, insofar as we see that the numerically monitored events suggest the stretched exponential behavior rather than the inverse power law prescription to be the general consequence of cooperation. However, we now prove that it is not so, if we make a distinction between actions and events. The action generator is assumed to not be fully successful, and a success rate parameter $g < 1$ is introduced with the limiting condition $g = 1$ corresponding to full success. To turn this perspective into a theory, yielding the theoretical prediction of Eq. (6.10), we assume that the time distance between two consecutive actions is described by the function

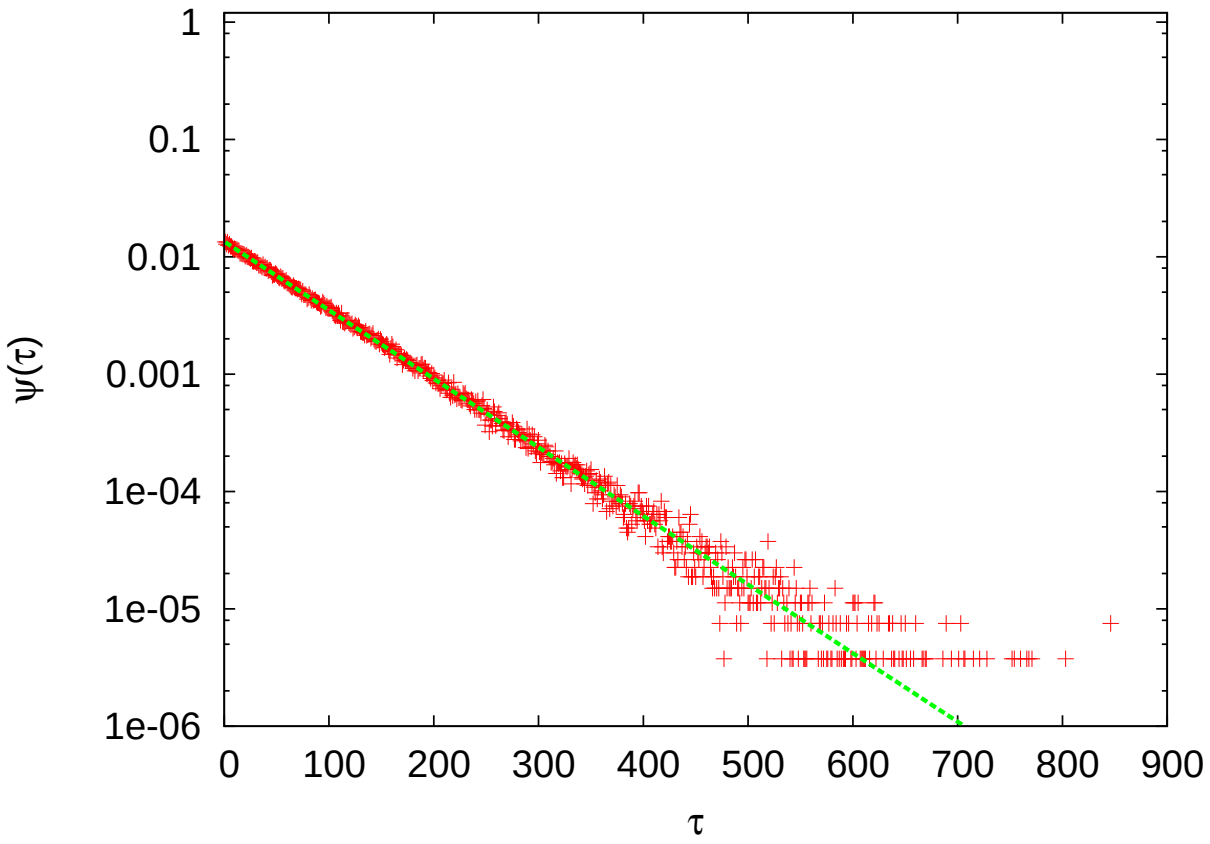

Figure 6.6: The function $\Psi(\tau)$ as a function of τ. The numerical result corresponds to curve 1 of Fig. 6.5. The dashed line is the analytical expression of Eq. (6.13) with $G = 0.0135$.

$\psi^{(S)}(\tau)$, where the superscript (S) indicates that from a formal point of view we realize a process corresponding to the subordination theory advocated by the authors of [81, 83]. It is evident that when $g = 1$ the survival probability $\Psi(\tau)$ is equal to $\Psi^{(S)}(\tau) = \int_\tau \psi^{(S)}(\tau')d\tau'$. When, $g < 1$, using the formalism of the subordination approach [81, 80, 59], we easily prove that the Laplace transform of $\Psi(\tau)$ (we adopt the notation $\hat{f}(u) = \int_0 \infty d\tau exp(-u\tau)f(\tau)$) is given by

$$\hat{\Psi}(u) = \frac{1}{u + g\hat{\Phi}(u)}, \tag{6.18}$$

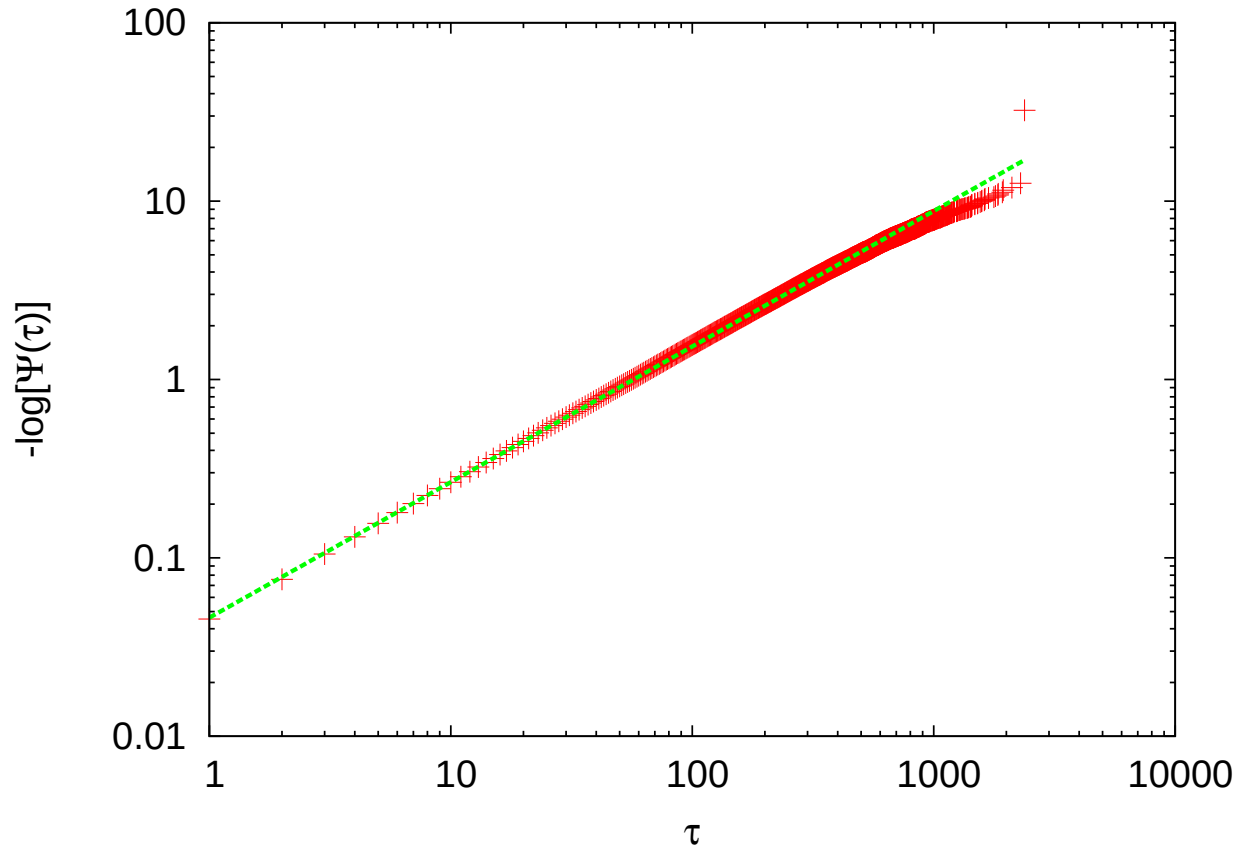

Figure 6.7: The function $-log[\Psi(\tau)]$ as a function of τ. This is curve 2 of Fig. 6.5. The dashed line is a straight line with $\alpha = 0.77$. k $= 0.002$.

where

$$\hat{\Phi}(u) = \frac{u\hat{\psi}^{(S)}(u)}{1 - \hat{\psi}^{(S)}(u)}. \tag{6.19}$$

To prove the emergence of Eq. (6.10) from this approach let us consider for simplicity's sake the case where $\psi^{(S)}(\tau)$ is not truncated, namely the case $\Gamma_t = 0$ of Eq. (6.10). We assign to $\psi^{(S)}(t)$ the form

$$\psi^{(S)} = (\mu_S - 1)\frac{T_S^{\mu_S - 1}}{(\tau + T_S)^{\mu_S}}. \tag{6.20}$$

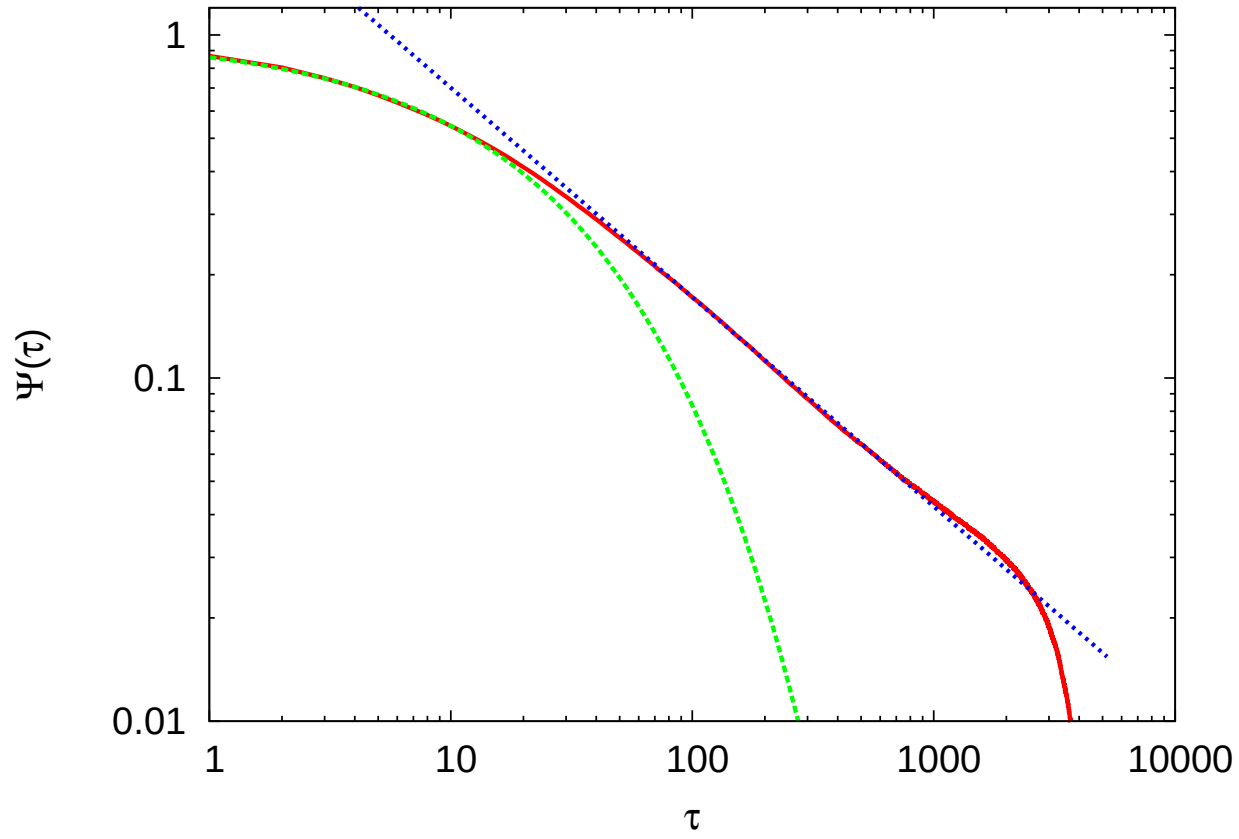

Figure 6.8: The function $\Psi(\tau)$ as a function of τ. The dotted straight line has the slope $\alpha = 0.61$. The dashed curve is Eq. (6.17) with $\lambda = 0.0445$ and $\alpha = 0.61$. k = 0.01.

In the non-ergodic case $\mu_S < 2$, using the Laplace transform method of Ref. [44], we obtain that the limiting condition $u \to 0$ yields (6.10) with

$$\lambda = \left[\frac{g}{T_S^{\alpha}\Gamma(1-\alpha)}\right]^{1/\alpha} \tag{6.21}$$

where $\Gamma(1-\alpha)$ is the Gamma function. Let us make also the assumption

$$T_S^{\alpha}\Gamma(1-\alpha) = C, \tag{6.22}$$

where C is constant that for simplicity's sake we set equal to 1. Thus, for the interval $(0, k_{bd}]$ we obtain

$$g(k) = \lambda(k)^{\alpha(k)}. \tag{6.23}$$

The parameters $\alpha(k)$ and $\lambda(k)$, for any value of k belonging to the interval $(0, k_{bd}]$ are safely obtained by fitting the numerical $\Psi(t)$ with the stretched exponential of Eq. (6.17), because the early time region is not affected by $\Gamma_t > 0$. Note that α and λ decreases and increases respectively, moving from their respective initial conditions $\alpha = 1$ and $\lambda = G$. From this fitting procedure we get the dependence of α and λ, and so of the success rate g on k. The result is plotted in Fig. 6.9. We see that, as expected g moves from the very small value $g = 0.02$, at $k = 0.001$, and increases so as to become of the order of 0.14 at $k = 0.01$. As we have earlier seen $g = 1$ corresponds to a regime totally dominated by the inverse power law behavior. Upon increase of the coupling k we reduce the size of stretched exponential regime and we make it possible for the inverse power law behavior to emerge. It is interesting to noticing that due to condition of Eq. (6.22), since the Gamma function diverges for $\alpha \to 1$, $T_S \to 0$ thereby making for the actions faster the transition to the inverse power law in the coupling region where for the events is significantly postponed so as to become virtually invisible. It is also evident that due to $\Gamma_t > 0$, the long-time regime of $\psi^{(S)}(\tau)$ is exponentially truncated in accordance with Ref. [53].

6.4. Role of Complex Networks in Stochastic Neuron Synchronization

We can now address the important issue of adopting a network with a finite number of connecting links rather than the ATA condition. The result is illustrated in Fig. 6.10. We adopt the log-log representation of $-log[\Psi(\tau)]$ as a function of τ so as to emphasize the emergence of the stretched exponential condition for the R network. We see that for the same value of k the complex networks already yield a pronounced transition to the inverse power law behavior, thereby suggesting that the complex networks favor also the emergence of the high synchronization condition.

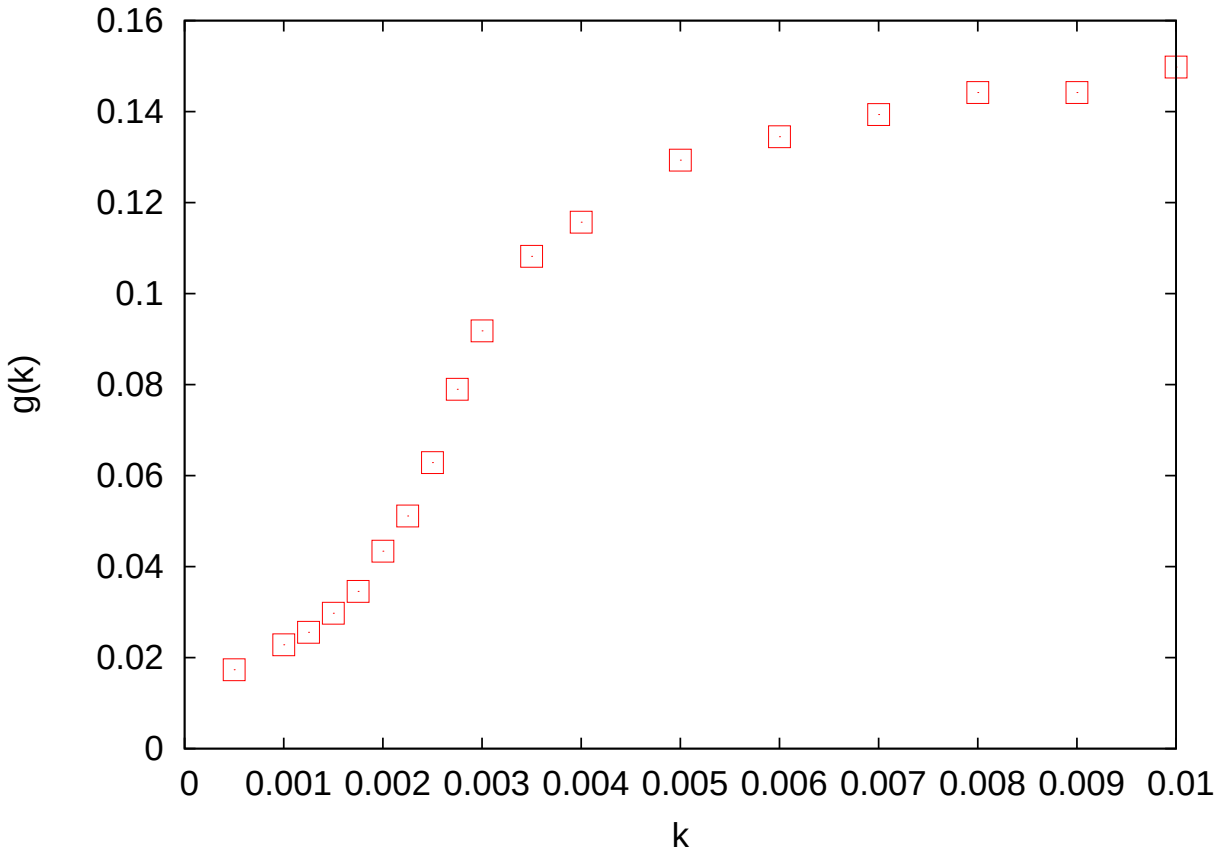

Figure 6.9: The function g(k) of Eq. (6.23) as a function of k.

Let us go back to Fig. 6.8. We see that in the region $\tau \approx T_{MS}$ immediately before the fast drop to 0 a little bump appears. This is a preliminary sign of the high synchronization condition that will produce at values of k of the order of 0.1 the step-like behavior corresponding to a regular firing process with the period of T_{MS}. We are convinced that this model can be used to reproduce the main properties of healthy brain, located in the region $(0, k_{bd}]$ and those of pathological brains [79] with $k > k_{bd}$.

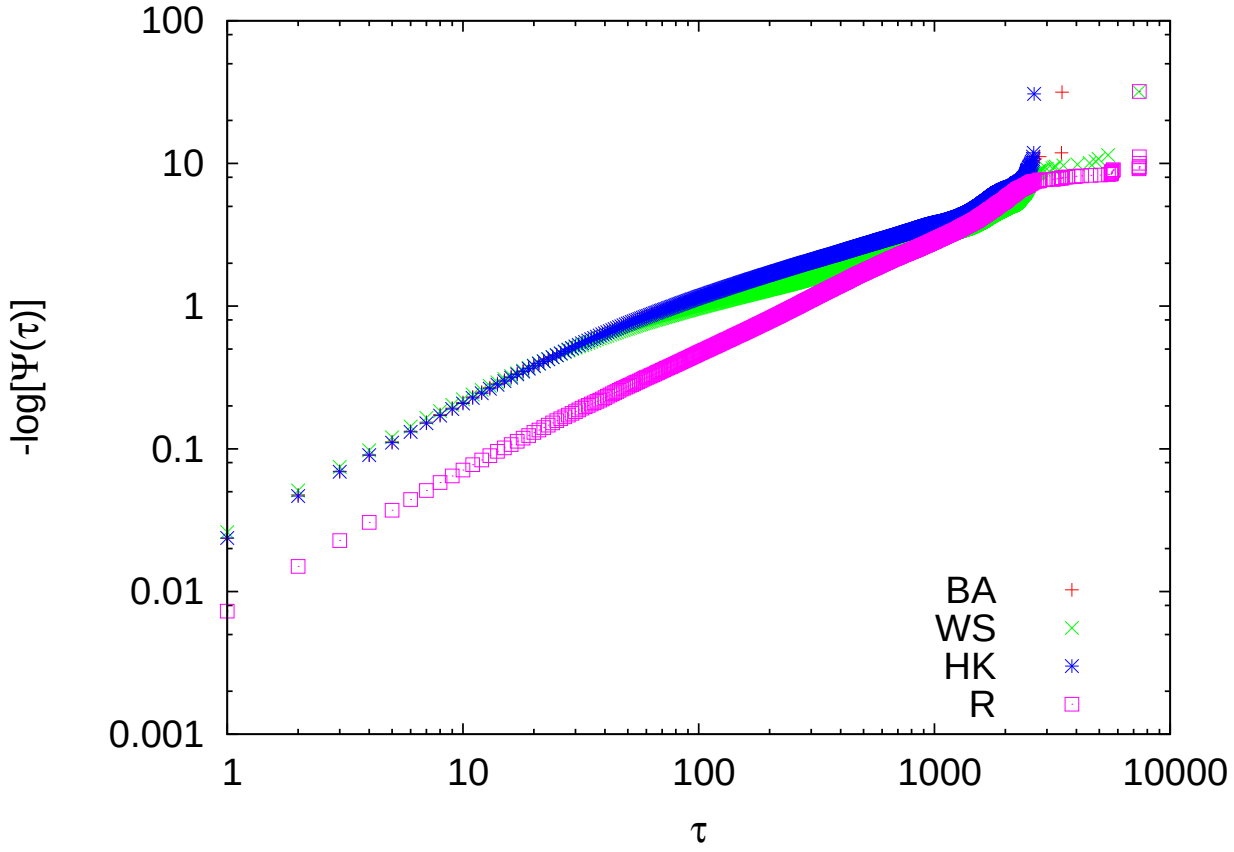

Figure 6.10: The function $\Psi(\tau)$ as a function of τ. We adopt the condition $m_l = 10$. The bottom line corresponds to the condition of a regular network. The other three networks, WS, AB and HK, merge into to top curve. Parameters are $\gamma = 0.0001$, $S = 0.00019$, $\sigma = 5 \times 10^{-5}$ and k = 0.3.

CHAPTER 7

CONCLUSIONS

In conclusion, the results of this dissertation affords the following benefits: (a) It offers a satisfactory model for blinking nanocrystals which is characterized by an inverse-power law distribution of sojourn times in "on" and "off" states, and in addition, we found that adopting a complex network topology results to change in the power index of the state sojourn time distribution; (b) It builds up a foundation for the dynamics of human brain by adopting a complex network topology for stochastic neuron synchronization; (c) It offers a clear proof that synchronization of oscillators is enhanced through the adoption of complex networks; (d) It supports the widely accepted view of complexity, that is, a condition intermediate between total randomness and cooperation-generated excessive order; (e) It supports the view that the experimentally observed deviations from the ordinary exponential behavior rests on the inverse power-law nature of the distribution density of the time distances between two consecutive actions, even when the actions cannot be directly observed.

APPENDIX A

ASYMPTOTIC BEHAVIOR OF POWER-LAW WAITING TIME DISTRIBUTION

Let us consider the following inverse power-law distribution of waiting times:

$$\psi(\tau) = (\mu - 1)\frac{T^{\mu-1}}{(\tau + T)^{\mu}} \tag{A-1}$$

Using the result from [48], the Laplace transform of (A-1) gives

$$\hat{\psi}(u) = \frac{(\mu - 1)\Gamma(1 - \mu)}{(uT)^{1-\mu}}\Big[e^{uT} - E_{\mu-1}^{uT}\Big] \tag{A-2}$$

where

$$E_{\mu-1}^{uT} \equiv \sum_{n=0}^{\infty} \frac{(uT)^{n+1-\mu}}{\Gamma(n + 2 - \mu)}. \tag{A-3}$$

Using (A-3) and the Taylor series expansion of (A-1), we get:

$$\begin{aligned}\hat{\psi}(u) = -\frac{(\mu - 1)\Gamma(1 - \mu)}{(uT)^{1-\mu}} \times \Big[&\frac{(uT)^{1-\mu}}{\Gamma(2 - \mu)} + \frac{(uT)^{2-\mu}}{\Gamma(3 - \mu)} + \frac{(uT)^{3-\mu}}{\Gamma(4 - \mu)} + \dots \\ &-1 - uT - \frac{1}{2}(uT)^2 - \frac{1}{6}(uT)^3 + \dots\Big] \\ = \Big[1 + &\frac{\Gamma(2 - \mu)}{\Gamma(3 - \mu)}(uT) + \frac{\Gamma(2 - \mu)}{\Gamma(4 - \mu)}(uT)^2 + \dots \\ -\Gamma(2 - \mu)\Big[&(uT)^{\mu-1} + (uT)^{\mu} + \frac{1}{2}(uT)^{\mu+1} + \frac{1}{6}(uT)^{\mu+2} + \dots\Big]\Big]\end{aligned} \tag{A-4}$$

where in the last step we applied the Γ function property

$$\Gamma(1 + x) = x\Gamma(x). \tag{A-5}$$

Let us approximate (A-4) in two different regions $1 < \mu < 2$ and $2 < u < 3$. In the case $1 < \mu < 2$ the slowest decay is given by $(uT)^{\mu-1}$. Thus, in the limiting case $u \to 0$ we get

$$\lim_{u\to 0} \hat{\psi}(u) = 1 - \Gamma(2-\mu)(uT)^{\mu-1}. \tag{A-6}$$

The case $2 < u < 3$ gives

$$\lim_{u\to 0} \hat{\psi}(u) = 1 - < \tau > u - \Gamma(2-\mu)(uT)^{\mu-1}. \tag{A-7}$$

where we made use of the mean waiting time $< \tau >= T/(\mu - 2)$.

APPENDIX B

DERIVATION OF THE RATE OF EVENTS

Let us evaluate the forms of the rate of events

$$\mathcal{P}(t) = \sum_{n=0}^{\infty} \psi_n(t) \tag{B-1}$$

in two cases $2 < \mu < 3$ and $1 < \mu < 2$. The condition $2 < \mu < 3$ gives, using Eqn. (3.54) and (3.50),

$$\begin{aligned} \hat{\mathcal{P}}(t) &= \frac{1}{<\tau> u + \Gamma(2-\mu)(\mu T)^{\mu-1}} \\ &= \frac{1}{<\tau> u} \frac{1}{1 + \Gamma(2-\mu)\frac{(uT)^{\mu-1}}{<\tau> u}} \\ &\approx \frac{1}{<\tau> u} - \frac{\Gamma(2-\mu)T^{\mu-1}}{<\tau>^2} \frac{1}{u^{3-\mu}}. \end{aligned} \tag{B-2}$$

The anti-Laplace transform of (B-2) can be easily evaluated using the Tauberian theorem (see Appendix C). This gives

$$\mathcal{P}(t) = \frac{1}{<\tau>} - \frac{\Gamma(2-\mu)T^{\mu-1}}{<\tau>^2 \, \Gamma(4-\mu)} \frac{1}{t^{\mu-2}}. \tag{B-3}$$

Using the Γ function property

$$\Gamma(1+x) = x\Gamma(x) \tag{B-4}$$

and the mean waiting time $<\tau> = T/(\mu-2)$, Eqn. (B-3) is simplified to

$$\mathcal{P}(t) = \frac{1}{<\tau>} + \frac{T^{\mu-2}}{(3-\mu)<\tau>} \frac{1}{t^{\mu-2}}. \tag{B-5}$$

In the case $1 < \mu < 2$, using Eqns. (3.54) and (3.49) we arrive at

$$\hat{\mathcal{P}}(t) = \frac{1}{\Gamma(2-\mu)T^{\mu-1}} \frac{1}{u^{\mu-1}} \tag{B-6}$$

which gives us

$$\mathcal{P}(t) = \frac{1}{\Gamma(\mu-1)\Gamma(2-\mu)T^{\mu-1}} \frac{1}{t^{2-\mu}}. \tag{B-7}$$

APPENDIX C

TAUBERIAN THEOREM

Suppose that $\hat{f}(u)$ is the Laplace transform of $f(t)$, and that $L(u)$ is a slowly varying function at $u = 0$. Suppose further that as $u \to 0$, $\hat{f}(u)$ behaves like

$$\hat{f}(u) = \frac{1}{u^{\alpha}} L\Big(\frac{1}{u}\Big) \tag{C-1}$$

where $\alpha \geq 0$. Let us define the function $F(t)$ to be the indefinite integral of $f(t)$:

$$F(t) = \int_0^t f(\tau)\mathrm{d}\tau. \tag{C-2}$$

Thus, the singular behavior shown in (C-1) implies that

$$F(t) \approx \frac{t^{\alpha} L(t)}{\Gamma(1+\alpha)}. \tag{C-3}$$

Using (C-2) yields

$$f(t) \approx \frac{\alpha t^{\alpha-1} L(t)}{\Gamma(1+\alpha)} = \frac{t^{\alpha-1} L(t)}{\Gamma(\alpha)}. \tag{C-4}$$

Therefore,

$$f(t) = \frac{t^{\alpha-1} L(t)}{\Gamma(\alpha)} \Rightarrow \hat{f}(u) = \frac{1}{u^{\alpha}}. \tag{C-5}$$

This is known as the Tauberian Theorem.

BIBLIOGRAPHY

[1] S.M. Mason, Geoforum **32**, 405 (2001).

[2] F. Reitsma, Geoforum **34**, 13 (2003).

[3] D.C. Mekulecky, Computational Chemistry (Oxford) **25**, 341 (2001).

[4] S. Mukamel, I. Procaccia, and J. Ross, J. Chem. Phys. **68**, 1205 (1978).

[5] P. Jung, U. Behn, E. Pantazelou and F. Moss, Phys. Rev. A **46**, R1709 (1992).

[6] A. Pikovsky, A. Zaikin, M.A. de la Casa, Phys. Rev. Lett. **88**, 050601 (2002).

[7] B. Cleuren and C. Van den Broeck, Europhys. Lett. **54**, 1 (2001).

[8] D. Huber and L.S. Tsimring, Phys. Rev. Lett. **91**, 260601 (2003).

[9] D.J. Watts and S.H. Strogatz, Nature (London) **393**, 440 (1998).

[10] A.-L. Barabási and R. Albert, Science **286**, 509 (1999).

[11] P. Erdös, and A. Rényi, *Random graphs* Publication of the Mathematical Institute of the Hungarian Academy of Science, 5, pages 17-61, 1960.

[12] P. Holme and B.-J. Kim, Phys. Rev. E **65**, 026107 (2002).

[13] R. Albert and A.-L. Barabási, Rev. Mod. Phys., bf 74, 47 (2002)

[14] B Mandelbrot, *Multifractals and 1/f Noise: Wild Self-Affinity in Physics (1963-1976)* Springer-Verlag, (1999).

[15] P. Bak, C. Tang, and K. Weisenfield, Phys. Rev. Lett. **59**, 381 (1987).

[16] C. Beck, E.G.D. Cohen, Physica A **322**, 267 (2003).

[17] H. J. Jensen, *Self-Organized Criticality*, Cambridge Lecture Notes in Physics, Cambridge University Press, Cambridge UK (2000).

[18] L. E. Reichl , A Modern Course in Statistical Physics, John Wiley, New York (1998).

[19] P. Grigolini, Adv. Chem. Phys, in press.

[20] G.H. Weiss, Aspects and Applications of the Random Walk, North-Holland, Amsterdam, 1994.

[21] W. Paul and J. Baschnagel, *Stochastic Processes: From Physics to Finance*, Springer, Berlin Germany (1999).

[22] Y. Fukui and T. Morita, J. Phys. A (Great Britain), **41** (1971).

[23] A. Einstein, A. Phys. (Leipzig), **33** 1105 (1910).

[24] B.D. Hughes, Random Walks and Random Environments, Vol. 1: Random Walks, Oxford University Press, Oxford, 1995.

[25] G.H. Weiss, R.J. Rubin, Adv. Chem. Phys. 52 (1983) 363.

[26] S. Alexander, J. Bernasconi, W.R. Schneider, R. Orbach, Rev. Mod. Phys. 53 (1981) 175.

[27] S. Havlin, D. Ben-Avraham, Adv. Phys. 36 (1987) 695.

[28] J.-P. Bouchaud, A. Georges, Phys. Rep. 195 (1990) 12.

[29] M.B. Isichenko, Rev. Mod. Phys. 64 (1992) 961.

[30] J.W. Haus, K.W. Kehr, Phys. Rep. 150 (1987) 263.

[31] M. Grifoni, P. Hänggi, Phys. Rep. 304 (1998) 229.

[32] B.J. West, W. Deering, Phys. Rep. 246 (1994) 1.

[33] R. Balescu, Statistical Dynamics, Matter out of Equilibrium, Imperial College Press, London, 1997.

[34] M.F. Shlesinger, G.M. Zaslavsky, J. Klafter, Nature 363 (1993) 31.

[35] J. Klafter, M.F. Shlesinger, G. Zumofen, Phys. Today 49 (2) (1996) 33.

[36] G.M. Zaslavsky, S. Benkadda, Chaos, Kinetics and Nonlinear Dynamics in Fluids and Plasmas, Springer, Berlin, 1998.

[37] R. Metzler and J. Klafter, Phys. Reports **339**, 1 (2000).

[38] S. Redner, *A Guide to First-Passage Processes*, Cambridge University Press, Cambridge, England (2001)

[39] H. A. Kramers, Physica **7**, 284 (1940).

[40] K. Connors, *Chemical Kinetics*, VCH Publishers (1990).

[41] E. W. Montroll and G. H. Weiss, J. Math. Phys. **6**, 178 (1965).

[42] M.F. Shlesinger, B.D. Hughes, Physica A, **109** 597 (1981).

[43] C. Beck, *Phys. Rev. Lett.* **87**, 180601 (2001).

[44] M. Bologna, P. Grigolini, M. Pala, L. Palatella, Chaos, Solitons and Fractals **17**, 601 (2003).

[45] S. Bianco, P. Grigolini, P. Paradisi, J. Chem. Phys. **123**, 174704 (2005).

[46] B.J. West, M. Bologna and P. Grigolini, *Physics of Fractal Operators*, Springer, New York (2003).

[47] P. Allegrini, F. Barbi, P. Grigolini, and P. Paradisi, Chaos, Solitons & Fractals, Volume 34, Issue 1, October 2007, Pages 11-18.

[48] M. Bologna, P. Grigolini, and B. J. West, Chem. Phys. 284 (2002), 115.

[49] G. Aquino, M. Bologna, P. Grigolini, and B.J. West, Phys. Rev. E **70**, 036105 (2004).

[50] E. Barkai, *Phys. Rev. Lett.* **90**, 104101 (2003).

[51] P. Allegrini, G. Aquino, P. Grigolini, L. Palatella, A. Rosa, and B. J. West, Phys. Rev. E **71**, 066109 (2005).

[52] D. R. Cox, *Renewal Theory*, Metheun & Co, London (1967).

[53] A. -L. Barabási, Nature **435**, 207 (2005).

[54] A. Vazques, B. Rácz, A. Lukács, A.-L. Barabási, Phys. Rev. Lett. **98**, 158702 (2007).

[55] R. Metzler, J. Klafter, Phys. Rep. **339**, 1 (2000).

[56] R. Cakir, A. Krockin and P. Grigolini, Chaos, Solitons & Fractals, Volume 34, Issue 1, October 2007, Pages 19-32.

[57] M. Kardar, G. Parisi, and Y.-C. Zhang, Phys. Rev. Lett. **56**, 889 (1986).

[58] R. Failla, P. Grigolini, M. Ignaccolo, and A. Schwettmann, Phys. Rev. E **70**, 010101 (R) (2004).

[59] S. Bianco, M. Ignaccolo, M. S. Rider, M. J. Ross, P. Winsor, and P. Grigolini, Phys. Rev. E **75**, 061911 (2007).

[60] A. T. Winfree, *The Geometry of Biological Time*, Springer-Verlag, Berlin (1990).

[61] Y. Kuramoto, *Rhythms and Turbulence in Populations of Chemical Clocks* Physica A **126**, 128 (1981).

[62] C. J. Stam, Clinical Neurophysiology **116**, 2266 (2005).

[63] O. E. Rössler, Phys. Lett. **57 A**, 397 (1976).

[64] T. Prager, B. Naundorf, and L. Schimansky-Geier, Physica A **325**, 176 (2003).

[65] H. E. Stanley, Introduction to Phase Transitions and Critical Phenomena, Oxford University Press, Oxford (1971).

[66] K. Wood, C. Van den Broeck, R. Kawai, and K. Lindenberg, Phys. Rev. Lett. **96**, 145701 (2006).

[67] G. Margolin and E. Barkai, Phys. Rev. E **72**, 025101 (R) (2005).

[68] K. Wood, C. Van den Broeck, R. Kawai, and K. Lindenberg, Phys. Rev. Lett. **96**, 145701 (2006).

[69] G. Margolin and E. Barkai, J. Chem. Phys. **121**, 1566 (2004).

[70] M. Kuno, D. P. Fromm, H. F. Hamann, A. Gallagher, and D. J. Nesbitt, J. Chem. Phys. **115**, 1028 (2001); K. T. Shimizu, R. G., Neuhauser, C. A. Leatherdale, S. A. Empedocles, W. K. Woo, and M. G. Bawendi, Phys. Rev. B **63**, 205316 (2001).

[71] D. Plenz and T. C. Thiagarajan, Trends in Neurosci. **30**, 101 (2007).

[72] D. Plenz and T. C. Thiagarajan, Trends in Neurosciences, **30**, 101 (2007).

[73] B. J. Kim, Phys. Rev. Lett. 93, 168701 (2004).

[74] R. E. Mirollo and S. H. Strogatz. SIAM J. Appl. Math. **50**, 1645 (1990).

[75] C. S. Peskin, *Mathematical Aspects of Heart Physiology*, Courant Institute of Mathematical Sciences, New York University, New York, pp. 268-278, 1975.

[76] H.C. Tuckwell, *Stochastic processes in the neurosciences*, Society for Industrial and Applied Mathematics, Philadelphia (1989).

[77] R. Metzler, J. Klafter, Journal of Non-Crystalline Solids, **305**, 81(2002).

[78] T. Nakamura, K. Kiyono, K. Yoshiuchi, Z. R. Struzk, and Y. Yamamoto, Phys. Rev. Lett. **99**, 138103 (2007).

[79] S. Ponten, F. Bartolomei, C. Stam, Clinical Neurophysiology, **118**, 918 (2007).

[80] R. Failla, M. Ignaccolo, P. Grigolini and A. Schwettmann, Phys. Rev E **70**, 010101 (2004).

[81] I. M. Sokolov, Phys. Rev. A **63**, 011104 (2000); E. Barkai and R.J. Silbey, J. Phys. Chem. B (**104**), 3866 (2000); R. Metzler and J. Klafter, J. Phys. Chem. B, **104**, 3851 (2000).

[82] I. M. Sokolov, Phys. Rev. E **73**, 067102 (2006); I. M. Sokolov, J. Klafter, Phys. Rev. Lett. **97**, 140602 (2006).

[83] I. M. Sokolov, J. Klafter,Chaos, **15** 026103 (2005); R. Gorenflo, F. Mainardi and A. Vivoli, Chaos, Solitons and Fractals, **34**, 87 (2007).